December 2017

Towards a Better Understanding of the Molecular Mechanisms Underlying Plant Development and Stress Response

Peipei Wu
Clemson University, peipeiw88@gmail.com

TOWARDS A BETTER UNDERSTANDING OF THE MOLECULAR MECHANISMS UNDERLYING PLANT DEVELOPMENT AND STRESS RESPONSE

A Dissertation
Presented to
the Graduate School of
Clemson University

In Partial Fulfillment
of the Requirements for the Degree
Doctor of Philosophy
Biochemistry and Molecular Biology

---

by
Peipei Wu
December 2017

Accepted by:
Dr. Hong Luo, Committee Chair
Dr. Julia Frugoli
Dr. Rajandeep Sekhon
Dr. Liangjiang Wang

`

ABSTRACT

The spectacular array of diverse plant forms as well as the predominantly sessile life style of plants raises two questions that have been fascinating to scientists in the field of plant biology for many years: 1) how do plants develop to a specific size and shape? 2) how do plants respond to environmental stresses given its immobility?

Plant organ development to a specific size and shape is controlled by cell proliferation and cell expansion. While the cell proliferation process is extensively studied, the cell expansion process remains largely unknown, and can be affected by several factors, such as cell wall remodeling and the incorporation of new wall materials. To better understand the genetic basis of plant development, we identified an *Arabidopsis* T-DNA insertion mutant named *development related Myb-like 1* (*drmy1*), which showed altered size and shape in both vegetative and reproductive organs due to defective cell expansion. We further demonstrated that the defective cell expansion in the *drmy1* mutant is linked to the change in cell wall composition. Complementation testing by introduction of *DRMY1* into the mutant background rescued the phenotype, indicating that *DRMY1* is a functional regulator of plant organ development. The DRMY1 protein contains a single Myb-like DNA binding domain and is localized in the nucleus, and may cooperate with other transcription factors to regulate downstream gene expression as DRMY1 itself does not possess transactivation ability. *DRMY1* expression analysis revealed that its expression is reduced by the plant hormone ethylene (a negative regulator of cell expansion) while induced by ABA (a positive regulator of cell expansion). Furthermore, whole transcriptome profiling suggested that DRMY1 might control cell expansion directly by regulating genes

`

related to cell wall biosynthesis/remodeling and ribosome biogenesis or indirectly through regulating genes involved in ethylene and ABA signaling pathways.

Plants cannot “escape” from salinity stress but have evolved different mechanisms for salt tolerance over the time of adaptation to salinity. About 1% of plant species named halophytes can survive and thrive in environments containing high salt concentrations, which makes it important to understand their salt tolerance mechanisms and the responsible genes. Here, we investigated salt tolerance mechanisms in Supreme, the most salt-tolerant cultivar of a halophytic warm-seasoned perennial grass, Seashore paspalum (*Paspalum vaginatum*) at the physiological and transcriptomic levels by comparative study with another cultivar Parish, which possesses moderate salinity tolerance. Our results suggest that Na^+ accumulation under normal conditions and further increased accumulation under high salinity conditions (400 mM NaCl), possibly by vacuolar sequestration is a crucial mechanism for salinity tolerance in Supreme. Our data suggests that Na^+ accumulation in Supreme under normal conditions might trigger the secondary messenger Ca^{2+} for signal transduction and the resulting upregulation of salt stress related transcription factors in addition to serving as cheap osmolytes to facilitate water uptake. Moreover, the retention of K^+ under salt treatment, which can counteract the toxicity of Na^+, is a protective mechanism for both cultivars. A strong oxidation-reduction process and nucleic acid binding activity under high salinity conditions are two other contributors to the salinity tolerance in both cultivars. We also identified ion transporters including NHXs and H^+-PPases for Na^+ sequestration and K^+ uptake transporters, which can be used as candidate

`

genes for functional studies and potential targets to engineer plants for enhanced salinity tolerance, opening new avenues for future research.

`

DEDICATION

I dedicate this dissertation to my parents, Jinlin Lu and Xiuyun Liu, who give me their best love and support. This work is also dedicated to my husband Yijian Qiu, who helped me get through tough times during my PhD study with encouragement and support.

`

ACKNOWLEDGMENTS

Firstly, I would like to express my sincere gratitude to my advisor Dr. Hong Luo for his invaluable guidance and enormous support for my PhD study. I also greatly appreciate my committee members Dr. Julia Frugoli, Dr. Liangjiang Wang, and Dr. Rajandeep Sekhon for their insightful and helpful suggestions on my projects. I would also like to thank my current and previous lab members, Qian Hu, Dr. Zhigang Li, Dr. Ning Yuan and Dr. Zhihui Chang for their generous help and support. I'm also very grateful for the following people: Dr. Steven Cogill (Stanford University), Yijian Qiu (Clemson University), Dr. Christopher Saski (CUGI), Dr. Rooksana Noorai (CUGI), Xiaoxia Xia (CUGI), Dr. Vijay Shankar (CUGI), Wei Li (Clemson University) for their help in RNAseq data analysis; Computing experts Dr. Marcin Ziolkowski, Dr. Linh Ngo, Ashwin Srinath, Jeff Denton from Clemson University Computing and Information Technology (CCIT) for their help in programming and troubleshooting; Dr. Rhonda Reigers Powell from Clemson Light Imaging Facility (CLIF) for her guidance in fluorescence imaging; Dr. Cliff Foster from Michigan State University for his help with cell wall composition analysis; Dr. Cora MacAlister from University of Michigan and Dr. David Jackson from Cold Spring Harbor for providing *Lat52B-GUS* transgenic *Arabidopsis* seeds and protocols; Dr. Dayong Li from Chinese Academy of Sciences for providing yeast systems for transactivation assay; Dr. Paul Raymer from University of Georgia for providing Seashore paspalum cultivars.

`

TABLE OF CONTENTS

`

LIST OF TABLES

LIST OF FIGURES

List of Figures (Continued)

CHAPTER ONE

LITERATURE REVIEW AND RESEARCH OBJECTIVES

`

Part I: The Regulation of Plant Development

Plant organ growth is regulated by a complex gene regulatory network that enables two successive but overlapping processes of cell proliferation and cell expansion. Over the past decades, our understanding of the molecular pathways controlling cell proliferation and cell expansion has been considerably moved forward by forward and reverse genetic studies. In this review, I will summarize our current knowledge about how the intrinsic genetic control of cell proliferation and cell expansion is executed during organ development at the cellular level and how these two processes are coordinated by organ-wide regulatory mechanisms.

Cell Proliferation

Cell proliferation determines the number of cells in the leaf (Powell and Lenhard 2012). Cell proliferation rate is an important factor that contributes to this process. Assuming that the duration of cell proliferation in which new cells are generated is constant, the time to complete an entire cell cycle will decide the total number of cells that form a leaf. Cell proliferation rate is tightly controlled by the plant cell cycle machinery that ensures correct DNA replication and successful progression through different phases of the cell cycle.

The basic cell cycle machinery is composed of the catalytic cyclin-dependent kinases (CDKs) and the regulatory cyclins (CYCs) that control CDK activity. Plant CDKs are classified into eight classes based on their cyclin-binding domain, namely CDKA to CDKG and CDKL. Different CDKs-CYCs complex phosphorylate an array of substrates to drive the progression of the cell cycle from one phase to another. The major drivers of the plant cell cycle are CDKA and CDKB. CDKA controls the G1-S and G2-M transition

`

by association with CYCD and CYCB respectively while CDKB functions in association with CYCA and CYCB, which is necessary for G2-phase and M-phase, respectively.

CDKA and CYCD play a central role in G1 to S transition and progression of the S phase in which cells undergo DNA replication. Overexpression of a dominant negative allele of *CDKA;1* in meristematic cells decreased the cell division rate within the SHOOT MERISTEMLESS (STM) domain of the shoot apex as well as the developing organs (Gaamouche et al. 2010). Triple loss-of-function mutants *cycd3;1-3* in *Arabidopsis* showed reduced cell number in developing leaves by regulating the duration of the mitotic phase (Dewitte et al. 2007). In the presence of plant hormones such as auxin, cytokinins (CK), brassinosteroids (BR), CYCD associates with CDKA, forming an inactive CDKA/CYCD complex (Inzé and De Veylder 2006). The CDKA/CYCD complex is then activated by phosphorylation which is catalyzed by CDK activating kinases (CDKF and CDKD associated with CYCH). The activity of the CDKA/CYCD complex is also regulated by two different families of CDK inhibitors, Kip-Related Proteins (KRPs) and the plant-specific SIAMESE (SIM)-related protein (Verkest et al. 2005) (Churchman et al. 2006). The *Arabidopsis* genome encodes seven KRPs, designated as KRP1-7. KRP1 is the target of two different ubiquitin protein ligases for its degradation, SCF and the RING protein RKP, suggesting the important role of proteolysis in the cell cycle regulation (Ren et al. 2008). Ectopic expression of KRP2 inhibited cell proliferation in the leaf primordia without affecting the timing of cell cycle exit (De Veylder et al. 2001). Using *Arabidopsis* pollen development as a model system, Zhao et al. (2012) identified a quadruple negative regulatory cascade regulating the G1/S transition, which is composed of four components: CDKA;1, KRPs, the F-box protein (FBL17) and RBR1. FBL17 plays a central role in this

`

regulatory network which mediates the degradation of KRPs but itself is repressed by RBR1 (Zhao et al. 2012).

Upon activation by phosphorylation, the CDKA/CYCD complex phosphorylates RBR, which triggers its dissociation from the transcriptional activator E2Fa/b-DP heterodimeric complex. In addition, the activated CDKA/CYCD complex also phosphorylates the transcriptional repressor E2Fc-DP, which is targeted for protein degradation by the SCF E3 ubiquitin protein ligase. Once the E2Fa/b-DP complex is released from RBR, it triggers the onset of G1 to S transition by activating gene expression relevant to DNA replication initiation, including CDC6, CDT1, ORC3, and MCM3. CDC6 and CDT1 together with ORC3 enable the loading of MCM3 to the replication initiation site. Then, the DBF-CDC7 complex phosphorylates and dislodges ORC3, exposing the replication origins to the replisome complex and allowing DNA replication to start (Francis 2007).

Arabidopsis has six E2Fs: E2Fa, E2Fb, E2Fc, E2Fe/DEL1, E2Fd/DEL2 and E2Ff/DEL3 with the former three in association with two DPs (DPa and DPb) (Mariconti et al. 2002). E2Fa and E2Fb perform as transcriptional activators and stimulate the G1 to S transition and the progression of the S phase. Overexpression of AtE2Fa and AtDPa can induce non-dividing leaf cells to reenter the S phase (Rossignol et al. 2002). E2Fb is induced by auxin and coexpression of E2Fb with its dimerization partner DPa stimulated cell proliferation and shortened cell cycle duration time, resulting in increased cell numbers (Magyar et al. 2005). On the other side, E2Fc acts as a transcription repressor of the S phase, the stability of which is regulated by proteolysis. Overexpression of a stable form of AtE2Fc negatively affects cell division and represses the expression of CDC6 (Del Pozo,

`

Boniotti, and Gutierrez 2002). For three atypical E2Fs/DELs, it is still elusive whether they can repress gene expression actively or compete with three typical E2Fs (E2Fa, E2Fb and E2Fc) for binding the target sites (Berckmans and De Veylder 2009).

After DNA replication, cells exit from S phase to enter G2 phase, in preparation for cell division through mitosis. CDKA and CDKB associated with CYCA, CYCB and CYCD are involved in this process. Some B-type CDKs are regulated by the E2Fa/b-DP complex, suggesting a potential mechanism by which different cell cycle phases communicate with each other. Similar to G1/ S phase, the CDK/CYC complex during G2/M phase can be activated by the CDK-activating kinase pathway, which involves CDKF and CDKD coupled with CYCH. The activated CDK/CYC complex phosphorylates and activates three repeat MYB transcription factors, which then promote the expression of G2/ M phase specific genes by binding to the M phase specific activator (MSA) element in their promoter regions (Berckmans and De Veylder 2009). In tobacco, there are three MYB3R proteins, namely NtMYBA1, NtMYBA2 and NtMYBB, which are structurally similar to animal c-MYB proteins. Transient expression assays showed that NtMYBA1 and NtMYBA2 act as transcriptional activators whereas NtMYBB performs as a repressor by modulating B-type cyclin genes (Ito et al. 2001). In *Arabidopsis*, *MYB3R1* and *MYB3R4*, which encode homologs of NtMYBA1 and NtMYBA2, respectively, act as positive regulators in cytokinesis and are functionally redundant. The *myb3r1myb3r4* double mutant is defective in cytokinesis, mainly caused by a reduced expression of an MSA element containing gene called *KNOLLE*, which is essential for the cell plate formation during cytokinesis (Haga et al. 2007).

`

On the other hand, like in the G1/S phase, the activity of CDK/CYC complex is also inhibited by KRPs during G2/M phase. Additionally, its activity can be negatively regulated through phosphorylation by the WEE1 protein kinase which is upregulated in response to DNA replication termination or DNA damage. WEE1-deficient mutant plants exhibited no obvious phenotype under normal growth conditions but the mutant showed hypersensitivity to agents that inhibit DNA replication. Overexpression of the *WEE1* gene inhibited plant growth by limiting cell cycle in the G2 phase (De Schutter et al. 2007).

Cell cycle progression is an irreversible process. Exit from mitosis requires rapid degradation of cell cycle regulatory proteins by the 26S proteasome upon ubiquitination by the anaphase-promoting complex/cyclosome (APC/C) and its two activators, CCS52 and CDC20. In addition, there are two negative regulators of APC/C activity, named UVI4 and DEL1, suggesting a fine-tuning of APC/C activity during the cell cycle. The APC/C is an E3 ubiquitin ligase, which destroys cell cycle proteins and promotes exiting from mitosis. Overexpression of APC10, a subunit of APC/C complex, leads to enhanced leaf size due to accelerated cell division during early stage of leaf development. Further analysis revealed that the proteolysis rate of CYCLIN B1;1(CYCB1;1) was increased in *35S-APC10* transgenic plants (Eloy et al. 2011). Similarly, Ectopic overexpression of another subunit of APC/C, *Arabidopsis* CDC27a, in tobacco also promotes plant growth by enhancing the cell division rate (Rojas et al. 2009). Changes in GA metabolism in stress conditions lead to stability of the DELLA protein, which triggers mitotic exit by modulating the APC/C activity through down regulation of DEL1 and UVI4 (Claeys et al. 2012).

`

Cytoplasmic Growth

Cytoplasmic growth is coupled with cell proliferation to maintain cells at a constant cell size while proliferating. It mainly relies on macromolecular biosynthesis, mostly proteins, which is an energy-consuming process. Therefore, cytoplasmic growth is tightly linked to the nutritional and energy level of plants. Given the sessile attribute of plants, plants must evolve a regulatory mechanism that connects the environmental nutritional conditions to growth regulation in order to maintain survival under the available resources. Recent findings illuminated the central role of the Target of Rapamycin (TOR) signaling pathway in conveying the nutrient-derived signals and regulating cell growth. TOR is a serine/threonine protein kinase, which operates in a multi-protein complex with the Regulatory-associated protein of TOR (RAPTOR) and the Lethal with Sec Thirteen 8 (LST8) protein. Overexpressing AtTOR produces bigger leaves with larger cells while inducible down-regulation of TOR produces smaller leaves with smaller cells, which is related to decreased polysome accumulation and soluble proteins (Deprost et al. 2007). Ribosomal protein S6K is one of the well-characterized substrates of TOR, as evidenced by decreased S6K phosphorylation under the conditions of chemical inhibition or knockdown of TOR gene activity (Xiong and Sheen 2012; Schepetilnikov et al. 2013). TOR-activated S6K contributes to translation-mediated cell growth by several mechanisms. Firstly, TOR-activated S6K showed increased kinase activity towards the ribosomal protein S6 that contributes to ribosome biogenesis (Rexin et al. 2015). Moreover, TOR-activated S6K in plants has been shown to promote reinitiation of mRNA translation after upstream open reading frame (uORF) translation by phosphorylating eukaryotic initiation

`

factor 3H (eIF3H) and thus stabilizing the association of the ribosomes with mRNAs in *Arabidopsis* (Schepetilnikov et al. 2013).

The TOR signaling pathway is also involved in a wealth of other biological outputs related to plant development. A recent study identified the E2Fa transcription factor as a novel TOR kinase substrate for activation of S-phase genes during cell cycle, bypassing or acting downstream of the universal CYC-CDK-RBR cascade (Xiong et al. 2013). By performing metabolite profiling in combination with transcript profiling, Caldana *et al.* (2013) revealed regulation of genes involved in the cell cycle, cell wall remodeling and nutrient recycling processes such as senescence or autophagy, together with substantial accumulation of lipids and starch in *Arabidopsis* plants with down-regulation of *AtTOR* expression (Caldana et al. 2013). The TOR pathway also affects cell wall structures. LRR-extensin1 (LRX1) is known as an extracellular protein involved in cell wall development in *Arabidopsis* root hairs (Diet et al. 2006). Inhibition of TOR signaling by rapamycin led to specific changes to galactan and arabinogalactan proteins of cell walls and caused suppression of the aberrant root hair phenotype in the *lrx1* mutant (Leiber et al. 2010).

Endocycle

After several rounds of mitosis, many of the newly formed cells then switch into endocycle, a process in which cells increase their ploidy level by successive rounds of DNA replication without mitosis. For cells to timely transit into the endocycle, they should be directed by developmental signals. For example, the auxin gradient in the root meristem plays a vital role in coordinating the developmental switch from mitotic cycle into endocycle. A high concentration of auxin in the proximal region of the meristem is required

`

to maintain mitotic cycles and repress endocycles while a lower concentration of auxin triggers an exit from mitotic cycle and an entry into endocycle (Ishida et al. 2010).

To promote the progression of endocycle, the activity of CDK has to be kept below a level that inhibits mitosis. Different mechanisms account for the CDK inhibition to initiate endocycle. The first mechanism is transcriptional repression of premitotic/mitotic CDKs. CDKB1;1 along with CYCA2;3, which form an active complex during the G2-M transition are down-regulated in leaves undergoing endoreduplication (Boudolf et al. 2009). Mitotic CDKs activity can also be down-regulated by APC-mediated proteolysis of A- and B-type cyclins, which are required for the functions of mitotic CDKs. CCS52, which is an APC substrate targeting subunit, plays a central role in promoting the transition into the endocycle by physical interacting with several A-type and B-type CYCs in *Arabidopsis* (Fülöp et al., 2005). This type of mechanism seems to be conserved among higher plants as elevated transcript levels of CCS52 were observed in endoreduplicating nodule cells in Medicago and its downregulation decreases cell size by altering the ploidy level (Cebolla et al., 1999). Another mechanism of CDKs inhibition is through direct binding to cyclin kinase inhibitors (CKIs). The SIAMESE-RELATED (SMR) family is a class of plant-specific CKIs that potentially targets both CDKA and CDKB. SIAMESE (SIM) is the founding member of the SMR family, which is required for endoreduplication in leaf trichomes. In *sim* recessive mutants, the endocycle is repressed in trichomes, resulting in multicellular trichomes with low ploidy level. This phenotype is strikingly different from wild-type trichomes, which are unicellular with a ploidy level of 16 to 32C (Churchman et al. 2006).

`

Maintaining endoreduplication cycle also requires a plant orthologue of archaeal topoisomerase VI, which belongs to type IIB subclass of type II topoisomerases in archaea and is composed of an A2B2 heterodimer complex with subunit A (topo VIA) and subunit B (topo VIB). In archaea, topoisomerase VI functions to decatenate replicated chromosomes. In plants, the mutation of topoisomerase VI components such as RHL1/HYP7, AtSPO11-3/RHL2/BIN5, AtTOP6B/RHL3/HYP6/BIN3, and MIDGET (MID) caused a dwarf phenotype, implying the structural requirements for endoreduplication in plants too (Sugimoto-Shirasu et al. 2002; Sugimoto-Shirasu et al. 2005; Hartung et al. 2002; Yin et al. 2002; Kirik et al. 2007). Bin4 is a DNA binding protein that functions as another component of the plant DNA topoisomerase VI complex through interaction with both AtSPO11-3/RHL2/BIN5 and RHL1/HYP7. The loss of Bin4 initiates various DNA damage repair processes by activating the expression of genes involved in the DNA damage response, thus leading to an early arrest of endocycles (Breuer et al. 2007).

Most of the factors identified in the regulation of the plant endocycle act at the entry point and how plants terminate endocycling is not well known. GT-2-LIKE1 (GTL1), a trihelix transcription factor was found to be involved in mediating endocycle termination in leaf trichomes. The GTL1 loss-of-function mutation leads to an additional round of endocycle and growth extension of trichomes without altering trichome branching (Breuer et al. 2009). Further study demonstrated that GTL1 directly represses the transcription of CCS52 to stop the endocycle progression, implying the important role of APC-mediated proteolysis in endocycle termination (Breuer et al. 2012).

`

Ploidy levels vary greatly among different species and cell types. High ploidy usually occurs in the cells with specialized differentiation such as leaf epidermal pavement cells, trichomes, and xylem cells or cells of high metabolic activity, such as endosperm cells (Sugimoto-Shirasu and Roberts 2003). In *Arabidopsis*, leaf epidermal pavement cells, trichomes, hypocotyls and roots often exhibit high ploidy level varying from 2C to 32C (Sonoda et al. 2009). Maize endosperm cells possess a DNA content as high as 96C or 192C (Kowles and Phillips 1985). Increased ploidy level is strongly correlated with cell growth, which supports the "nuclear-cytoplasmic ratio" theory that cytoplasmic growth is adjusted with respect to the DNA content of nucleus by a controlled mechanism (Sugimoto-Shirasu and Roberts 2003). However, it should be noted that uncoupling of cell growth from ploidy level has also been reported. One example involves *Arabidopsis* root cells from different ecotypes, which are varied in sizes but no correlation was found between cell size with ploidy level (Beemster et al. 2002). Thus, it was suggested that an increase in ploidy level may set the maximum capacity for cell growth instead of determining the exact level of cell growth with its contribution depending on the developmental context (Breuer, Ishida, and Sugimoto 2010; De Veylder, Larkin, and Schnittger 2011).

Cell Expansion

Cell growth occurs in both proliferating cells and expanding cells where the former grows by increasing cytoplasmic volume while the latter grows by increasing vacuolar volume (Kalve, De Vos, and Beemster 2014). Cytoplasmic growth is closely related to the energy and nutritional status of the cell as discussed previously while post-mitotic cell expansion is triggered by turgor pressure, which is generated by water uptake and pushes up against the cell wall, inducing wall loosening for stress relaxation. The extended cell

`

wall allows further water uptake and volume enlargement of the cell. Finally, biosynthesis and deposition of new wall materials is required to reinforce the stretched cell wall (Cosgrove 2014). The following cell wall related processes are involved in turgor driven cell expansion: first, cell wall hydration; second, cell wall loosening; third, synthesis and deposition of new cell wall materials.

Cell wall hydration is induced by acidification of apoplast and membrane hyperpolarization as a result of the activation of the P-type plasma membrane proton ATPase (AHA) in the presence of auxin or BR (Cleland 2010; Caesar et al. 2011). The increased hydration promotes the subsequent cell wall loosening, which refers to the cell wall modification that leads to relaxation of cell wall stress imposed by turgor pressure. There are four mechanisms of wall loosening which involve the following wall loosening agents: expansin, xyloglucan endotransglucosylase (XET), endo-(1,4)-β-d-glucanase (EGases) and hydroxyl radicals.

The plant primary cell wall is a complex structure with cellulose microfibrils embedded in a matrix of hemicelluloses, pectins and a small amount of proteins (Cosgrove, 2005). Expansins are small secreted proteins in the cell wall, which are thought to promote cell wall loosening by disrupting the hydrogen bonds between cellulose and the main hemicellulose called xyloglucan (XGs) (Cosgrove 2005). Plant expansins are a large superfamily with 36 and 58 members in *Arabidopsis* and rice, respectively and can be divided into four families: EXPA, EXPB, EXLA and EXLB. EXPA and EXPB families have been demonstrated to have the ability to extend cell wall and mediate cell expansion (Cosgrove 2005). For example, when *AtEXP10* was expressed maximally in the growing leaf, *Arabidopsis* had larger leaf blades and cells than the controls (Cho and Cosgrove

`

2000). *35S-AtEXP3* transgenic plants also showed better growth performance than the controls when they are allowed to germinate in the soil (Kwon et al. 2008).

Xyloglucan endotransglucosylase (XET) is part of a large family of xyloglucan endotransglucosylase/hydrolase (XTH). XET is capable of cutting pre-existing xyloglucans and grafting newly secreted xyloglucans. The role of XTH in the regulation of cell wall loosening is controversial as contradictory results were observed. Saladie *et al.* showed that the biomechanical properties of plant cell walls were not affected by incubation with tomato SlXTH5, in the presence or absence of xyloglucans (Saladié et al. 2006). However, Van Sandt *et al*. demonstrated that exogeneous XTH can act on isolated onion epidermis cell walls by significantly increasing cell wall extension (Van Sandt et al. 2007).

Endo-(1,4)-β-d-glucanase (EGase) induces wall loosening probably by digesting the non-crystalline parts of the cellulose, which releases xyloglucans from cellulose microfibrils (Cosgrove 2005). In *Arabidopsis*, the EGase gene family is composed of more than 20 members, which are divided into two groups: membrane-bound and wall secreted. Knockdown of the secreted EGase gene *CEL1* in *Arabidopsis* plants led to shorter stems and roots with abnormal cell wall deposition, which relates to defects in cell wall relaxation during cell expansion (Tsabary et al. 2003).

Hydroxyl radicals have been proposed as a cell wall loosening reagent by cleaving cell wall polysaccharides non-enzymatically based on the result that exogenous application of artificially generated hydroxyl radicals can induce cell wall extension in vitro (Liszkay and Schopfer 2003). A plasma membrane NADPH oxidase, which is activated by increasing cytoplasmic calcium as a result of opening calcium channels under cell wall

`

relaxation, can generate superoxide at the extracellular regions. The produced monovalent O_2 is further converted into hydrogen peroxide, which then forms hydroxyl radicals. The site-specific production of the hydroxyl radicals in the apoplast space can cleave polysaccharides present in the cell wall (Cosgrove 2005). Studies showed that auxin promotes the generation of hydroxyl radicals, which is required for inducing elongation growth of coleoptile in maize seedlings (Schopfer et al. 2002).

Biosynthesis and deposition of new cell wall materials is the final step in the cell expansion process to reinforce the thickness and strength of the loosened cell wall. While cellulose microfibrils are synthesized at the plasma membrane by a membrane localized cellulose synthase complex (CSC), hemicelluloses and pectins are generated in the Golgi apparatus and delivered to the cell wall through vesicles (Cosgrove 2005). CSC consists of cellulose synthase (CESA) proteins that are arranged into a rosette-shaped structure. In *Arabidopsis*, the CESA family contains 10 genes, of which CESA1, 3, and 6 are required for the primary cell wall synthesis while CESA4, 7 and 8 are required for the secondary cell wall formation (Taylor et al. 2003). KORRIGAN (KOR), which is a membrane-bound endoglucanase, is also required for the formation of cellulose microfibrils, as suggested by its mutant phenotype, which is a defect in crystallizing the synthesized (1,4)-linked β-D-glucan properly into microfibrils (Nicol et al. 1998). The CSC synthesizes the cellulose microfibrils along the cortical microtubule (CMT) arrays (Paredez, Somerville, and Ehrhardt 2006). Thus, the pattern of CMT arrangement can impact the deposition of the cellulose microfibrils, which will determine the direction of growth. For example, the abnormal CMT arrangement was found in *angustifolia (an)* leaf which exhibited reduced growth in the leaf width direction, suggesting that the plant CtBP family member AN might

`

regulate the polarity of cell expansion by modulating the CMT arrangement (Kim et al. 2002).

Compensation Mechanism: Organ-Wide Regulation

Compensation is a phenomenon in which enhanced/decreased post-mitotic cell expansion is associated with a decrease/increase in cell number during determinate organ development. It is a heterogeneous phenomenon that is governed by at least three mechanisms revealed by genetic and kinetic study of the compensation-exhibiting mutants (Ferjani et al. 2007; Ferjani et al. 2013). The first mechanism is the increase of the post-mitotic expansion rate with its duration unaffected while the second mechanism is the increase of duration with its rate unchanged. The third type of compensation, which is represented by a cyclin-dependent kinase KRP2, was reported to show larger cell size in proliferating cells and further increase in cell size by an enhanced post-mitotic expansion rate but not the period.

Compensation is triggered when the cell number is reduced below a certain threshold, which is suggested by mutants in which the cell number is decreased but not enough to induce compensation (Horiguchi and Tsukaya 2011). For example, compensation did not occur when single *oligocellula* (*oli*) mutants *oli2*, *oli5* and *oli7* had moderate reduction in their cell number. However, when cell number was further reduced in double mutants, compensation was induced (Fujikura et al. 2009). Compensation syndrome is also observed in mutants with more but smaller cells (Usami et al. 2009; Hur et al. 2015). These studies are suggestive of a monitoring system for cell number measurement existing during plant development but how it works remains to be elucidated.

`

The above observations demonstrate that altered cell proliferation serves as a trigger for compensation. Conversely, is there any possibility of an opposite type of compensation in which altered post-mitotic cell expansion affects cell proliferation in the same developing organs? So far there is no clear evidence supporting this possibility as none of the genes identified in compensation exhibiting mutants are known to have specific functions involved in post-mitotic cell expansion. Rather, observations in several mutants with altered cell expansion but normal cell number suggested that alteration of post-mitotic cell expansion may not influence cell proliferation (Hu, Poh, and Chua 2006; Kim et al. 2002; Qin et al. 2014). Further studies are needed in the future to gain insights into this possibility.

Compensation occurs in both cell-autonomous and non-cell-autonomous manners. In the cell autonomous mode of compensation, the seesaw-like relationship between cell proliferation and cell expansion occurs at a single cell level while in the non-cell-autonomous case, compensation occurs when the intercellular signal is generated and transmitted. These two modes of action were well illustrated by Kawade *et al.* (Kawade, Horiguchi, and Tsukaya 2010). It was shown that in KRP2 overexpressing chimeric leaves, only KRP2 overexpressing cells but not WT cells exhibit compensated cell expansion, indicating a cell-autonomous compensation. In *an3* chimeric leaves, not only *an3* mutant cells but also WT cells exhibit compensated cell expansion, indicative of a non-cell-autonomous compensation and cell-to-cell communication. In this situation, interesting questions such as what intercellular signals are generated and how the signal is transmitted remains to be explored to increase our knowledge regarding the coordination of cell proliferation and post-mitotic cell expansion.

`

Part II: The Regulation of Plant Salt Stress Response

Salinity is a major abiotic stress that causes substantial reduction in agricultural productivity in about 20% of the world cultivated lands (Rhoades and Loveday 1990). Low concentrations of salt have little or no effect on the yield of agricultural crops (Maggio et al. 2001). However, high salinity affects plants in two major ways. First, a water potential gradient between plant cells and the soil solution of high salt concentration results in the disturbance of water uptake by the roots. Second, intracellular accumulation of salts can be toxic to the plants as it inhibits enzymes and metabolic pathways (Munns and Tester 2008). As a consequence of these two primary effects, secondary effects often occur, such as oxidative stress due to the generation of reactive oxygen species (ROS) and nutrient imbalance as a result of competitive uptake of high levels of Na^+ and Cl^- (Lodeyro and Carrillo 2015). Taken together, these effects lead to reduction in plant growth and survival.

Over the time of acclimation to salinity, plants have evolved different types of adaptive mechanisms for salt tolerance, which will be briefly discussed in the forthcoming sections. It is worth noting that despite these tolerance mechanisms that plant has developed, crop yield is still decreased under salt stress, which is compounded by the increasing demand for food because of a rapidly expanding population (predicted to reach 9.6 billion by 2050, http://www.un.org/en/development/desa/news/population/un-report-world-population-projected-to-reach-9-6-billion-by-2050.html) and limited arable lands. In this context, a deeper understanding of salt tolerance mechanisms and engineering crops with candidate genes for enhancement of their salt tolerance ability is a very promising strategy to ameliorate these problems.

`

Na^+ Transporters and Plant Salt Tolerance

Excessive Na^+ accumulation in the cytoplasm is toxic to the plants. At the cellular level, plants have evolved three major mechanisms to prevent excessive cytoplasmic Na^+ accumulation: 1) restriction of Na^+ entry into the root cells, which is mediated largely by non-selective cation channels (NSCCs); 2) exclusion of Na^+ out of the cells, which is controlled by the plasma membrane localized Na^+/H^+ antiporter Salt Overly Sensitive 1 (SOS1, also known as AtNHX7 in *Arabidopsis*); and 3) compartmentalization of excessive Na^+ into the vacuoles, which is regulated mainly by the vacuolar Na^+/H^+ antiporter NHX. At the whole plant level, inhibition of Na^+ transport from root to the shoot through xylem or recirculation of Na^+ from shoot to the root through phloem is also crucial for salinity tolerance (Tester and Davenport 2003). Studies in *Arabidopsis* suggested that the class I High-affinity K^+ Transporter (HKT) plays an essential role in mediating Na^+ exclusion from leaves by removing Na^+ from xylem sap to root under salt stress, thus preventing Na^+ accumulation in leaves and maintaining their photosynthesis activity (Horie, Hauser, and Schroeder 2009).

NSCC transporters

NSCCs show a high preference for mediating passive fluxes of cations over anions through the plant membranes. They typically have a low selectivity among different monovalent cations and several of them are also permeable to divalent cations (Demidchik and Maathuis 2007; Pottosin and Dobrovinskaya 2014). The functions of NSCCs are well established on the basis of electrophysiological experiments but molecular studies are still lacking. A previous study suggested that NSCCs are primary mediators of Na^+ influx to the root cells (Demidchik and Tester 2002). This could be beneficial by decreasing tissue

`

osmotic potential but could also be toxic if excess Na^+ is not sequestrated (Shabala and Cuin 2008). It was suggested that NSCC may also play a role in mediating Ca^{2+} influx and K^+ efflux in *Arabidopsis* root epidermis cells (Demidchik et al. 2011).

SOS1 transporters

Na^+ efflux is another mechanism for eliminating Na^+ accumulation. It is mediated by the plasma membrane-localized Na^+/H^+ antiporter Salt Overly Sensitive 1 (SOS1), which is empowered by the function of plasma membrane H^+-ATPase. SOS1-mediated Na^+ efflux involves the SOS pathway, in which SOS3, sensing the cytosolic increase in $[Ca^{2+}]$ induced by excess Na^+ and high osmolarity, activates SOS2, a Ser/Thr protein kinase, to the plasma membrane where the SOS3-SOS2 protein complex phosphorylates and activates SOS1 (Qiu et al. 2002; Yamaguchi, Hamamoto, and Uozumi 2013). *SOS1* transcripts are predominantly expressed in epidermal cells at the root tip region and in xylem parenchyma cells at the root, leaf and stem (Shi et al. 2002). It was suggested that SOS1 not only functions in excluding Na^+ from root at the root-soil interface but also plays a role in mediating Na^+ efflux from the xylem vessels under severe salinity (Shi et al. 2002). Knockout of SOS1 in *Arabidopsis* led to greater Na^+ accumulation in the root, xylem sap and shoot under severe salt stress (100 mM NaCl) (Shi et al. 2002). Consistent with the phenotype of the *atsos1* mutant, overexpression of *SOS1* by the CaMV 35S promoter in *Arabidopsis* resulted in less Na^+ in the xylem stream and shoot, thus conferring salt tolerance (Shi et al. 2003).

Vacuolar Na^+/H^+ antiporters from NHX family

Another mechanism that plant cells employ to alleviate the excessive cytosolic Na^+ accumulation is to compartmentalize Na^+ into the vacuoles by vacuolar NHX transporters,

`

whose ion exchange activity is empowered by the electrochemical gradient created by the H^+-ATPase and H^+-pyrophosphatases (H^+-PPases) (Roy, Negrão, and Tester 2014). Constitutive overexpression of *AtNHX1* in *Arabidopsis* led to enhanced salt tolerance with a concomitant increase in Na^+ content (Apse et al. 1999). Recent studies have also shown that vacuolar NHX transporters are also important for K^+ uptake into vacuoles for turgor regulation and stomatal function (Barragán et al. 2012). Transgenic tomatoes overexpressing *AtNHX1* had more K^+ accumulation in vacuoles but no consistent increase in Na^+ accumulation was observed under salt stress. The greater capacity of the transgenic tomatoes to retain intracellular K^+ made them more salt tolerant when salt-shock was applied (Leidi et al. 2010). Besides the vacuolar NHX antiporters NHX1-4, a recent study by double knockout of endosomal NHX antiporters NHX5 and NHX6 in *Arabidopsis* suggested that endosomal NHX5 and NHX6 are also involved in salt tolerance in addition to their role in mediating cell growth and vesicular trafficking (Bassil et al. 2011).

HKT transporters

The identification of the first HKT transporter in wheat (*TaHKT2;1*) (Schachtman and Schroeder 1994) which is responsible for Na^+/K^+ transport has led to the identification of many HKT transporters from various plant species (Horie, Hauser, and Schroeder 2009). HKT transporters can be divided into two groups: the class 1 HKT transporters that mediate Na^+-selective transport and the class 2 HKT transporters that mediate both Na^+ and K^+ transport (Horie, Hauser, and Schroeder 2009; Deinlein et al. 2014). *AtHKT1;1* was identified as a class 1 HKT transporter in *Arabidopsis*, which is localized at the plasma membrane of xylem parenchyma cells (Horie et al. 2005). *AtHKT1;1* was suggested to be an important Na^+ influx system in root as *hkt1;1* knockout plants showed reduced

`

accumulation of Na^+ in the root and higher salt resistance in the short-term root growth assay (Mäser et al. 2002). The current model in *Arabidopsis* suggests that AtHKT1;1 may play a major role in protecting leaf blades from excessive accumulation of Na^+ by unloading of Na^+ from the xylem sap (Davenport et al. 2007). In support of this model, *hkt1;1* knockout plants exhibited higher Na^+ sensitivity with increased Na^+ accumulation in the leaf in a long-term growth assay (Mäser et al. 2002). Moreover, overexpression of *AtHKT1;1* in mature root stele led to improved salt tolerance by decreasing root-to-shoot transfer of Na^+ (Møller et al. 2009). Interestingly, *Arabidopsis* plants constitutively overexpressing *AtHKT1;1* driven by CaMV 35S promoter accumulated more Na^+ in the leaves and displayed salt sensitivity probably due to the increased influx of Na^+ into the roots (Møller et al. 2009). Thus, cell type-specific overexpression of *HKT1;1* is essential to improve salinity tolerance.

Compatible Solutes and Osmotic Adjustment

Plant response to the osmotic effect of salt stress lies in osmotic adjustment. One low energy-cost way to achieve this is to accumulate Na^+ and Cl^- ion in the vacuoles as cheap osmolytes. However, it also increases the risk of enhanced accumulation of toxic ions in the cytoplasm. Another way is *de novo* synthesis of compatible solutes (Shabala and Cuin 2008). Compatible solutes are a class of organic compounds that can accumulate to a high concentration without interfering with metabolic pathways because of their compatibility with metabolism (Lodeyro and Carrillo 2015). They are comprised of nitrogen-containing compounds, such as free amino acids (proline), quaternary ammonium compounds (glycine betaine), and polyamines; soluble sugars such as glucose, fructose, sucrose and raffinose; and sugar alcohols such as mannitol, sorbitol, myo-inositol, ononitol

`

and pinitol (Munns 2005a). Besides their role in providing osmotic protection and attenuating water loss, these compounds also serve other functions, such as stabilizing proteins and membrane structures (Lodeyro and Carrillo 2015), and scavenging ROS such as hydroxyl radical ($OH^{\cdot}$) which cannot be efficiently detoxified by enzymes (Bose, Rodrigo-Moreno, and Shabala 2014).

Antioxidative Defense Mechanism

Salt stress can disrupt the balance of cellular metabolism, resulting in oxidative stress with elevated level of reactive oxygen species (ROS). ROS mainly comprises of free radicals like the superoxide radical anion ($O_2^{\cdot -}$) and hydroxyl radicals ($OH^{\cdot}$) and non-radicals like hydrogen peroxide (H_2O_2) and singlet oxygen($^1O_2$). ROS acts as a double edged sword as on one hand, it acts as a secondary messenger under salt stress; on the other hand, it can cause oxidative damage to protein and membrane lipid peroxidation, DNA and RNA damage (Das and Roychoudhury 2014). Plants have developed two antioxidant defense systems to work in concert for ROS scavenging, and these include both enzymatic and non-enzymatic machinery. The major enzymatic antioxidants include catalase (CAT), superoxide dismutase (SOD), ascorbate peroxidase (APX), glutathione peroxidase (GPX), glutathione reductase (GR), monodehydroascorbate reductase (MDHAR), and dehydroascorbate reductase (DHAR) while the major non-enzymatic antioxidants include ascorbic acid (AA), glutathione (GSH), phenolic compounds, etc. (Gill and Tuteja 2010; Das and Roychoudhury 2014).

Salt Signaling and Regulatory Pathways

To mount various effective responses under salt stress, plants have developed a stress signaling pathway in which the stress signal of the hyperosmotic component and Na^+

`

ion is perceived/sensed, which results in the generation of many secondary messengers, such as Ca^{2+}, ABA and ROS. The stress signal is then transduced downstream with the involvement of many proteins such as protein kinases and transcription factors, resulting in a change of stress-responsive gene expression and ultimately leading to physiological responses (Deinlein et al. 2014; Wang et al. 2016). So far, the identities of sensors for hyperosmotic component and Na^+ ion still remained elusive. It was speculated that hyperosmotic stress is sensed by a mechanically gated Ca^{2+} channel on the basis of the following evidence: first, interfering with cuticle development which provides structural support to the cell affected many osmotic-induced responses, such as ABA production (Wang et al. 2011); second, cytosolic Ca^{2+} levels increase rapidly (within seconds) in response to NaCl or mannitol treatment (Knight, Trewavas, and Knight 1997). Although how salt stress is sensed is still largely unknown, substantial progress has been made in dissecting the Ca^{2+} signaling pathway, ABA-dependent and -independent signaling pathways and transcriptional regulation during salt stress response.

Ca^{2+} signaling pathway

Ca^{2+} is a very important second messenger in response to a wide range of external stimuli. The nature and the intensity of different external stimuli can be distinguished by specific Ca^{2+} signatures such as amplitude and duration (Bartels and Sunkar 2005). High salinity causes a rapid and transient increase in cytosolic Ca^{2+}. The Ca^{2+} signal is further decoded by Calcineurin B-like protein (CBL)-CBL-interacting protein kinase (CIPK) complex, which can activate Na^+ transporters including the plasma membrane Na^+/H^+ antiporter SOS1 and vacuolar Na^+/H^+ antiporter NHX to maintain cytosolic Na^+ homeostasis (Manik et al. 2015; Tuteja 2007).

`

ABA-dependent and -independent signaling pathways

ABA biosynthesis and accumulation are induced by osmotic stresses, including drought, high salinity or cold stress. ABA produced in roots in response to osmotic stress is transported to the leaves through the xylem. ABA can also be synthesized in leaf cells under water-deficit conditions and distributed around the plant (Chaves, Flexas, and Pinheiro 2009). It was suggested that the ABA signal can be perceived by different cellular receptors and elicit specific cellular responses (Golldack et al. 2014). Under osmotic stress, the ABA signal is perceived intracellularly by Pyrabactin Resistance1/PYR1-like/Regulatory Components of ABA Receptors (PYR1/PYL/RCARs) receptors, which inhibit type 2C phosphatases (PP2Cs) such as ABI1 and ABI2 (Ma et al. 2009; Park et al. 2009). The inactivation of PP2Cs activates their downstream targets, such as the sucrose nonfermenting 1-related protein kinase 2 (SnRK2) (Vlad et al. 2009; Umezawa et al. 2009). SnRK2 regulates the ABA-responsive element binding protein/factors (ABRE/ABFs), which belongs to a distinct subfamily of bZIP transcription factors (TFs) and other TFs such as myelocytomatosis oncogene (MYC) and myeloblastosis oncogene (MYB) for regulation of ABA-responsive gene expression (Nakashima and Yamaguchi-Shinozaki 2013). In guard cells, this ABA signaling cascade impedes stomatal opening and induces stomatal closure through regulation of ion fluxes in Ca^{2+} dependent and independent pathways (Jacob et al. 1999). Moreover, it also mediates transcriptional reprogramming for the expression of osmotic tolerance proteins, such as Late Embryogenesis Abundant (LEA) proteins (Nakashima and Yamaguchi-Shinozaki 2013).

Gene expression in response to osmotic stress is also regulated by an ABA-independent signaling pathway. Dehydration-responsive element binding protein 2

`

(DREB2) transcription factors play a pivotal role in ABA-independent gene expression regulation in response to osmotic stress (Yoshida, Mogami, and Yamaguchi-Shinozaki 2014). Recent studies have shed light on the crosstalk between the ABA-dependent and ABA-independent pathways. DREB2A promoter regions contain an ABRE motif and ChIP analyses have demonstrated that DREB2A is regulated by ABF2, ABF3, ABF4 under osmotic stress (Kim et al. 2011). Moreover, DREB1A and DREB2A were shown to interact with ABF2 while DREB2C was shown to interact with ABF2, ABF3 and ABF4 (Lee et al. 2010). By contrast, transcriptional regulation of AREB/ABFs is not well understood.

Evidence has been emerging that ABA-mediated abiotic stress response is linked and integrated with GA-mediated developmental signaling. GA stimulates growth by 26S proteasome–dependent degradation of DELLA (Fu et al. 2004). ABA treatment on wild-type roots but not *abi1-1* roots increased the accumulation of DELLAs and consequently induced growth inhibition. The quadruple DELLA mutant with functional losses of GAI, RGA, RGL1, and RGL2 is more resistant to the inhibitory effects of ABA. These results suggest that ABA-mediated growth inhibition is at least in part advanced by means of enhancement of DELLA restraint (Achard et al. 2006).

Transcription regulation of salt stress response

In the past decades, considerable progress has been made to identify and characterize various transcription factors (TFs) in plant response to abiotic stress and to engineer these TFs to enhance plant stress tolerance in model and crop species (Wang et al. 2016). These TFs mainly include AREB/ABF, AP2/EREBP (such as DREB and ERF), MYB, WRKY, etc, functioning in either an ABA-dependent or ABA-independent manner.

`

AREB/ABF

AREB/ABF TFs are major transcriptional regulators modulating ABA-responsive gene expression by binding to the ABA-responsive *cis*-element (PyACGTGG/TC) in the promoter region of the target genes (Joshi et al. 2016). AREB/ABF TFs have a bZIP domain and four SnRK2 phosphorylation sites, which are activated upon phosphorylation by SnRK2 in a ABA-dependent manner (Fujita et al. 2011).

DREB

DREB TFs belong to the APETALA 2/Ethylene-responsive Element Binding Proteins (AP2/EREBPs) superfamily, which is defined by the presence of a AP2 DNA binding domain (Riechmann and Meyerowitz 1998). The AP2/EREBPs superfamily also includes AP2, RAV, ERF and other TFs (Sakuma et al. 2002). The DERB subfamily can be further classified into two major groups: DREB1 and DREB2, which regulate the expression of many stress-responsive genes mostly in an ABA-independent manner by binding to the Dehydration-responsive Element/C-Repeat Responsive Element (DRE/CRT) cis-element present in the promoter region of various stress-responsive genes (Lata and Prasad 2011). In *Arabidopsis*, the DERB1 subgroup consists of six proteins, which are involved in plant response to drought, salt, cold and freezing stress (Lata and Prasad 2011; Wang et al. 2016). For example, overexpression of *OsDREB1A* in rice led to enhanced tolerance to drought, high salinity and low temperatures, although the growth of transgenic plants was retarded under normal growth conditions (Dubouzet et al. 2003). The DREB2 subgroup consists of eight proteins, which are involved in drought, salt and heat response (Wang et al. 2016; Lata and Prasad 2011). DREB2A and DREB2B are two major players under osmotic stress. Overexpression of AtDREB2A did not lead to any phenotypic

`

changes in *Arabidopsis* in the aspects of growth and stress tolerance, implying the requirement for post-translational modification for its activity (Liu et al. 1998). Following this up, overexpression of AtDREB2A-CA, which is a constitutively active form with the deletion of a negative regulatory domain within AtDREB2A, resulted in growth inhibition and higher drought tolerance with up-regulation of many stress-inducible genes in *Arabidopsis* (Sakuma et al. 2006).

MYB

MYB TFs function in many physiological and biochemical processes, such as development, metabolism and plant response to abiotic and biotic stresses (Ambawat et al. 2013; Dubos et al. 2010). MYB TFs that are active in abiotic stress signaling are well documented (Li, Ng, and Fan 2015). Studies show that a single MYB TF can regulate a diversity of target genes, thus impacting various processes under abiotic stress. For example, studies of a ABA-responsive MYB TF, MYB96 in *Arabidopsis* showed that it can activate cuticular wax biosynthesis for drought resistance (Seo et al. 2011). Moreover, AtMYB96 can also activate the transcription of the lipid-transfer protein LTP3 for plant tolerance to drought and freezing stress (Guo et al. 2013).

WRKY

Previous studies have demonstrated that WRKY TFs are involved in various abiotic stresses such as drought, salt, cold, heat, nutrient starvation, UV radiation, high light and oxidative stresses, which have been extensively reviewed recently (Banerjee and Roychoudhury 2015).

`

In addition to the above-mentioned TFs, there are other TF families that are involved in plant response to multiple abiotic stresses, such as basic leucine zipper (bZIP) TFs, NAC TFs, heat shock TFs (HSFs), basic helix-loop-helix (bHLH) TFs, and homeodomain-leucine zipper (HD-Zip) TFs. It was suggested that these TFs not only function independently but also interact with each other by regulating common downstream targets (Wang et al. 2016).

Salt Tolerance Mechanisms in Halophytes

Plants exhibit significant variations in their abilities to tolerate salinity. About 1% of the plant species named halophytes can survive and thrive under conditions with above 200 mM NaCl (Flowers and Colmer 2008). It has been proposed that different mechanisms at the molecular and physiological levels work in concert for salinity tolerance in halophytic plants (Kosová, Prášil, and Vítámvás 2013; Zhang and Shi 2013).

It was suggested that three mechanisms contribute to high salinity tolerance in halophytes at the molecular level (Kosová, Prášil, and Vítámvás 2013). First, halophytic plants may possess higher copy number of salt-tolerant genes at their genome. For example, Genome sequencing of *Thellungiella parvula*, which is related to *Arabidopsis thaliana* and is endemic to saline environment revealed that *Thellungiella parvula* genome contains higher gene copy number of several genes related to salt stress adaptation than *Arabidopsis thaliana*, such as AVP1 and NHX8 (Dassanayake et al. 2011). Second, halophytic plants may have subtle gene expression at the transcriptomic level in both qualitative and quantitative ways. For example, a comparative transcriptome study of a salt-tolerant rice cultivar Pokkali and a salt-sensitive rice cultivar IR64 suggested that a higher expression of a set of salt stress responsive genes such as V-ATPase and GST in Pokkali than IR64

`

may contribute to higher salinity tolerance in Pokkali (Kumari et al. 2009). Third, halophytic plants may have higher activity levels for proteins involved in salt stress response. A few studies comparing the proteomic response to salt stress between related plant species with different levels of salt tolerance have been published (Pang et al. 2010; Sengupta and Majumder 2009). Two-dimensional gel electrophoresis (2-DE) coupled with mass spectrometry (MS) has enabled the identification of protein spots showing differential abundance. Functional analysis of these proteins needs to be conducted to unravel their roles in conferring salinity tolerance.

At the physiological level, halophytes have also developed different mechanisms for salinity tolerance and different types of halophytes may utilize specific mechanisms for adaptation to their habitats. Three different mechanisms at the physiological level will be discussed briefly below. In salt-accumulating halophytes, such as plants from the genus of *Suaeda*, vacuole compartmentalization is a primary mechanism for salinity tolerance. Under NaCl treatment, the increased activity of vacuolar Na^+/H^+ antiporters and V-H^+-ATPase was observed in the leaves of *Suaeda salsa* (Qiu et al. 2007). *Suaeda salsa* also possesses an effective anti-oxidative defense system in chloroplasts which scavenges superoxide radicals in situ, reducing oxidative damage caused by NaCl (Qiu-Fang et al. 2005). Salt-excluding halophytes, such as an *Arabidopsis thaliana* relative *Thellungiella halophila* from the genus of *Thellungiella*, accumulate less Na^+ and more K^+ in both shoot and root thus maintaining a higher K^+/Na^+ ratio compared to *Arabidopsis thaliana* under salinity stress, resulting in higher salinity tolerance (Volkov et al. 2004). In salt-secreting halophytes, such as mangrove plants, salt excretion is considered to be an essential contributor to high salinity tolerance. Salt excretion is mediated by specialized tissues such

`

as salt glands and salt hairs for halophytes in arid areas, which are responsible for excreting excessive Na^+ onto the leaf surface (Zhang and Shi 2013).

Part III: The Objectives of the Current Research

The regulation of plant development and stress response are two major research areas in the field of plant biology that have captured a lot of attention and achieved fruitful accomplishments in the past. Understanding the mechanisms underlying plant development and stress response has significant practical meanings in the context of rapidly expanding human populations and changing environment, such as sea level rise due to global warming. Genes that are involved in the regulation of plant organ growth and stress response are good candidates to engineer crops for enhanced yield as the former has the potential to alter plant architecture improving production and the latter can help enhance plant stress tolerance and maintain yield where unfavorable environmental conditions exist. However, the genetic basis underlying plant development and response to environmental stresses including high salinity has not been completely deciphered. For a better understanding of the genetic control of plant development and salt stress response, my dissertation research focuses on the following two projects. One is functional characterization of a novel Myb-like gene in plant development; another is comparative study of two cultivars Supreme (high salt-tolerance) and Parish (moderate salt-tolerance) from a halophyte named Seashore paspalum at the physiological and transcriptomic levels to better understand plant salt tolerance mechanisms and identify potential candidate genes for future molecular studies.

`

CHAPTER TWO

DRMY1, A NOVEL MYB-LIKE TRANSCRIPTION FACTOR REGULATES CELL EXPANSION DURING PLANT DEVELOPMENT AND AFFECTS SEED PRODUCTION IN *ARABIDOPSIS*

`

Abstract

Plant organ development depends on the coordination of cell proliferation and cell expansion. Although many genetic factors have been identified for organ development, the underlying mechanism especially for cell expansion is still largely unknown. Here we identify a novel Myb-like protein, Development Related Myb-like1 (DRMY1), which controls cell expansion during development of both vegetative and reproductive organs, and affects fertility in *Arabidopsis thaliana*. The loss-of-function mutant *drmy1* leads to reduced organ growth and cell expansion, which is associated with increased accumulation of cell wall matrix polysaccharides. We demonstrate that *DRMY1* is strongly expressed in developing organs and vascular tissues and its expression is reduced by the plant hormone ethylene while induced by Abscisic Acid (ABA). Furthermore, DRMY1 is localized in the nucleus but itself alone does not confer transactivation activities. Transcriptome analysis reveals that DRMY1 may control cell expansion directly by regulating the expression of genes involved in cell wall biosynthesis/remodeling as well as genes encoding for ribosome proteins. DRMY1 also regulates the expression of genes in ethylene and ABA signaling pathways, indicating that it may control cell expansion indirectly via hormone signaling pathways. Our results suggest that DRMY1 plays a vital role in organ development by regulating cell expansion either directly or indirectly through ethylene and ABA signaling pathways.

Introduction

Plant organ development is regulated by genetic programs as well as the developmental and environmental cues, such as hormones, light, temperature and nutrients (Chaiwanon et al. 2016). Plant organ growth to its characteristic size and shape occurs

`

through two successive but overlapping processes: cell proliferation and cell expansion, increasing cell number and cell size, respectively (Gonzalez, Vanhaeren, and Inzé 2012; Hepworth and Lenhard 2014; Powell and Lenhard 2012; Kalve, De Vos, and Beemster 2014). Cell proliferation is tightly controlled by plant cell cycle machinery composed of the catalytic cyclin-dependent kinases (CDKs) and the regulatory cyclins (CYCs) that control CDK activity. Different CDKs-CYCs complexes phosphorylate an array of substrates, ensuring correct DNA replication and successful progression through different phases of the cell cycle (Komaki and Sugimoto 2012). Cytoplasmic growth is coupled with cell proliferation to maintain cells at a constant cell size while proliferating. It mainly relies on macromolecular biosynthesis, mostly proteins, which is an energy-consuming process and is tightly linked to the nutritional and energy level of plants (Sablowski and Dornelas 2014). Target of Rapamycin (TOR) is a central regulator of cytoplasmic growth by sensing and integrating the nutritional conditions and different developmental and environmental signals into growth decisions in order to maintain survival under the available resources (Zhang, Persson, and Giavalisco 2013). As cytoplasmic growth mainly relies on protein biosynthesis, the biogenesis of ribosomes as a translational machinery is essential for cell growth. Ribosomal proteins are known for playing a fundamental role in ribosome assembly and protein translation. Recent studies also highlighted their functions in many aspects of plant development (Byrne 2009; Micol 2009). Deficiency in specific r-proteins causing developmental abnormalities with change in leaf shape have most frequently been reported (Byrne 2009; Micol 2009). For instance, *Arabidopsis* with mutations in PGY genes, PGY1, PGY2, and PGY3, which correspond to ribosome protein L10a, L9, and L5,

`

produced pointed and narrow rosette leaves with more pronounced marginal serrations than wild type (Pinon et al. 2008).

Cell proliferation to cell expansion transition then takes place progressively in a basipetal manner though cells committed to stomata and vascular lineage continue to divide (Powell and Lenhard 2012). Several mutants that are defective in this transition exhibited altered final leaf size, such as *angustifolia 3* and *aintegumenta*, suggesting its important role in regulating organ size (Horiguchi, Kim, and Tsukaya 2005; Mizukami and Fischer 2000). Post-mitotic cell expansion is a complex process which is triggered by turgor pressure and followed by cell wall remodeling and deposition of newly synthesized wall materials (Cosgrove 1993). Given the fact that plant cells are surrounded by cell walls, it is not surprising that alterations in cell wall content and organization affect cell size and shape. Such alterations are mediated by proteins involved in cell wall biosynthesis (such as cellulose synthase (CESA) proteins), deposition (such as microtubules and microtubule-associated proteins), or remodeling (such as expansins, Xyloglucan Endotransglucosylase/Hydrolases (XTHs), Endo-β-1, 4-glucanases (EGases) and Pectin Methylesterases (PMEs)) (Cosgrove 2005). However, the mechanistic evidence regarding their transcriptional regulation remains largely unknown, making cell expansion a much more elusive process than cell proliferation. Cell expansion is often accompanied by ploidy increase through endoreduplication, which occurs through successive rounds of DNA replication without mitosis. However, there is evidence that ploidy level is often but not always associated with cell size (Sugimoto-Shirasu and Roberts 2003).

Cell expansion in plants is modulated by different plant hormones via their specific or cross-talk pathways. For instance, brassinosteroid (BR) plays an important role in

`

controlling polar cell expansion during organ development. BR deficient mutant *rotundiolia 3* (*rot3*) and BR insensitive mutant *brassinosteroid-insensitive 1* (*bri1*) exhibited a defect in cell expansion in the leaf-length direction (Kim et al. 2005; Clouse, Langford, and McMorris 1996). Ethylene also functions as an important modulator of cell expansion. The constitutive ethylene response mutant *ctr1* produced smaller rosette leaves with a reduction in the size of epidermal cells, protruding gynoecium out of the unopened bud and infertile early flowers. Leaf epidermal cells from ethylene-treated WT plants were also smaller than those from air-grown WT plants, indicating that ethylene inhibits cell expansion (Kieber et al. 1993). Overexpression of an ethylene-induced gene *RhNAC100* in *Arabidopsis* significantly reduced the petal size by inhibiting cell expansion, suggesting a negative role of ethylene in cell expansion (Pei et al. 2013). Ethylene also inhibits primary root length by reducing cell elongation (De Cnodder et al. 2005) (Růžička et al. 2007; Swarup et al. 2007). Despite the general view of ABA as a growth inhibitor, paradoxically there are a number of studies showing its stimulatory effect on cell expansion and organ growth (Humplík, Bergougnoux, and Van Volkenburgh 2017). In tomato, ABA-deficient mutants *flacca (flc)* and *notabilis (not)* showed inhibited leaf and stem growth. The stunted growth persisted when they were grown under well-watered conditions but can be restored by treatment of exogenous ABA, suggesting that ABA is required to maintain shoot growth, independently of its effects on water balance in plants (Sharp et al. 2000). In *Arabidopsis*, the ABA-deficient mutant *abscisic acid deficient 1* (*aba1*) is characterized by reduced size of rosette leaves, inflorescence and flowers. The reduced growth of rosette leaves is due to a decreased cell size, which can be improved by exogenous application of ABA with low concentrations (up to 50 nM). Moreover, low concentrations of exogenous ABA increase

`

the mesophyll cell size of WT plants (Barrero et al. 2005), revealing a positive role for ABA in cell expansion during organogenesis. The *Arabidopsis* ABA-deficient mutant *abscisic acid deficient 2* (*aba2*) exhibited severe growth defects in all vegetative organs and siliques in the absence of exogenous sugars and stress conditions, which is another important piece of evidence suggesting the role of ABA as a growth stimulator (Cheng et al. 2002).

In the *Arabidopsis thaliana* genome, there are 197 Myb family members. They are characterized by the presence of a Myb DNA-binding domain (DBD) that contains three α-helices. The second and third helices which form a helix-turn-helix structure are responsible for interaction with the major grooves of DNA (Ogata et al. 1994). Myb family proteins are classified into four major groups according to the number of Myb DBD present within the sequence, namely 1R-Myb/Myb-like, which usually but not always contain one Myb repeat, R2R3-Myb, R1R2R3-Myb and 4R Myb (Katiyar et al. 2012; Yanhui et al. 2006). R2R3-Myb proteins are most extensively studied in *Arabidopsis*. They are involved in many biochemical and physiological processes, including primary and secondary metabolism, developmental processes, cell differentiation and defense responses (Dubos et al. 2010). Compared with R2R3-Myb proteins, Myb-like proteins are not well characterized. The first plant Myb-related protein (StMyb1) was isolated from potato. It has a Myb-like motif in the central region of the protein that confers DNA binding specificity and a C-terminal proline-rich region that functions as a transcriptional activation domain (Baranowskij et al. 1994). Functions of Myb-like proteins were then assigned for circadian clock control, such as CIRCADIAN CLOCK ASSOCIATED1 (CCA1) and LATE ELONGATED HYPOCOTYL (LHY) (Alabadí et al. 2002; Mizoguchi et al. 2002;

`

Schaffer et al. 1998; Wang and Tobin 1998); epidermal cell differentiation, such as CAPRICE (CPC) (Wada et al. 1997); trichome patterning, such as TRIPTYCHON (TRY) (Pesch and Hülskamp 2011); telomeric DNA binding, such as AtTBP1 (Hwang et al. 2001); and controlling cell expansion by regulating ROS homeostasis, such as KUODA1 (Lu et al. 2014).

To better understand the underpinnings of cell expansion during organ development, here we identify a novel Myb-like protein, Development Related Myb-like1 (DRMY1), which controls growth of both vegetative and reproductive organs by regulating cell expansion, and affects seed production. By performing RNAseq, we hypothesized that DRMY1, possibly through interaction with other transcription factors, may regulate cell expansion either directly through regulating cell wall biosynthesis/remodeling and ribosome biogenesis or indirectly through ethylene and ABA signaling cascades to set the final size and shape of the organ.

Methods

Plant materials and growth conditions

The *Arabidopsis thaliana* ecotype Columbia-0 (Col-0) was used as the wild type (WT) in this study. The *drmy1* T-DNA insertion mutant (SALK-012746) was obtained from Arabidopsis Biological Resource Center (ABRC) stock center. Seeds were planted in commercial nutrient-rich soil (3-B Mix, Fafard) and synchronized in darkness at 4℃ for three days before transferring to the growth chamber with photoperiod (16h, 22℃/8h, 20℃) and illumination of 100 μmol/m^2/s. Fully expanded fifth leaves in 36-day-old plants were used to characterize the leaf phenotype. Bolting time was measured as the date when the inflorescence stem elongated by 1cm while flowering time was measured as the date when

`

the first flower opens. Flower buds and mature flowers from the primary inflorescence stem were used for observation of the flower phenotype. 45-old-day plants were used for measurement of seed production while 7-week-old plants were used for measurement of plant height. For phenotypic analysis of primary root length and lateral root number, sterilized seeds were plated on half-strength Murashige and Skoog (MS) medium supplemented with 1% sucrose and 0.6% agar and chilled in 4℃ for three days to synchronize germination before growing vertically in the growth chamber under the conditions described above. 1-week-old *Arabidopsis* seedlings were used for measurement of primary root length. Lateral root number was measured by counting the lateral root number emerged from the primary root in 10-day-old *Arabidopsis* seedlings.

Cytological analyses

To assess the contribution of cell number and cell size to the organ size, fully expanded fifth leaves were excised and placed in a destaining solution (75% ethanol and 25% acetic acid). After infiltration for 1 h and staying at room temperature for at least 24 h, the destaining solution was exchanged with the basic solution (7% NaOH in 60% ethanol) for 15-20 min at room temperature followed by rehydration via an ethanol series (40, 20, and 10%) for 10-15 min at each step. After infiltration for 30 minutes in 25% glycerol (vol/vol) diluted in 5% ethanol, leaves were finally mounted in 50% glycerol and imaged under the microscope (MEIJI EMZ-5TR, Meiji Techno, Japan) (Yang, Wang, et al. 2014). The palisade cells at the central region beside leaf mid-vein were photographed to determine cell number and cell size. The total cell number per leaf was estimated as the product of total leaf area and average cell number per unit area. Average cell size was measured with ImageJ software (http://rsb.info.nih.gov/ij/).

`

For observation of leaf adaxial epidermal cells and flower stigmatic papillae, leaves and flowers were fixed at FAA fixation solution (50% ethanol 89 ml, glacial acetic acid 6 ml, formaldehyde 5 ml) for at least 24 h. They were then dehydrated through an ethanol series (70, 80, 90, 95 and 100%) for 15 min at each step followed by CO_2 critical point drying in a K850 critical point drier (Quorum Technologies, UK), coated with Platinum in an HUMMER 6.2 sputtering system (ANATECH LTD, US), and then examined with a Variable-Pressure Scanning Electron Microscope S-3400N-2 (Hitachi, Japan).

To detect fluorescence of DRMY1 tagged with GFP using Confocal Laser Scanning Microscope (CLSM), WT (negative control), *35S-GFP* transgenic plants (positive control) and *35S-DRMY1-GFP* transgenic plants were grown on half-strength MS media for 4-5 days with the bottom of the petri dish wrapped with aluminum foil to avoid fluorescence quenching by light. Roots were mounted under a coverslip with 20 µg/ml DAPI and photographed using the Leica TCS SPE confocal microscope with the following settings: laser excitation at 488 nm and a 505–550 nm emission filter for GFP; laser excitation at 358 nm and a 461nm emission filter for DAPI.

Pollen tube growth assay

Transgenic pollen harboring *lat52-GUS* was manually applied to WT and *drmy1* stigma at flower stage 13 (Smyth, Bowman, and Meyerowitz 1990). After 24 h, WT and *drmy1* pistils were excised and mounted on double-sided tape to remove the ovary walls under the microscope (MEIJI EM-5, Meiji Techno, Japan). They were then immediately placed in a microcentrifuge tube containing 80% acetone overnight to fix cells and remove chlorophyll. WT and *drmy1* pistils were then incubated in X-Gluc solution (2 mM 5-bromo-4-chloro-3-indolyl β-D-glucuronide, 2 mM ferrocyanide, 2 mM ferricyanide, 0.2%

`

TritonX in 50 mM phosphate buffer, pH 7.2) at 37°C overnight. They were cleared in 70% ethanol, mounted under a coverslip with 50% glycerol and imaged under the microscope (MEIJI EM-5, Meiji Techno, Japan).

Plasmid construction and plant transformation

For construction of the *DRMY1* genomic DNA construct, genomic *DRMY1* including 2296bp of 5'UTR sequence, 4282bp of exons and introns, and 1145bp of 3'UTR sequence was cloned into pGEM-T Easy vector (Promega) and sequenced. The genomic *DRMY1* fragment was then subcloned into the binary vector, p35S-*bar*. For the pDRMY1-*GUS* construct, a 3.6 kb genomic fragment from the *DRMY1* promoter was cloned into pGEM-T Easy vector and sequenced. The promoter sequence was then subcloned upstream of *GUS* gene in the binary vector, p35S-*bar/GUS*. To generate the *DRMY1-GFP* fusion construct, the *DRMY1* coding sequence without the stop codon was amplified from cDNAs by RT-PCR, ligated into the pGEM-T Easy vector and sequenced. *DRMY1* was then subcloned into the pCambia binary vector, p35S-C4ppdk1-*sGFP*(S65T)/p35S-*hptII*, in frame upstream of *sGFP* (S65T). For the *DRMY1* overexpression construct, p35S-*DRMY1*/p35S-*hptII*, *DRMY1* coding sequence was amplified from cDNAs by RT-PCR, ligated into the pGEM-T Easy vector and sequenced, and was then subcloned into the pCambia vector. Primers used for generation of the above constructs are listed in Supplemental Table A-1. The generated constructs were transformed into *Agrobacteria tumefaciens* strain LB4404 by electroporation. Floral dip method was used for *Arabidopsis thaliana* transformation as described previously (Clough and Bent 1998).

Sequence alignment and phylogenetic tree construction

`

The full-length amino acid sequences of DRMY1 and its paralog named DRMY1 Paralog 1 (DP1) were obtained from the Arabidopsis Information Resource (TAIR) database. Sequence alignment of DRMY1 and DP1 full-length amino acid sequences was performed with the MultAlin software with default settings (Corpet 1988). The conserved domain of DRMY1 and DP1 was predicted using NCBI Conserved Domains Database (Marchler-Bauer et al. 2011). The BLAST tool in The Universal Protein Resource (Uniprot) database was used to search for proteins possessing similar domain with DRMY1 and DP1 (Consortium 2017). Sequence alignment of DNA binding domains was conducted using Clustal Omega software with default settings (Goujon et al. 2010; Sievers et al. 2011). To elucidate the phylogenetic relationships among DRMY1 and its homologous proteins from land plants, full-length amino acid sequences of DRMY1 were blasted against non-redundant (nr) protein database in NCBI. Proteins with similarity > 40% were retained and aligned with BioEdit software (Hall, 1999). Phylogenetic tree was constructed by the Maximum Likelihood method in MEGA 6 using 1,000 bootstrap replicates (Tamura et al. 2013).

Histochemical *β*-Glucuronidase (GUS) staining

GUS activity was assayed by histochemical staining with X-Gluc solution. Plant samples immersed in X-Gluc solution were vacuum infiltrated for 1 h, followed by incubation at 37°C overnight in the dark and then cleared in 70% ethanol and imaged under the microscope (MEIJI EM-5).

Hormone treatment and gene expression analysis

For the hormone treatment, nine-day-old seedlings grown on half-strength MS solid medium were transferred to half-strength MS liquid medium containing GA_3 (100 μm),

`

IAA (5 μm), ACC (5 μm), BL (1 μm) or ABA (50 μm) as previously reported (Qin et al. 2014). Samples were collected after 3-h treatment.

Total RNA was isolated from 100 mg of plant materials using Trizol reagent (Invitrogen) following the manufacturer's guided protocols. After digestion with DNaseI, RNA was reverse transcribed into first strand cDNA with ProtoScript II Reverse Transcriptase (Biolabs) and oligo (dT) primers for subsequent RT-PCR or real-time quantitative PCR (qRT-PCR) analysis.

qRT-PCR was performed with SYBR Green Supermix (Bio-Rad) according to the manufacturer's guided protocols. *AtACTIN2* was used as an endogenous control for qRT-PCR analysis. The relative gene expression change was calculated based on the $2^{-\Delta\Delta CT}$ method (Livak and Schmittgen 2001). The experiments were conducted with two biological replicates (three technical replicates each). Primers used for expression analysis are shown in Supplemental Table A-1.

Transactivation assay in yeast

The transactivation assay was performed according to the method previously described (Yang, Li, et al. 2014). The Yeast strain Y2HGold (Clontech), which contains the following four reporter genes *HIS3*, *ADE2*, *AUR1-C*, *MEL1* (encoding α-galactosidase) with GAL4 binding elements in each of their promoters was used to examine whether DRMY1 possesses transactivation ability. *DRMY1* and *AtGRF1* coding sequence (CDS) were cloned into pGBKT7 vector (Clontech), respectively to produce the fusion protein with the GAL4 DNA-binding domain (DBD). The resulting construct pGBKT7-DRMY1, pGBKT7-AtGRF1 (positive control) and the empty vector pGBKT7 (negative control) were individually transformed into Y2HGold competent cells according to previously

`

described method (Agatep et al. 1998). The yeast cells were grown on synthetic dextrose (SD) medium without Trp (SD/-Trp) for 2-3 days at 30°C to select for successful transformants as the pGBKT7 vector harbors a tryptophan (Trp) selection gene. Transactivation activity was then assayed on the following selective media: SD/-Trp/-His, SD/-Trp/-Ade, SD/-Trp/-His/-Ade, SD/-Trp/-His/-Ade/+X-α-gal to test the expression of the reporter genes.

Cell wall biochemical assay

The cell wall biochemical analyses were carried out as described previously (Foster, Martin, and Pauly 2010a, 2010b). Briefly, the lignocellulosic cell wall material was isolated from aerial parts of 18-day-old plants. After trifluoroacetic acid (2M) hydrolysis and subsequent derivatization of the neutral monosaccharides in the hydrolysate by alditol acetate, the polysaccharide composition was analyzed via GC-MS system (Agilent 7890A GC/5975C MS). The content of crystalline cellulose was determined by using the colorimetric anthrone assay after isolation and purification from the insoluble residue remaining from the TFA hydrolysis and hydrolyzation in sulfuric acid (72%). For the lignin content analysis, the acetyl bromide soluble lignin (ABSL) method was performed and assayed using a photospectrometer at 280 nm (Spectromax 384 plus). For the lignin content calculation, the molar extinction coefficient for maize (17.75 $g^{-1}Lcm^{-1}$) was used, which was previously determined in literature (Fukushima and Hatfield 2004). The lignin composition was quantitated using GC-MS analysis (Agilent 7890A GC/5975C MS) after liberation of the p-Hydroxylphenyl (H), Guaiacyl (G), and Syringyl (S) monomers by thioacidolysis method and subsequent silylation with BSA according to the published procedure (Harman‐Ware et al. 2016).

`

RNAseq library preparation and data analysis

Three replicates of aerial parts of 15-day-old plants were harvested from WT and homozygous *drmy1* mutant plants. Total RNA was isolated using Trizol reagent (Invitrogen) following the manufacturer's guided protocols. After digestion with DNaseI, it was then purified using RNeasy Mini Kit (Qiagen). Total RNA fractions with 260/280 absorbance of 2.0 and RNA integrity of 8.0 or higher were used for RNAseq library construction. Each replicate was quantified by Qubit (Thermo Fisher Scientific) and normalized to 1 microgram. RNAseq libraries were constructed using the stranded TruSeq mRNAseq kit (Illumina Technologies) following the manufacturer's recommended procedures. Paired-end sequencing of each library (2x125bp) was collected on a HiSeq 2500 (Illumina Technologies). The raw paired-end reads were scored for quality using FastQC version 0.11.5 (http://www.bioinformatics.babraham.ac.uk/projects/fastqc/), and then trimmed to remove adapter sequences and low-quality bases using Trimmomatic version 0.36 (Bolger, Lohse et al. 2014). Preprocessed reads were aligned to the *Arabidopsis thaliana* reference genome assembly (TAIR10 release) using Tophat v2.1.1 (Trapnell, Pachter et al. 2009). Read counts per gene were quantified using the feature.Counts program that accompanies Subread (v1.5.3) (Liao, Smyth et al. 2013) for WT and *drmy1* samples. The differential gene expression analysis was performed using edgeR release 3.5 (Robinson, McCarthy et al. 2010). Genes with 2-fold change or above, $P < 0.05$ and $FDR < 0.05$ after multiple testing adjustment were defined as differentially expressed genes (DEGs). Heatmaps showing expression profiles between WT and *drmy1* samples were generated based on the $\log_2$ counts-per-million ($\log_2$CPM) values. Gene Ontology (GO) enrichment analysis was performed using the functional annotation tool in

`

The Database for Annotation, Visualization and Integrated Discovery (DAVID) v6.8 (Dennis, Sherman et al. 2003). Enriched GO terms were identified with P value cut-off of < 0.05 and Bonferroni value cut-off of < 0.05.

Results

drmy1 exhibits pleotropic phenotypes in vegetative growth

To study the genetic networks underlying plant organ development, an *Arabidopsis* T-DNA insertion mutant named *development related Myb-like 1 (drmy1)* with altered organ growth was identified . Detailed phenotypic characterization of *drmy1* revealed its delayed seed germination and reduced vegetative growth as compared to wild type (WT). As shown in Figure 2.1, when measuring daily seed germination frequencies over 7 days on half-strength MS solid media, about 70% of WT seeds germinated, whereas only 10% of *drmy1* seeds germinated at 24 hours. All the WT seeds germinated within 48 hours, while only 79% of *drmy1* seeds germinated at this time, indicating that the *drmy1* mutant seeds have a slower seed germination rate than WT seeds. It is also interesting to note that about 6.7% of the *drmy1* mutant seeds did not germinate at 168 hour, indicating that seed viability is affected in these seeds.

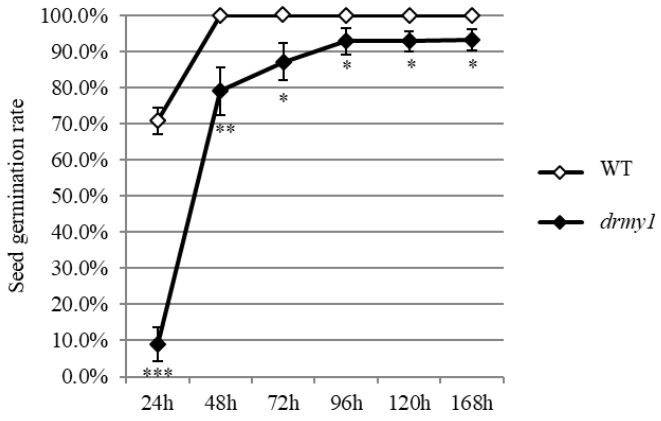

Figure 2.1. Seed germination assay of WT and the *drmy1* mutant. The germination frequencies were scored every 24 h for 5 days after sown on half-strength MS solid media. 48 h after that, the final germination frequency at the 7th day was measured. Error bars indicate SD. Asterisks represent statistically significant differences calculated by Student's t-test (*, P < 0.05; **, P < 0.01; ***, P < 0.001).

`

Another striking phenotype of *drmy1* was its reduced leaf growth (Figure 2.2A). The fifth rosette leaf was chosen as a representative for leaf growth kinetics (Figure 2.2B) because it was found to have the most reproducible features of all rosette leaves in *Arabidopsis* (Tsuge, Tsukaya, and Uchimiya 1996). As shown in Figure 2.2B, the *drmy1* mutant exhibited a slower leaf blade growth rate compared to WT. Fully expanded fifth leaves in 36-day-old plants were then used to characterize the final leaf phenotype. Leaf petiole length was not changed in the *drmy1* mutant (Figure 2.2C) but the average leaf blade area of *drmy1* was reduced by 16.8% compared to WT (Figure 2.2D). Leaf shape in the *drmy1* mutant was also altered with growth reduction in the width direction while not in the length direction (Figure 2.2E, 2.2F), leading to a narrower leaf with increased leaf index (the ratio of leaf blade length to leaf width).

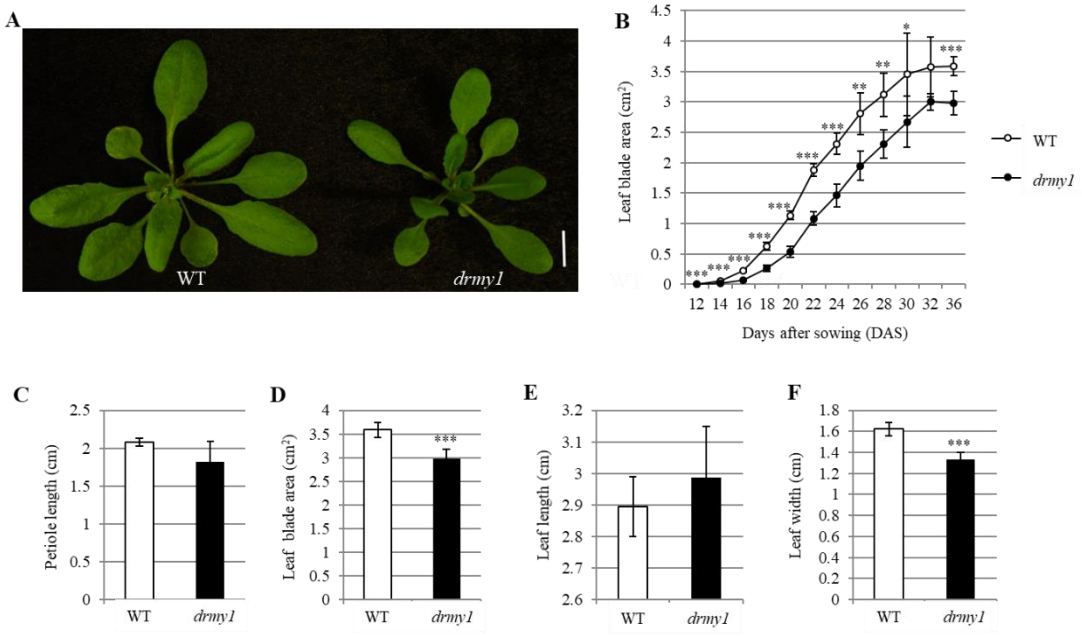

Figure 2.2. Leaf morphology of WT and the *drmy1* mutant. (A) 21-d-old plants of WT (left) and the *drmy1* mutant (right). Bar, 1 cm. (B) Growth kinetics of the fifth leaves in WT and the *drmy1* mutant plants. The leaf area was determined from at least four leaves for each genotype after their emergence at 2-day intervals. Five fully expanded fifth leaves from each genotype were used for determination of the following leaf parameters: (C) Petiole length of WT and the *drmy1* mutant leaves, (D) Leaf blade area of WT and the *drmy1* mutant leaves, (E) Leaf blade length of WT and the *drmy1* mutant leaves, (F) Leaf blade width of WT and the *drmy1* mutant leaves. Error bars indicate SD. Asterisks represent statistically significant differences calculated by Student's t-test (*, $P < 0.05$; **, $P < 0.01$; ***, $P < 0.001$).

`

In addition to leaf growth defects, *drmy1* also exhibited reduced primary root growth and lateral root number emerged from the primary root (Table 2.1). Moreover, *drmy1* plant height was reduced by 15.6% compared to WT (Table 2.1, Figure 2.4A), indicating that stem development of *drmy1* was also inhibited.

Table 2.1. Phenotype of WT and the *drmy1* mutant

Variables	WT	*drmy1*
Primary root length (cm)	2.3±0.2 (n=13)	1.4±0.3 (n=13)***
Lateral root number	12.8±2.9 (n=21)	5.0±1.8 (n=21)***
Bolting time (days)	22.9±1.4 (n=14)	23.5±0.7 (n=14)
Flowering time (days)	25.1±1.2 (n=14)	25.9±0.4 (n=14)
Plant height (cm)	52.5±2.1 (n=10)	44.3±1.5 (n=10)***

Student's t-test: *, P < 0.05; **, P < 0.01; ***, P < 0.001

As the leaf has been shown to be a good model to characterize organ development (Tsukaya 2003, 2008), we then further investigated the contribution of cell number and cell size to the reduced organ size in *drmy1*. Firstly, epidermal pavement cells in the *drmy1* mutants exhibit an abnormal shape compared to the jigsaw puzzle-like epidermal pavement cells in WT when observed under the scanning electron microscope (SEM) (Figure 2.3A). We then measured the number and size of palisade cells in *drmy1* fully expanded fifth leaves compared with those in WT (Figure 2.3B). As shown in Figure 2.3C and 2.3D, the average size of palisade cells in *drmy1* was decreased by 10.8% whereas the total palisade cell number remained almost unchanged. This result indicates that DRMY1 mainly impacts the process of cell expansion rather than cell proliferation during leaf development.

`

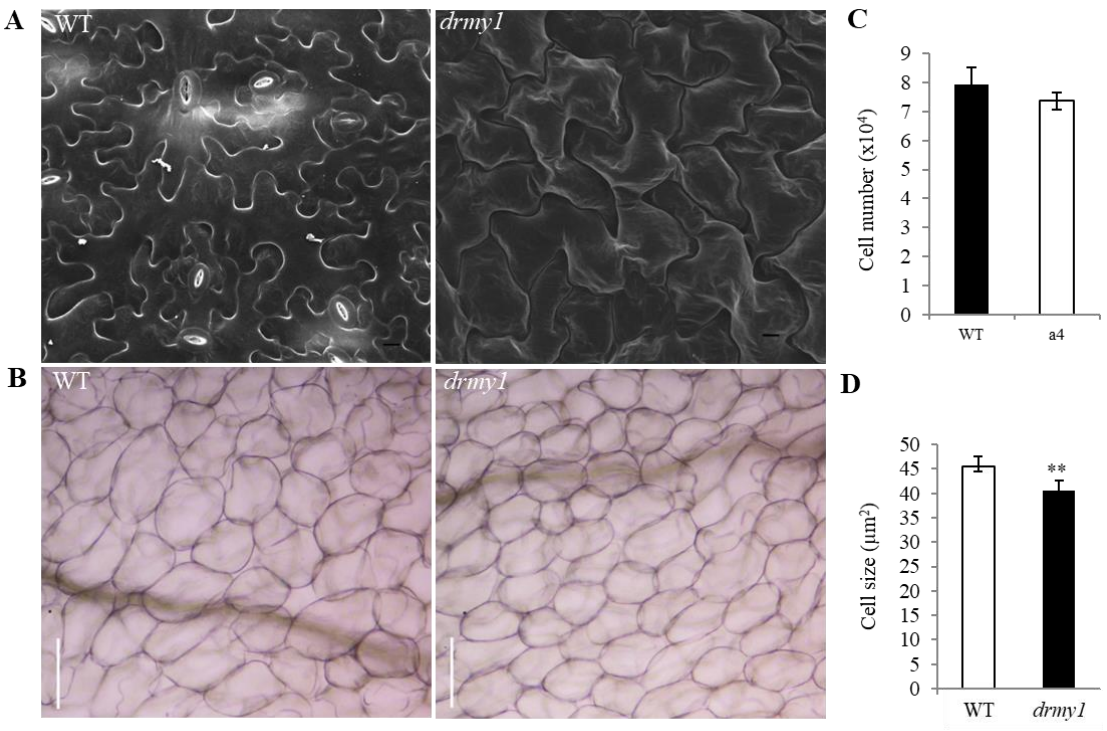

Figure 2.3. Cytological observation of WT and the *drmy1* mutant leaf. (A) Scanning electron microscopic photographs of adaxial epidermal cells of the fifth leaf in WT (left) and *drmy1* (right) 30-day-old plants. (B) Palisade cells of the fully expanded fifth leaf in WT (left) and *drmy1* (right) plants. Bars, 100 μm. (C) Estimated palisade cell number per leaf (top) and (D) cell size (bottom) in WT and *drmy1* plants. Five fully expanded fifth leaves from each genotype were cleared and visualized under a microscope to determine the palisade cell number per leaf and cell size. Error bars indicate SD. Asterisks represent statistically significant differences calculated by Student's t-test (*, $P < 0.05$; **, $P < 0.01$; ***, $P < 0.001$).

drmy1 produces fewer seeds than wild type, which is associated with abnormal flower development

Besides the growth defect in vegetative organs, *drmy1* was also partially sterile (Figure 2.4A, 2.4B) and produced shorter and curved siliques compared to WT (Figure 2.4C). We quantified the following four parameters to determine seed production in the *drmy1* mutant: the number of inflorescence stems, total silique number in the primary stem, percentage of siliques with different length and shape in the primary stem, and seed number per silique. The number of inflorescence stems in the *drmy1* mutant is similar to WT (Figure 2.4D), thus siliques in the primary stem were used as representatives for further characterization of seed production. The total number of siliques in the *drmy1* primary

`

stems didn't show significant change compared to those in WT (Figure 2.4E). However, they exhibited difference in length and shape, which could be divided into three categories: the long siliques (≥1cm), the short siliques (≤1cm) and the curved siliques that are completely sterile (Figure 2.4F). As shown in Figure 2.4F, the majority of *drmy1* siliques are short and seedless and only a small percentage of them are long. The long siliques of *drmy1* were then used to measure seed number per silique compared to WT normal siliques. There is an average of 57 seeds in WT siliques while only 13 seeds were set in *drmy1* long siliques (Figure 2.4G). These data suggest that *drmy1* has reduced seed production compared to WT.

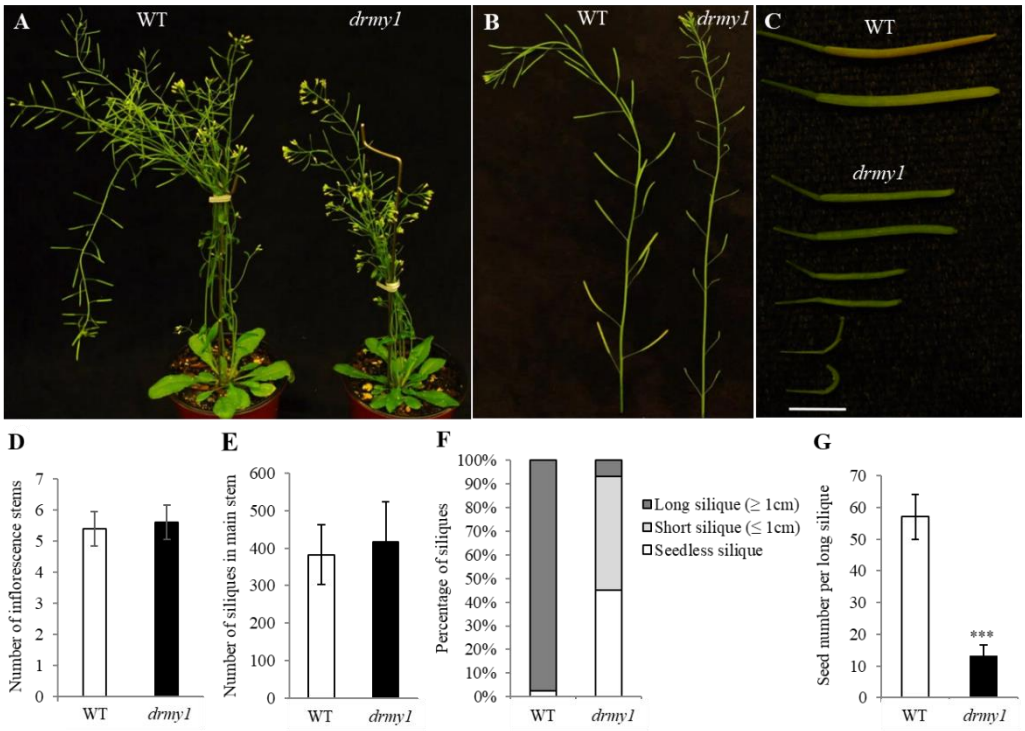

Figure 2.4. Silique phenotype and seed production in WT and the *drmy1* mutant. (A) Whole plant of 40-day-old WT and the *drmy1* mutant. (B) Main inflorescence stem of WT and the *drmy1* mutant, respectively. (C) Representative siliques of WT (top) and the *drmy1* mutant (bottom) plants. Bar, 0.5 cm. Seed production was measured based on the following parameters: (D) number of inflorescence stems, (E) number of siliques in the main inflorescence stem in WT and the *drmy1* mutant, (F) percentage of different types of siliques in WT and the *drmy1* mutant, (G) average number of seeds in WT normal siliques versus *drmy1* long siliques. Three plants from each genotype were measured. Error bars indicate SD. Asterisks represent statistically significant differences calculated by Student's t-test (*, $P < 0.05$; **, $P < 0.01$; ***, $P < 0.001$).

`

Seed production relies on normal flower development and a successful fertilization process. To investigate the cause for the reduced seed production in the *drmy1* mutant, we observed its flower development compared to that of WT. Before flowering, WT flower buds are enclosed by sepals (Figure 2.5A) while *drmy1* flower buds showed protruding pistils (Figure 2.5B), possibly due to the inhibited elongation of sepals. We also observed that mature *drmy1* flowers are smaller than WT flowers (Figure 2.5C). We then removed part of the sepals and petals for the observation of pistil and stamen morphology. When the WT flower matures, its stamen is level with the stigma so that the released pollen can land on the stigma, which facilitates fertilization (Figure 2.5D). But in the *drmy1* mutant, the fertilization process may be disrupted due to the defective growth of both pistils and stamens. First, we observed abnormal stigma papillae in *drmy1* flowers (Figure 2.5E). Second, we observed curved pistils in *drmy1* flowers (Figure 2.5F), which might lead to the curved siliques as observed previously. Moreover, some *drmy1* flowers show growth defect in filament elongation (Figure 2.5G), rendering the inaccessibility of pollens to the stigma and thus preventing pollination. Anther dehiscence and pollen maturation are not affected in the *drmy1* mutant, which is confirmed by microscopic observation and 1% iodine potassium iodide (I_2-KI) staining, respectively (Supplemental Figure A-1A and A-1B). We then used Scanning Electron Microscope (SEM) to better dissect the abnormal stigma papillae in *drmy1* flowers. At flower stage 12 (Smyth, Bowman, and Meyerowitz 1990), WT flowers showed elongating stigmatic papilla cells while the elongation of these cells is disrupted in *drmy1* flowers (Figure 2.6A). When the flower opens at stage 13, stigmatic papilla cells were fully expanded in WT flowers but not in *drmy1* flowers (Figure 2.6B). Stigmatic papilla cells have essential roles during pollination by mediating pollen-

`

pistil interactions (Elleman et al. 1988). Given their abnormal development, we hypothesized that the defective *drmy1* stigma might be less receptive to mature pollen grains. To test this hypothesis, we manually pollinated WT and *drmy1* defective stigma with pollens from transgenic plants harboring a pollen-specific *lat52-GUS* reporter (Figure 2.7A). GUS staining was then used to visualize pollen tube growth after 24 hours. Surprisingly, we found that the defective growth of *drmy1* stigmatic papilla cells did not seem to inhibit pollen germination and pollen tube growth. However, if pollinated pistilswere allowed to grow for two weeks for seed production, *drmy1* has much fewer seed set in the siliques compared to WT (Figure 2.7B), suggesting that fertilization did not succeed or the fertilization process did succeed but the fertilized eggs cannot develop into seeds, resulting in less seed production in *drmy1*.

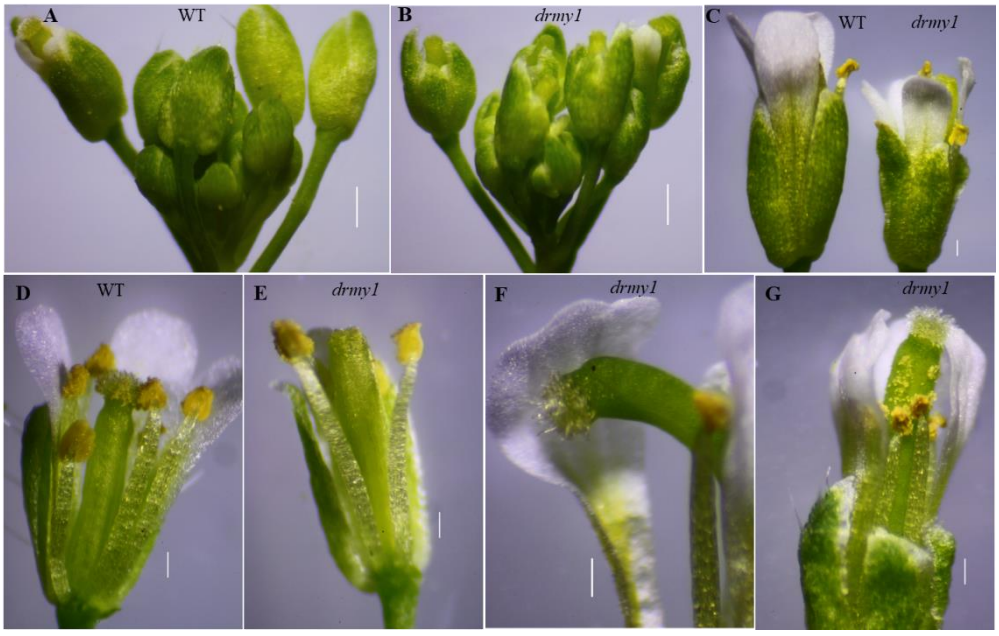

Figure 2.5. Flower phenotypes of WT and the *drmy1* mutant. (A) (B) Flower buds of WT and the *drmy1* mutant, respectively. Bars, 0.5 mm. (C) The first opened WT flower was larger than the *drmy1* mutant flower in the same position, but the floral organization was similar. Bar, 2 mm. (D) A dissected mature flower of WT. Bar, 2 mm. (E) The *drmy1* mature flower has abnormal stigma. Bar, 2 mm. (F) The *drmy1* mature flower has a curved pistil, preventing pollination. Bar, 2 mm. (G) The *drmy1* mature flower with the pistil longer than the stamens at floral stage 13, preventing pollination. Bar, 2 mm.

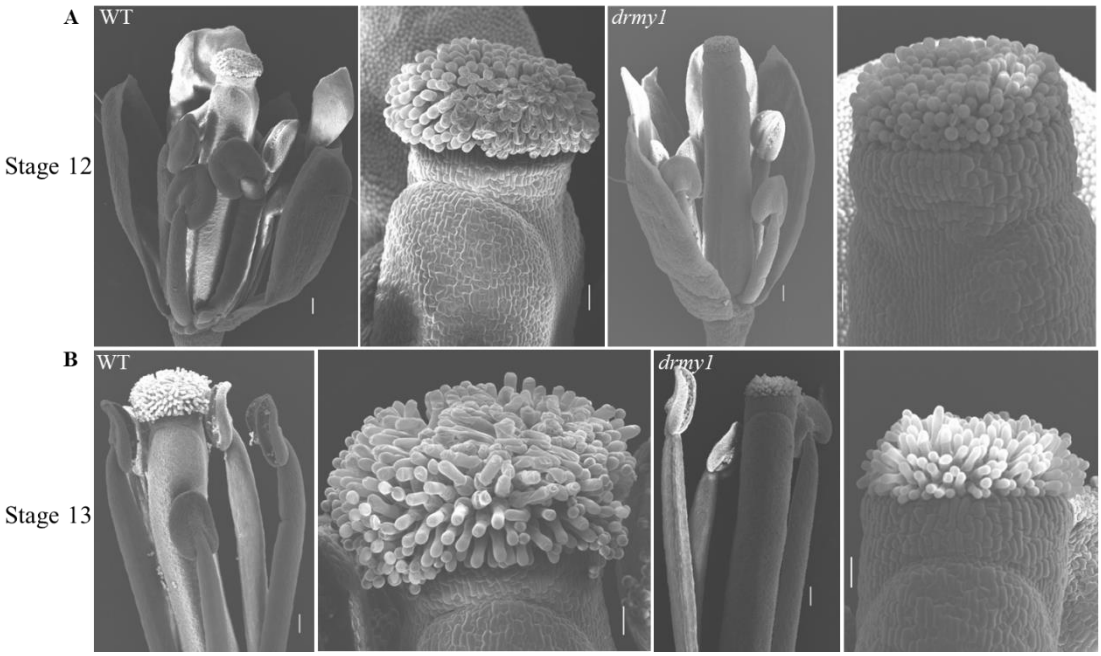

Figure 2.6. Flower development of WT and the *drmy1* mutant. (A) Scanning electron microscopic photographs of stage 12 flower buds of WT and the *drmy1* mutant with overall view (left, bar = 1 mm) and close-up view (right, bar = 400 μm). Note that stigmatic papillae of *drmy1* are shorter than those of WT. (B) Scanning electron microscopic photographs of stage 13 flowers of WT and the *drmy1* mutant with overall view (left, bar = 1 mm) and close-up view (right, bar = 400 μm). Note the retarded growth of stigmatic papillae cells in the *drmy1* mutant flower.

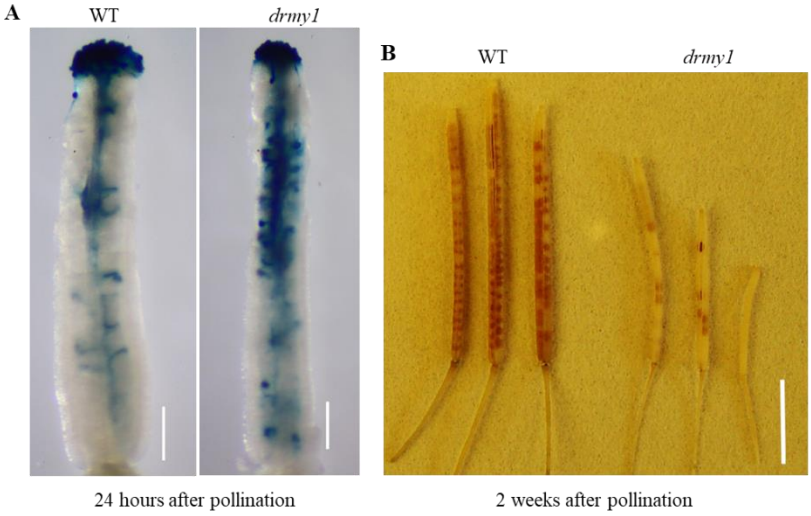

Figure 2.7. Observation of pollen penetration and seed production for WT and the *drmy1* mutant pistils pollinated with *lat52* promoter-GUS transgenic pollens. (A) Histochemical GUS staining for WT and *drmy1* pistils manually pollinated with transgenic pollens harboring pollen-specific *lat52* promoter-GUS. Note that pollens entered the transmitting tract of both genotypes. Bars, 0.5 mm. (B) Representative siliques WT and the *drmy1* mutant fertilized with *lat52* promoter-GUS transgenic pollens. Bar, 0.5 cm. Siliques were destained in 70% ethanol to remove chlorophyll.

`

The *drmy1* mutant phenotypes are caused by the disruption of a novel Myb-like DNA binding protein

PCR and DNA sequencing revealed that the T-DNA was inserted in the second exon of *DRMY1* (*At1g58220*) gene in an adjacent head-to-tail tandem configuration (Figure 2.8A, 2.8B), resulting in the disruption of *DRMY1* gene expression (Figure 2.8C). To confirm that the pleotropic mutant phenotypes of *drmy1* were indeed caused by the T-DNA insertion, we first examined the genetic linkage of the mutant phenotypes with T-DNA insertion. To this end, we backcrossed *drmy1* mutant with WT Columbia (Col-0) to generate F1, which were self-crossed to produce the F2 progeny. All F1 plants showed WT morphology and F2 plants showed a phenotypic segregation of WT: *drmy1* as 3:1 (97:31, P>0.8, Student's T-test) (Supplemental Figure A-2), indicating that the mutant phenotype co-segregates with the recessive mutation caused by the T-DNA insertion. To further confirm the functionality of *DRMY1* in organ development, we introduced a construct harboring genomic *DRMY1* into *drmy1* mutant and generated complementary transgenic lines. We used two lines, C1 and C3, for phenotypic characterization, in which the expression level of *DRMY1* is comparable to WT (Figure 2.9D). In the T1 generation, heterozygous C1 and C3 have segregating populations, in which plants with the restored phenotype correspond to the complemented transgenics while plants with the mutant phenotype correspond to the segregating *drmy1* mutants (Figure 2.9A, 2.9B, 2.9C), suggesting that the mutant phenotype is caused by the disruption of *DRMY1*.

`

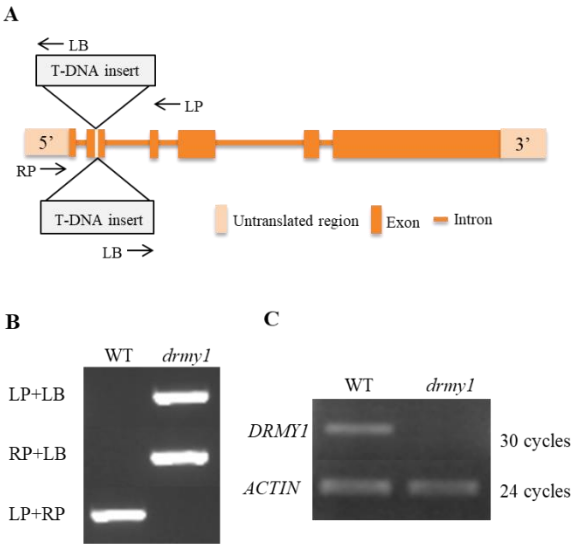

Figure 2.8. Schematic presentation of T-DNA insertions in the *drmy1* mutant and expression analysis of *DRMY1* in WT and the *drmy1* mutant. (A) Schematic diagram showing double T-DNA insertions in the *DRMY1* gene and primer locations. **(**B) PCR analysis of WT and *drmy1* genomic DNA using three pairs of primers. Primer LB are designed for T-DNA while primer LP and RP are designed for the genomic region. **(**C) RT-PCR analysis of *DRMY1* expression in WT and the *drmy1* mutant. *AtACTIN2* was used as an endogenous control.

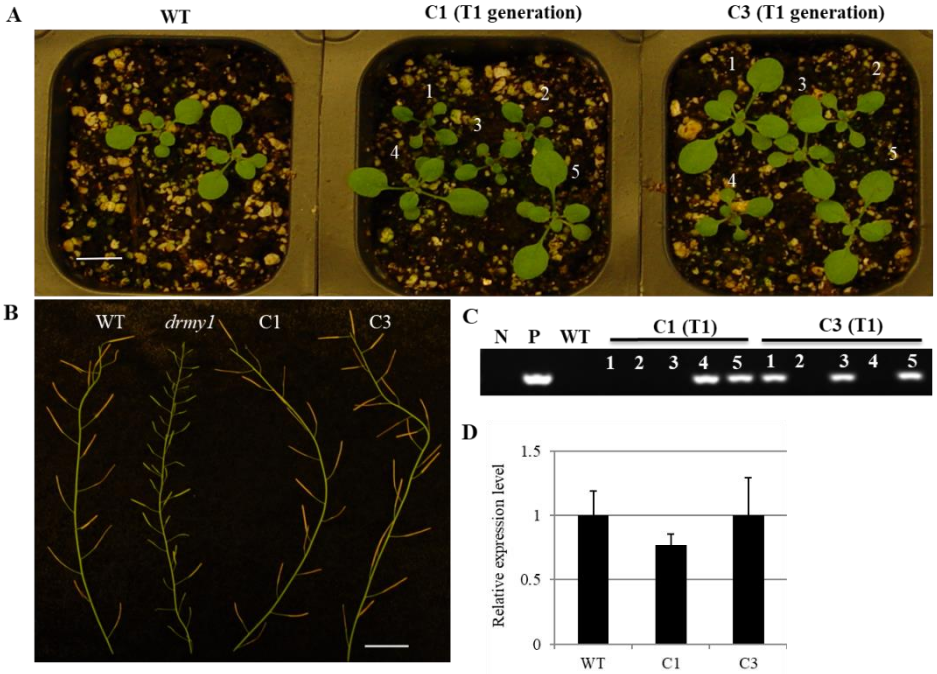

Figure 2.9. Phenotypic and molecular characterization of complementary transgenic plants with the introduction of genomic *DRMY1* sequence into the *drmy1* mutant. (A) Phenotypic observation of 2-week-old complementary transgenic lines C1 and C3 in T1 generation. Note the presence of both complemented transgenics and the *drmy1* mutant plants in T1 segregating populations. Bars, 1 cm. (B) Main inflorescence of WT, the *drmy1* mutant, C1 and C3 from left to right. Bar, 1 cm. (C) PCR analysis for individual plants in T1 generation using primers for the Basta resistance gene that is present in the complemented transgenic plants but not in WT and the *drmy1* mutant. Note the correspondence of the individual phenotype and the presence of amplicon. N: negative control; P: positive control. (D) qRT-PCR analysis for *DRMY1* expression levels in C1 and C3 lines.

`

DRMY1 protein has one Telomere Repeat Binding Factor (TRF)-like Myb DNA binding domain determined by searching Conserved Domains Database in NCBI (Marchler-Bauer et al. 2011), which belongs to the Myb-like subfamily that usually contains a single Myb repeat (Yanhui et al. 2006). In *Arabidopsis thaliana*, DRMY1 has a homolog we named DRMY1 Paralog 1 (DP1) with unknown function, which is predicted to have two alternatively spliced isoforms DP1-1 and DP1-2 with an overall protein sequence identity of 52.2% and 57.3% respectively to DRMY1 (Figure 2.10A). Interestingly, the *dp1* T-DNA insertion mutant (SALK_113831C) did not show any significant phenotypic variation regarding organ development as shown in Supplemental Figure A-3, suggesting that DP1 may not play a role in controlling plant growth.

To gain insight into the possible role of DRMY1, we blasted the DRMY1 Myb DNA binding domain against The Universal Protein Resource (UniProt) database to search for proteins possessing a similar domain (Apweiler et al. 2004), among which only the human Telomeric repeat-binding factor 2 (hTRF2) (domain similarity: 38.9%) has been functionally characterized and reported in the literature (Smogorzewska et al. 2000). hTRF2 is one of the six components of human shelterin, which together with hTRF1 functions in the protection of telomeres. TRF2 can also impose a restraint on telomerase, thereby a negative regulator of telomere length (Smogorzewska et al. 2000). To better characterize DRMY1's Myb DNA binding domain, sequence alignment was conducted using the Myb DNA binding domain of DRMY1 and DP1, the telomere binding domains of hTRF2 and other known telomere binding proteins in *Arabidopsis thaliana* (AtTBP1, AtTRP1), rice (RTBP1) and tobacco (NgTRF1). Interestingly, DRMY1 does not possess a highly conserved motif LKDKW(R/K)(N/T) within the Myb-like DNA binding domain

`

that is typical of telomere binding proteins (Figure 2.10B). To gain further insight into DRMY1's possible function, the complete amino acid sequence of DRMY1 was used to search for homologous proteins (similarity > 40%) in land plants (taxid: 3193) using NCBI BLASTP tool. A phylogenetic tree was generated as shown in Figure 2.10C, in which none of these proteins have known functions reported in the literature.

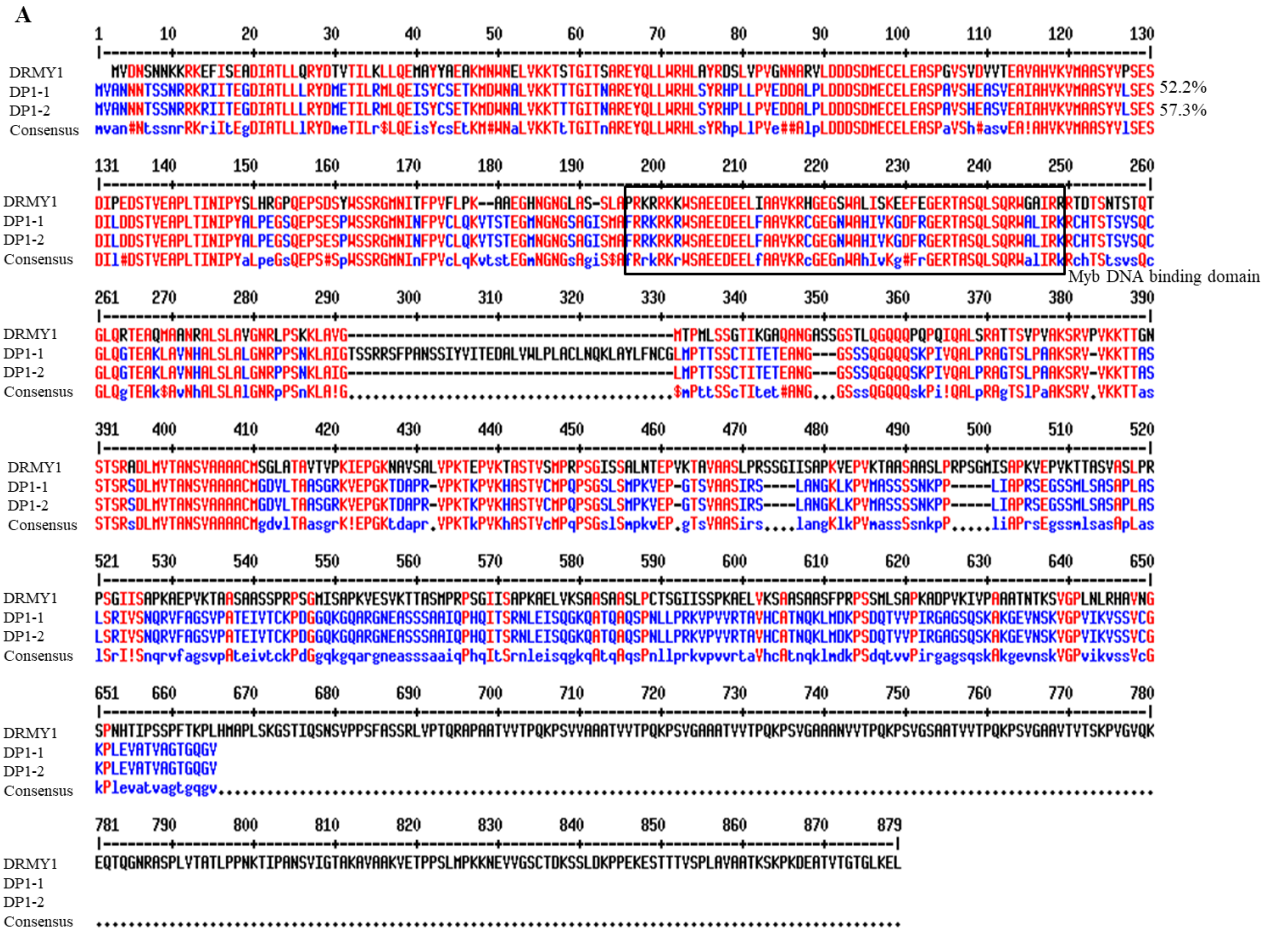

`

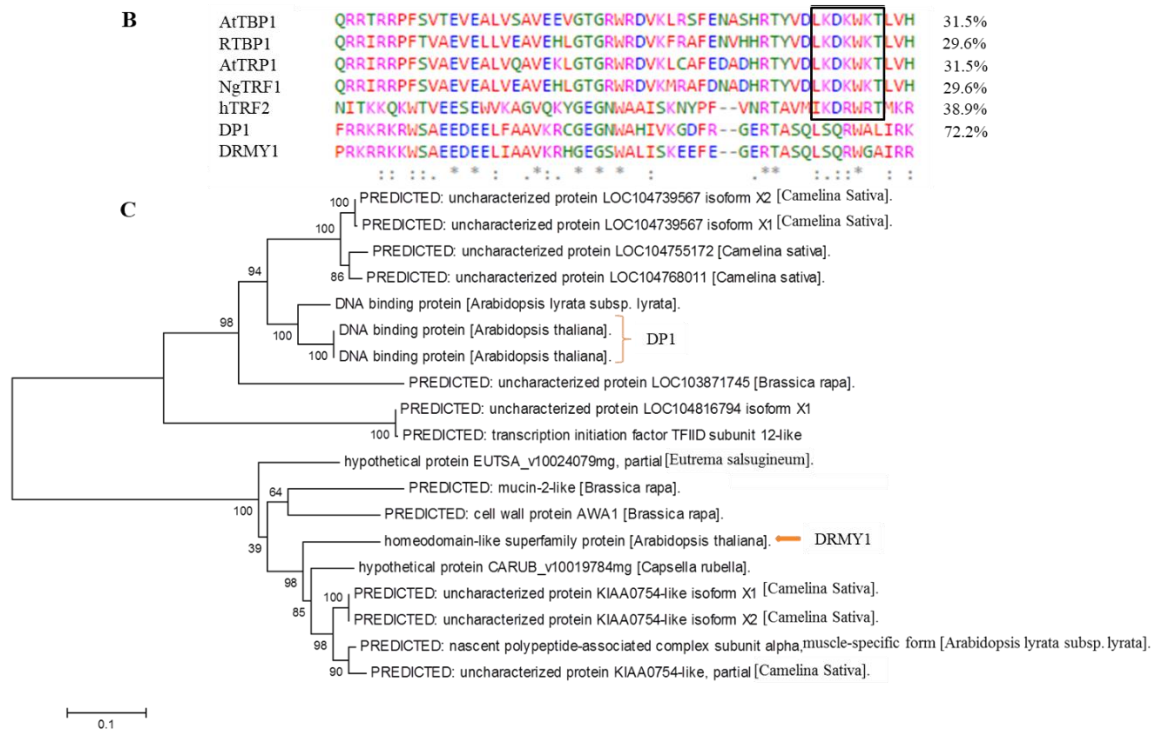

Figure 2.10. Sequence alignment and phylogenetic analysis of DRMY1 protein with its homologs. (A) Sequence alignment of DRMY1 protein and its paralog DP1 (two isoforms: DP1-1, DP1-2) in *Arabidopsis thaliana*. The amino acid sequence in the black box was predicted to be a Myb DNA binding domain. (B) Sequence alignment of the DNA binding domain in DRMY1, DP1, human hTRF2 and other known telomere binding proteins in *Arabidopsis thaliana* (AtTBP1, AtTRP1), rice (RTBP1) and tobacco (NgTRF1). The conserved motif LKDKW(R/K)(N/T) present in the telomere binding proteins is enclosed in the black box. (C) Phylogenetic analysis of DRMY1 and its closely related proteins (homology > 40%) in land plants by the Maximum Likelihood method using MEGA 6. Numbers on each branch correspond to bootstrap estimates for 1000 replicate analyses.

DRMY1 is highly expressed in developing organs and vascular tissues

To investigate the spatial and temporal expression pattern of *DRMY1*, we examined its expression in transgenic *Arabidopsis* harboring a *DRMY1*$_{pro}$*-GUS* fusion gene by histochemical GUS staining. In the seedling stage (Figure 2.11A, 2.11B, 2.11C), *DRMY1* was abundantly expressed at leaf primordia, roots tips and leaf vascular bundles. In the reproductive growth stage, strong *DRMY1* expression was observed in developing flowers, apices and bases of elongating siliques as well as the funiculus (Figure 2.11D, 2.11E, 2.11F, 2.11G). We also detected the expression of *DRMY1* in different organs at different developmental stages through qRT-PCR. Consistent with GUS staining assay, high

`

expression of *DRMY1* was detected in young rosette leaves and developing flowers, in support of its role in regulation of leave and flower development (Figure 2.11H). By contrast, *DRMY1* expression in the root and the stem is relatively low.

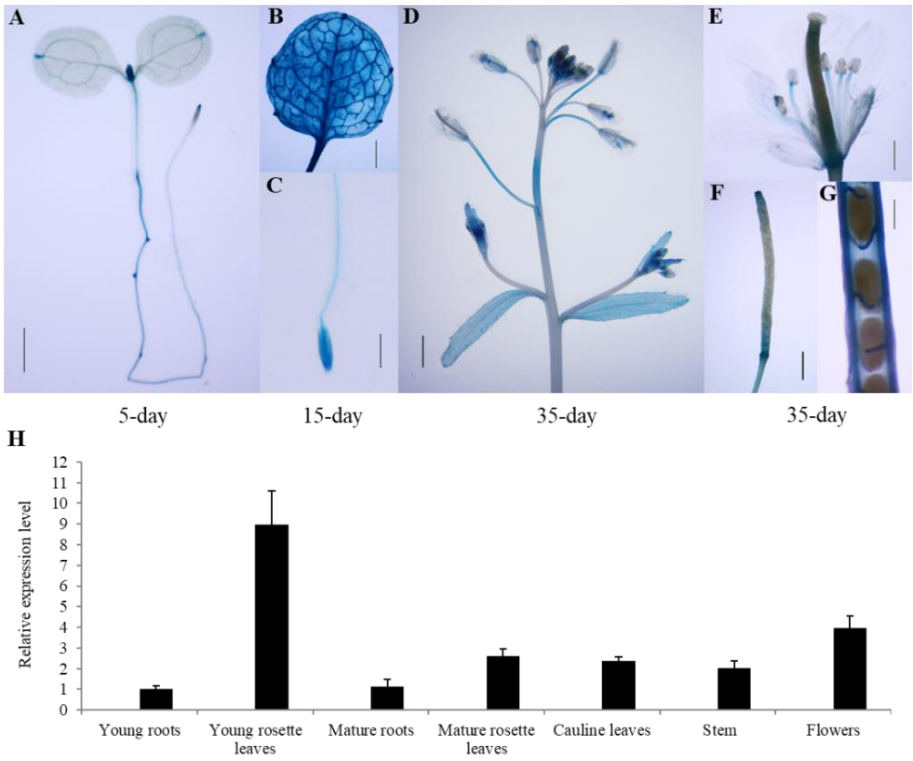

Figure 2.11. Spatial and temporal expression of *DRMY1*. (A-G) Histochemical GUS staining of (A) 5-day-old seedlings. Bar, 0.5 mm. (B) 15-day-old young leaf. Bar, 1 mm. (C) 15-day-old young root. Bar, 0.25 mm. (D) Flower cluster, cauline leaf and stem in the primary inflorescence of 35-day-old plant. Bar, 2 mm. (E) Opened flower. Bar, 0.5 mm. (F) Elongating silique. Bar, 1mm. (G) Developing seeds. Bar, 0.5 mm. (H) Real-time PCR analysis of *DRMY1* gene expression in different *Arabidopsis* organs with two biological replicates (three technical replicates each). *AtACTIN2* was used as an endogenous control.

DRMY1 is localized in the nucleus, but does not have transactivation ability

To elucidate the possible role of the DRMY1 protein, we then investigated the subcellular localization of the DRMY1 protein in *drmy1 Arabidopsis* roots carrying *35S-DRMY1-GFP*. The restored plant growth in the transgenic plants indicates that the fusion protein is functional (Supplemental Figure A-4). The GFP florescence signals were detected mainly in the nucleus with some signals also detected in the cell surface (Figure 2.12).

`

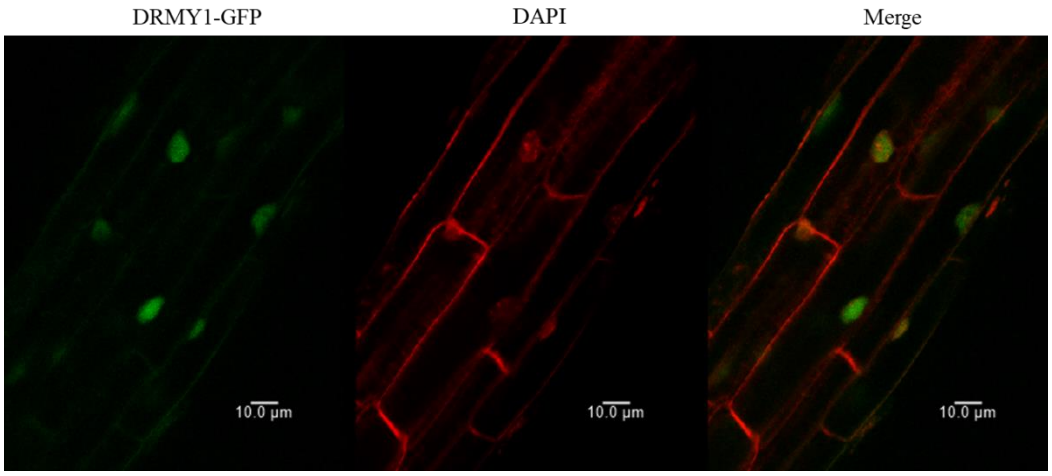

Figure 2.12. Subcellular localization of *DRMY1* in *Arabidopsis thaliana* root. *35S-DRMY1-GFP* transgenic plants were grown for 4-5 days on half-strength MS solid medium with the bottom of the petri dish covered with aluminum foil to avoid quenching of fluorescence by light. Fluorescent signals were then detected with confocal laser scanning microscope. Fluorescence from DRMY1-GFP fusion protein (left panel), DAPI (middle panel) and merged images (right panels) were shown. Bars, 10 µm.

A typical Myb family protein usually acts as a transcription factor. To test whether DRMY1 has transactivation ability, a transactivation assay was conducted in yeast cells. The *DRMY1* coding sequence was fused with the *GAL4* DNA binding domain (DBD) in the pGBKT7 vector and transformed into the Y2HGold yeast strain containing four reporter genes as shown in Figure 2.13A. The transcription factor *AtGRF1* fused with *GAL4* DBD in pGBKT7 vector and the pGBKT7 empty vector were used as positive and negative controls, respectively. As shown in Figure 2.13B, successful transformants can grow on SD/-Trp medium as the pGBKT7 vector harbors a tryptophan (Trp) selection gene. Yeast transformants harboring AtGRF1-GAL4 DBD can grow on SD/-Trp/-His medium (Figure 2.13C) but not in SD/-Trp/-Ade, SD/-Trp/-His/-Ade or SD/-Trp/-His/-Ade/+X-α-gal media (data not shown), indicating of a weak transactivation ability in yeast. DRMY1-GAL4 DBD transformants can grow on none of these media, suggesting that DRMY1 itself alone may not possess transactivation ability. It is possible that DRMY1 may require other transcription factors to form a complex to regulate the expression of downstream genes.

`

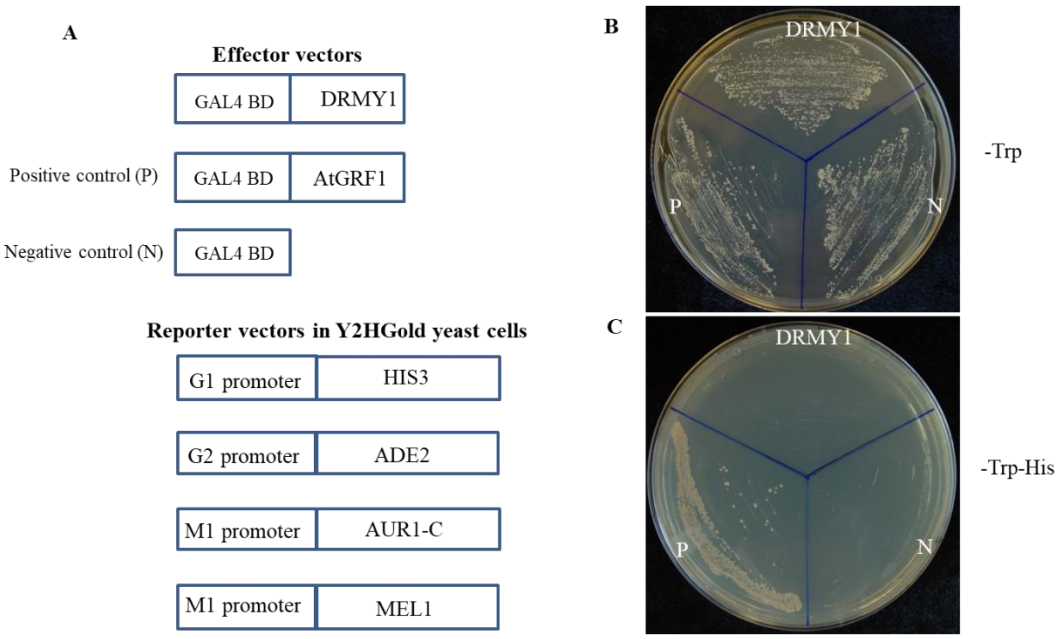

Figure 2.13. Transactivation assay of DRMY1 protein in yeast cells. (A) Schematic diagram illustrating the constructed effector vectors and the reporter vectors in Y2HGold yeast cells used for transformation. Growth of yeast cells transformed with GAL4BD-DRMY1, GAL4BD-AtGRF1 (positive control), GAL4BD empty vector (negative control) respectively on (B) SD/-Trp and (C) SD/-Trp-His media.

Overexpression of *DRMY1* does not lead to enhancement of plant growth and seed production

As the *drmy1* mutant has reduced organ growth, we asked whether *DRMY1* upregulation may promote organ growth. We therefore generated transgenic lines, in which *DRMY1* is constitutively overexpressed under the CaMV *35S* promoter. Two transgenic lines, OE12 and OE10, were used for phenotypic analysis (Supplemental Figure A-5A, A-5B). Interestingly, overexpression of *DRMY1* does not enhance plant organ growth. Conversely, rosette leaf growth was significantly reduced in OE10 (Supplemental Figure A-5C, A-5D, A-5E, A-5F). Moreover, there is no significant difference in root and stem growth (Supplemental figure A-6A, A-6B, A-6C) and seed production (Supplemental Figure A-6D, A-6E, A-6F) between WT and *DRMY1* overexpression transgenic plants.

`

The *drmy1* mutant phenotypes are associated with an increase of matrix polysaccharides in the cell wall

Plant cells are surrounded by two types of cell wall, primary cell wall (PCW) and secondary cell wall (SCW). While SCW provides mechanical stiffness and rigidity to specific cell types such as xylem cells (Cosgrove 2012), PCW has a relatively thin and extensible property, and functions as a major regulator for the size and shape of plant cells (Geitmann 2010; Hamant and Traas 2010). Given the evidence that *drmy1* mutant has a smaller cell size and altered cell shape, we speculated that it might have abnormal cell wall architecture. To this end, we analyzed the cell wall composition in 18-day-old developing WT and the *drmy1* mutant plants. As shown in Figure 2.14A, crystalline cellulose content did not show any significant difference between the two genotypes. However, all the analyzed matrix monosaccharide components that mainly constitute hemicellulose and pectin are significantly higher in the *drmy1* mutant than in WT (Figure 2.14B). The content and composition of the secondary cell wall component lignin was relatively low in both genotypes and did not show any change in *drmy1* (Figure 2.14C, 2.14D).

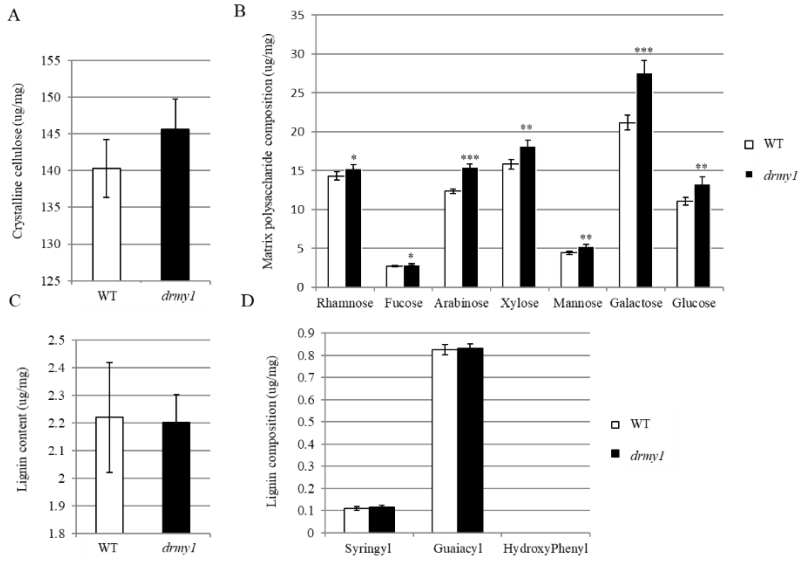

Figure 2.14. Cell wall composition analyses in WT and the *drmy1* mutant. The lignocellulosic cell wall materials were prepared from 18-day-old leaves of WT and the *drmy1* mutant and were then used to determine (A) crystalline cellulose content, (B) matrix polysaccharide composition, (C) lignin content, and (D) lignin composition. The results are given as average (ug/mg of lignocellulosic cell wall material) of four independent biological replicates with three technical replicates within each biological replicate. Error bars indicate SD. Asterisks represent statistically significant differences calculated by Student's t-test (*, $P < 0.05$; **, $P < 0.01$; ***, $P < 0.001$).

`

The expression of *DRMY1* is regulated by plant hormones ethylene and ABA

To investigate the possible upstream signals triggering *DRMY1* expression, we analyzed the promoter sequence of *DRMY1* using the Plant Cis-acting Regulatory Element (PlantCARE) database (Lescot et al. 2002). There are three different types of hormone-responsive elements that were identified in *DRMY1*'s promoter as shown in Table 2.2, including two gibberellin-responsive elements, an auxin-responsive element and an ethylene-responsive element. To elucidate whether *DRMY1* is responsive to plant hormones, qRT-PCR analysis of *DRMY1* expression was conducted in WT seedlings treated with various hormones including GA_3, IAA, ACC (ethylene precursor), and ABA. We found that the expression of *DRMY1* is significantly reduced by ACC while induced by ABA although the magnitude of change is small, indicating that *DRMY1* might function in hormone signaling pathways (Figure 2.15).

Table 2.2. Predicted hormone responsive elements in *DRMY1*'s promoter

Cis-acting elements	Position	Sequence
gibberellin-responsive element (GARE)	460 (-)	TCTGTTG
gibberellin-responsive element (GARE)	774 (+)	AAACAGA
auxin-responsive element (TGA-element)	141 (-)	AACGAC
ethylene-responsive element (ERE)	737 (-)	ATTTCAAA

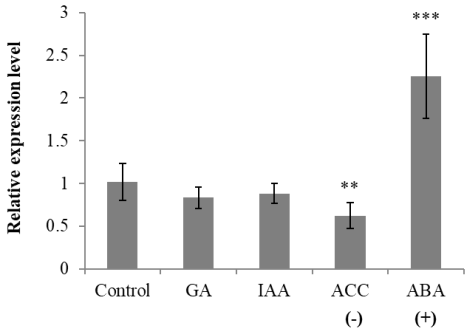

Figure 2.15. The transcriptional regulation of *DRMY1* by different plant hormones. Error bars indicate SD. Asterisks represent statistically significant differences calculated by Student's t-test (*, $P < 0.05$; **, $P < 0.01$; ***, $P < 0.001$). qRT-PCR was conducted with two biological replicates (three technical replicates each). *AtACTIN2* was used as an endogenous control.

`

DEGs genes in the *drmy1* mutant are involved in cell wall biosynthesis/remodeling, ribosome biogenesis and hormone signaling pathways

To investigate the downstream genes regulated directly or indirectly by DRMY1, we conducted RNAseq analysis of WT and *drmy1* aerial organs of 15-day-old soil grown seedlings. There are 443 genes that were differentially expressed (2-fold-change, $P < 0.05$, FDR < 0.05), of which 335 genes were upregulated and 108 genes were downregulated. 18 genes related to cell wall biogenesis/remodeling are differentially expressed (Figure 2.17A). To understand other possible biological functions of these differentially expressed genes (DEGs), we performed GO enrichment analysis and identified over-represented gene ontology (GO) terms ($P < 0.05$, Bonferroni < 0.05) for up-regulated and down-regulated genes, respectively. We found that GO terms related to ethylene and ABA signaling pathways are significantly enriched in the up-regulated genes (Figure 2.16). Average gene expression level of DEGs in these two categories were shown in Figure 2.17B and 2.17C, respectively. Many GO terms related to plant response to biotic and abiotic stresses are also significantly enriched among the up-regulated genes, including “response to chitin”, “response to water deprivation”, “response to cold”, “response to wounding”, “response to salt stress”, “response to osmotic stress” and “response to jasmonic acid” (Figure 2.16), suggesting that DRMY1 may also play a role in plant response to environmental stresses on top of regulating organ development. All the enriched GO terms for the down-regulated genes are related to ribosomes, including “structural constituent of ribosome”, “cytosolic large ribosomal subunit”, “ribosome” and “cytosolic ribosome” (Figure 2.16), suggesting a role of DRMY1 in regulating ribosome biogenesis. The average gene expression level of DEGs assigned with GO term “structural constituent of ribosome” are shown in Figure

`

2.17D. We also confirmed the expression of a select number of DEGs by qRT-PCR, which is in a good agreement with RNAseq data (Figure 2.18).

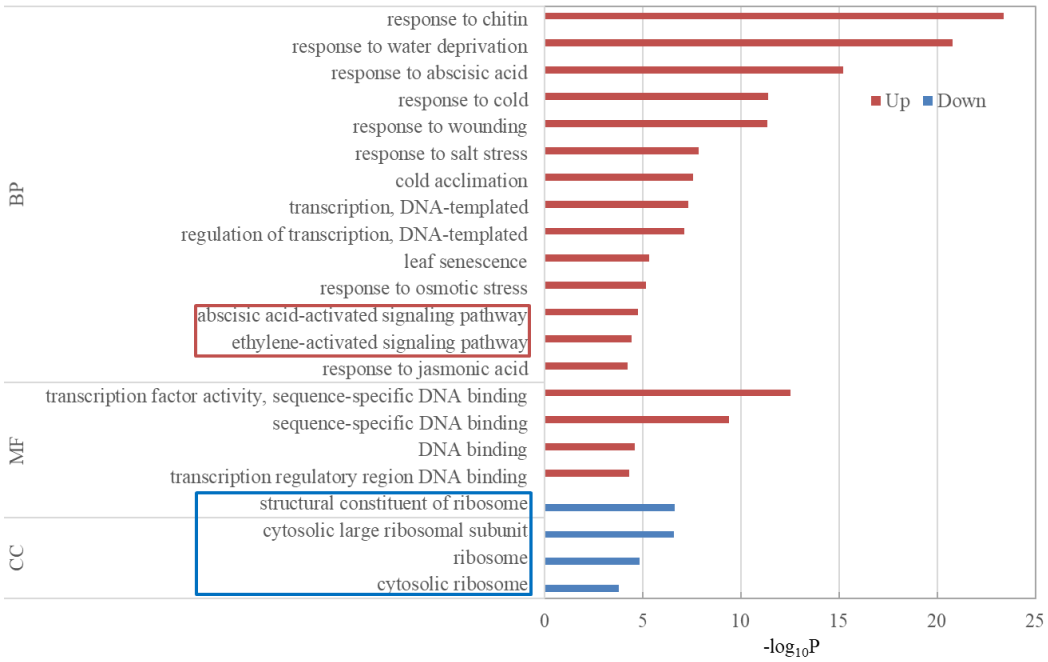

Figure 2.16. Functional enrichment analysis for DEGs identified in the *drmy1* mutant. The y-axis shows significantly enriched gene ontology (GO) terms (P < 0.05, Bonferroni < 0.05) in three categories, Biological Process (BP), Molecular Function (MF) and Cellular Component (CC). The x-axis shows the $-\log_{10}P$ values of these terms. Red bars indicate up-regulated genes; blue bars indicate down-regulated genes.

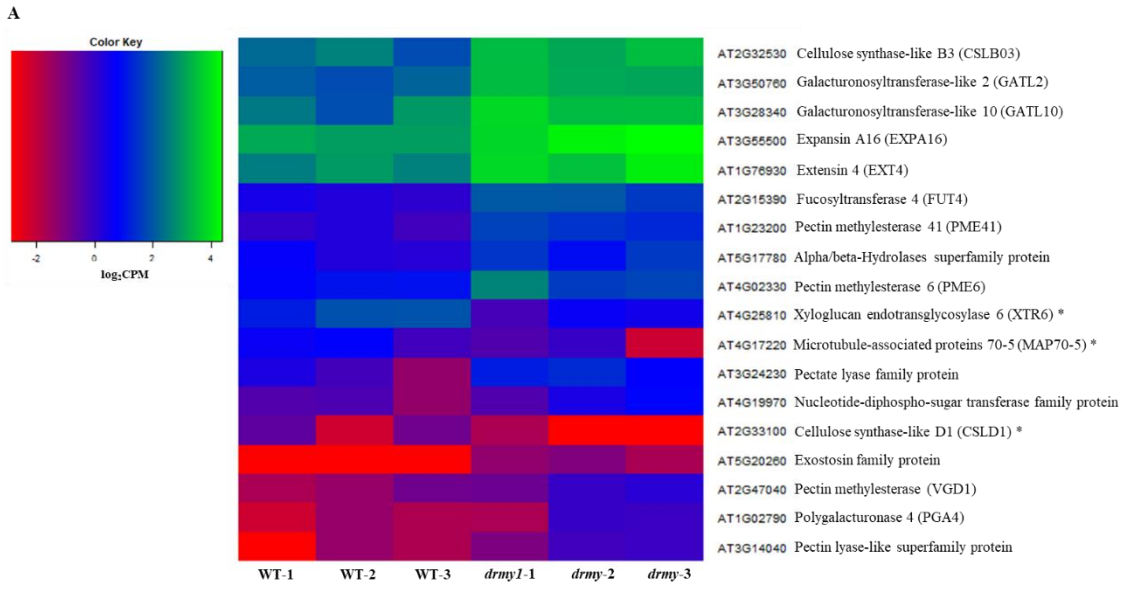

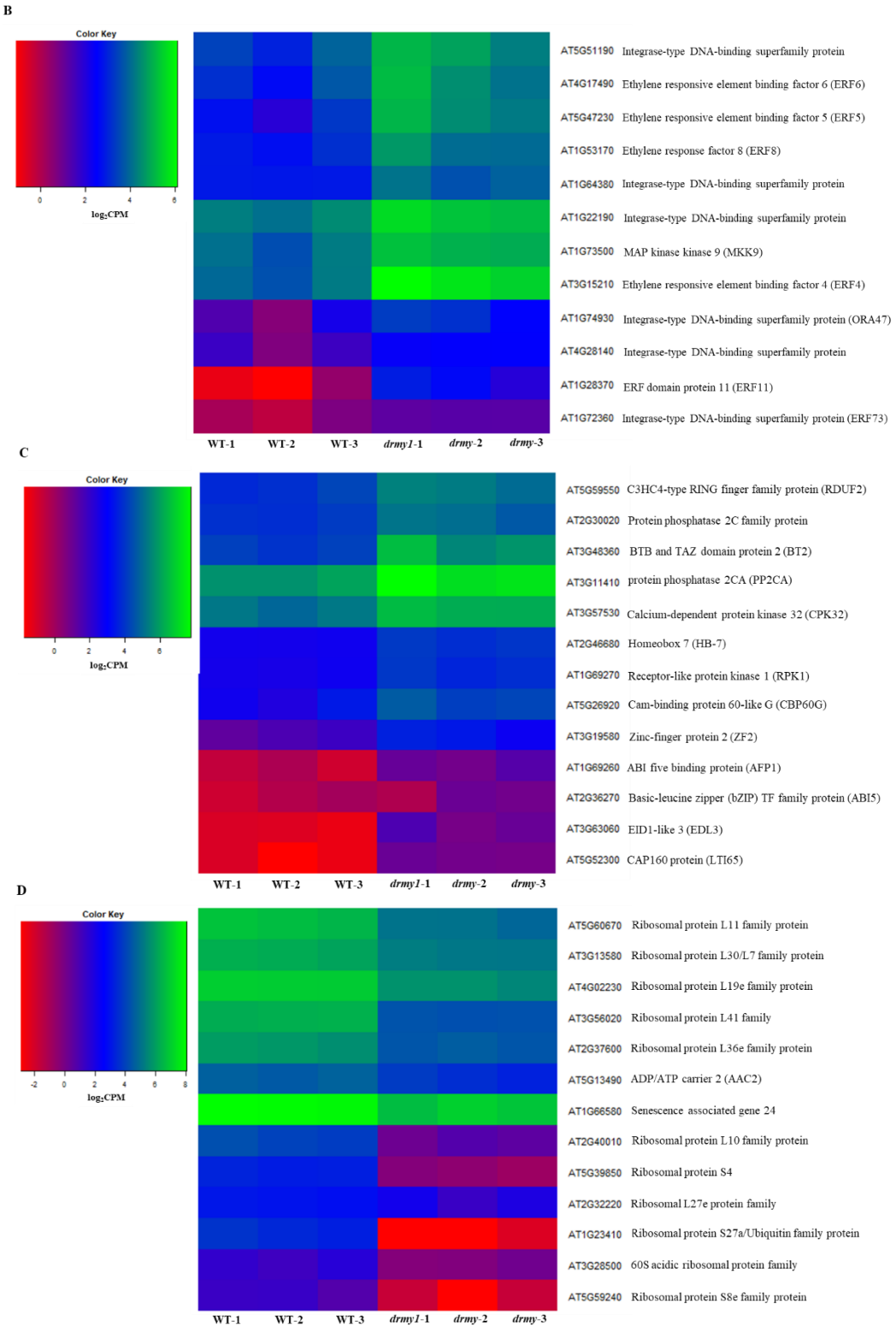

Figure 2.17. Heatmap diagrams depicting average expression level (log_2CPM) of DEGs in WT and the *drmy1* mutant. (A) differentially expressed cell wall biosynthesis and remodeling genes; (B) up-regulated genes with overrepresented GO term "ethylene-activated signaling pathway" in BP category; (C) up-regulated genes with over-represented GO term "ABA-activated signaling pathway" in BP category; (D) down-regulated genes with over-represented GO term "structural constituent of ribosome" in MF category.

`

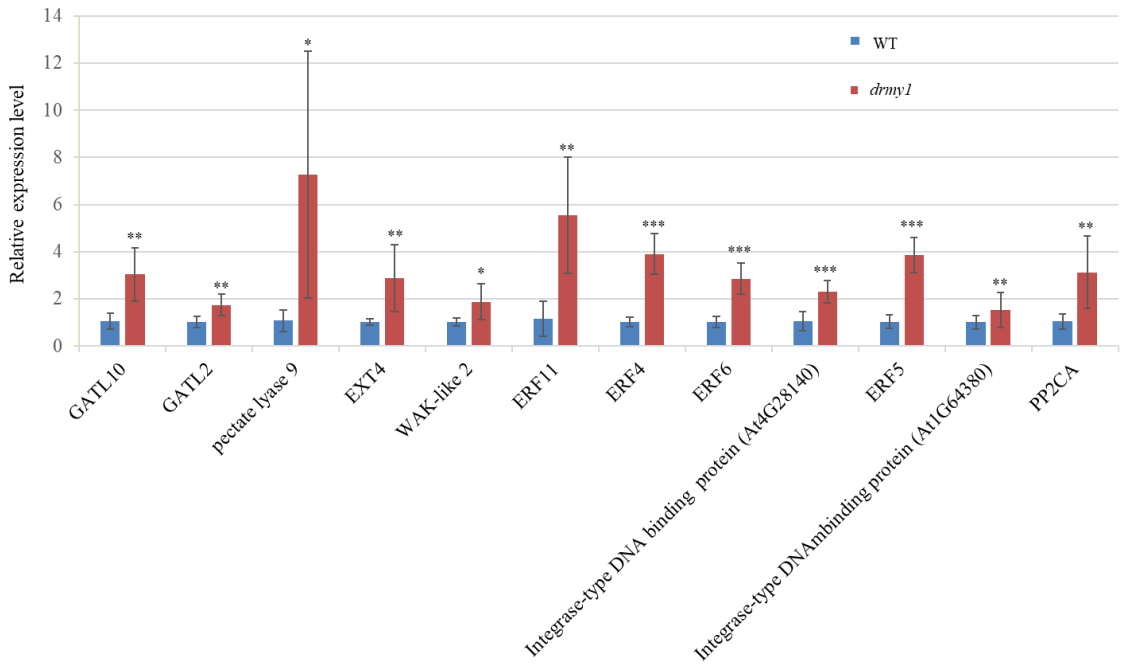

Figure 2.18. Gene expression confirmation by qRT-PCR. Data shown are mean $2^{-\Delta\Delta CT}$ value from two biological replicates. Error bars indicate SD. Asterisks represent statistically significant differences calculated by Student's t-test (*, $P < 0.05$; **, $P < 0.01$; ***, $P < 0.001$). qRT-PCR was conducted with two biological replicates (three technical replicates each). *AtACTIN2* was used as an endogenous control.

Discussion

Plant organ growth to its characteristic size and shape depends on the coordination of both cell proliferation and cell expansion. While several gene regulatory networks have been identified for cell proliferation, the cell expansion process remains largely unknown. Here we identified an *Arabidopsis* T-DNA insertion mutant named *drmy1*, which showed reduced growth in both vegetative and reproductive organs due to defects in cell expansion. We further demonstrated that the defective cell expansion in *drmy1* mutant is linked to changes in the composition of the cell wall, in which the matrix polysaccharides are more abundant in the *drmy1* mutant than in WT. Complementation by introduction of the *DRMY1* genomic DNA sequence into the mutant background rescued the phenotype, indicating that *DRMY1* mutation is responsible for the phenotype. *DRMY1* is strongly

`

expressed in developing organs and vascular tissues and its expression is reduced by the plant hormone ethylene while induced by ABA. The DRMY1 protein only contains a single Myb-like DNA binding domain and is localized in the nucleus, which may function with other transcription factors as a complex to regulate downstream gene expression as DRMY1 itself does not possess transactivation ability. Overexpression of DRMY1 did not lead to enhanced growth and yield, probably because there are not enough transcription factors as partners of DRMY1 to exert additional effect. Interestingly, DRMY1 overexpression line OE10 exhibited reduced leaf growth, which is probably because abundant DRMY1 may also bind to transcription factors that negatively affect leaf growth. Furthermore, whole transcriptome profiling suggested that DRMY1 may control cell expansion directly by regulating genes related to cell wall biosynthesis/remodeling and ribosome biogenesis or indirectly through regulating genes involved in ethylene and ABA signaling pathways.

DRMY1 may define novel binding targets in the Myb protein family

In the *Arabidopsis thaliana* genome, there are 197 Myb family members, among which 52 members were identified as Myb-like proteins that usually but not always contain one Myb repeat (Katiyar et al. 2012). Based on sequence alignment and phylogenetic analysis, Myb-like proteins are further divided into five major subfamilies: CIRCADIAN CLOCK ASSOCIATED1 (CCA1)-like, telomere binding proteins (TBP)-like, CAPRICE (CPC)-like, I-box-like and R-R-type (Yanhui et al. 2006; Du et al. 2013). DRMY1 and its paralog DP1 were classified into the TBP-like subfamily in a previous paper (Du et al. 2013), in which a highly-conserved motif LKDKW(R/K)(N/T) is usually present. However in our study, we found that DRMY1 and DP1 shared the conserved motif of

`

LSQRW(G/A)(A/L) instead, which raises the question whether or not DRMY1 and DP1 are telomere binding proteins. Furthermore, in *Arabidopsis thaliana*, known telomere-binding proteins are divided into two families: the Single-Myb-Histone-like (SMH) family and the TRF-like (TRFL) family 1 (Schrumpfová, Schořová, and Fajkus 2016). While SMH family proteins contain a Myb-like domain at the N-terminus, a central histone-like domain and a coiled-coil region at the C-terminus (Schrumpfová et al. 2004), TRFL family proteins possess a Myb-like domain at the C-terminus and a Myb-extension (Myb-ext) domain that are both essential for double-stranded telomeric DNA binding *in vitro* (Karamysheva et al. 2004). DRMY1 and DP1 do not have other characteristic domains of known telomere binding proteins besides a TRF-like Myb DNA binding domain, suggesting that DRMY1 may not function as a telomere binding protein. Instead, we hypothesize that DRMY1 may function as a typical Myb DNA binding protein and confers regulatory function by binding to the promoter regions of downstream genes but may require the cooperation of other transcription factors to regulate gene expression as itself did not show transactivation activity. The uniqueness of the Myb DNA binding domain in DRMY1 may define a novel binding motif in the Myb protein family.

DRMY1 may control cell expansion directly by regulation of cell wall biosynthesis/remodeling and ribosome biogenesis

It is proposed that cell expansion can be achieved by two major ways. One is cytoplasmic growth, which mainly relies on macromolecular biosynthesis, mostly proteins and is tightly linked to the nutritional and energy levels of plants as protein biosynthesis is an energy-demanding process. Another way is post-mitotic cell expansion, which is triggered by turgor pressure and requires cell wall remodeling to facilitate cell expansion

`

and deposition of newly synthesized wall materials to strengthen the stretched cell wall (Cosgrove 1993). How does DRMY1 contribute to cell expansion during organ development? We suggest that DRMY1 may regulate cell expansion directly in the following ways. First, DRMY1 may contribute to cell expansion by regulating cell wall biosynthesis/remodeling for the following reasons. On one hand, cell wall composition analysis revealed that the matrix monosaccharides in the walls of *drmy1* mutants, which mainly constitute hemicellulose and pectin, are all significantly increased compared to WT. The over-accumulation of the matrix polysaccharides in the *drmy1* mutant may impede cell expansion during organ development, leading to change in organ size and shape. On the other hand, expression of genes related to cell wall biosynthesis/remodeling is changed in the *drmy1* mutant, such as xyloglucan endotransglycosylase 6 (XTR6), expansin A16 (EXPA16) and extensin 4 (EXT4), although the direct binding of DRMY1 to their promoters needs to be further studied. Second, DRMY1 may contribute to cell expansion by downregulation of a variety of genes that encode ribosomal proteins (r-proteins). Evidence from previous studies shows that ribosomes have important developmental functions in addition to their fundamental role in protein biosynthesis (Byrne 2009; Micol 2009). A study of 13 r-protein deficient mutant lines showed that these mutants all displayed smaller and narrower leaves compared to wild type due to either reduced cell number, reduced cell size or both (Horiguchi et al. 2011). Thus, it is very likely that the deficiency of r-proteins in the *drmy1* mutant is another cause for the growth defect.

Could hormones be mediators of DRMY1-regulated growth?

DRMY1 may also control cell expansion indirectly via the signaling pathways of plant hormones ethylene and ABA. Ethylene was shown to be a negative modulator of cell

`

expansion. Ethylene-responsive factors (ERFs) are downstream transcription factors in the ethylene signaling pathway, which have been shown to regulate a set of developmental processes. For instance, an activation tagging of an ethylene responsive element binding protein (EREBP)-like transcription factor *LEP* produces leaves without a petiole and abnormal inflorescence branching and silique shape. DRMY1 may mediate cell expansion indirectly through the ethylene signaling pathway, possibly in the upstream of some ERFs, which is supported by two lines of evidence. First, the promoter of *DRMY1* has a predicted ethylene-responsive motif (ATTTCAAA) and its expression is significantly reduced by treatment with ACC, an ethylene precursor, although the extent of reduction is not high. Second, a number of ERFs are up-regulated in the *drmy1* mutant, suggesting that DRMY1 may be situated upstream of these ERFs. Among these ERFs, ERF6 and ERF11 are known to repress leaf growth (Dubois et al. 2015; Dubois et al. 2013). Overexpression of ERF6 and ERF11 led to reduced leaf growth by negatively affecting both cell number and cell size, partly consistent with the observed leaf phenotype in the *drmy1* mutant. Whether ERF6 and ERF11 are downstream of DRMY1 can be further investigated by ChIP-qPCR and double mutant analysis.

Although ABA has long been considered as a growth inhibitor when applied exogenously, studies of ABA-deficient mutants in tomato and *Arabidopsis* suggests its critical role in promoting cell expansion and organ growth. In our study, we found that *DRMY1* is significantly induced by ABA and its mutation resulted in up-regulation of a number of genes in the ABA signaling pathway, such as *homeobox 7* (*HB7*), which is a putative transcription activator. *AtHB7* is proposed to act as a negative regulator of growth and cell expansion. Constitutive overexpression of *AtHB7* led to reduction in

`

inflorescence stem and leaf cell expansion (Hjellström et al. 2003), partially resembling *DRMY1*'s phenotype. It deserves further examination as to whether DRMY1 functions through negative regulation of *HB7*.

Presumable role of DRMY1 in plant stress responses

Besides the fundamental role of DRMY1 in organ development, DRMY1 may also play a role in plant stress responses, as evidenced by enrichment of many GO terms related to a wide spectrum of stress responses among the up-regulated genes in *drmy1* mutant, including "response to chitin", "response to water deprivation", "response to cold", "response to wounding", "response to salt stress", "response to osmotic stress" and "response to jasmonic acid". A previous study showed that plants have evolved a fine-tuned balance of the growth-defense tradeoff given their sessile lifestyle (Chaiwanon et al. 2016). Although in this study we focused on the role of DRMY1 in regulating organ development, it would be very interesting to determine whether DRMY1 performs a function in plant response to biotic and abiotic stresses and balancing growth-defense tradeoff in the future.

Taking these results together, we suggest that DRMY1 plays a very important role in controlling cell expansion in *Arabidopsis*. We proposed a hypothetical model accounting for DRMY1's action in cell expansion and organ development (Figure 2.19). DRMY1 may affect cell expansion directly by regulating cell wall biosynthesis/remodeling and ribosome biogenesis or indirectly through ethylene and ABA signaling pathways.

`

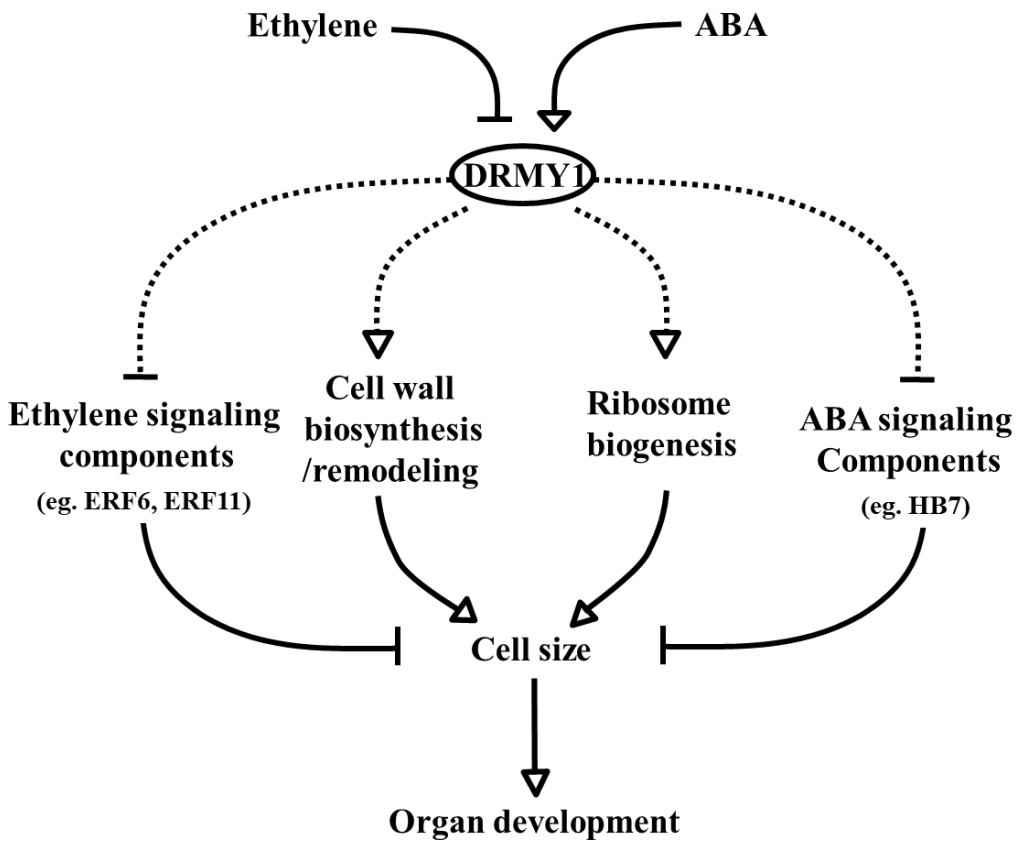

Figure 2.19. Proposed model of DRMY1-regulated cell expansion. DRMY1 modulates cell expansion either directly through regulating cell wall biosynthesis/remodeling and ribosome biogenesis or indirectly through ethylene and ABA signaling pathways.

In conclusion, we have identified a functional Myb-like protein controlling cell expansion and organ growth and propose a hypothetical mechanism by which it regulates cell expansion. ChIP-qPCR will be conducted in the future, which will help identify the direct binding targets of DRMY1 in combination with our RNAseq data and extend our knowledge about the regulatory pathways underlying cell expansion.

Accession Numbers

Gene sequence in *Arabidopsis thalinana* mentioned in this work can be found in Arabidopsis Information Resource (TAIR) database as the following accession numbers: DRMY1 (AT1G58220), DP1 (AT1G09710), ACTIN2 (AT3G18780), AtTBP1

`

(AT5G13820), AtTRP1 (AT5G59430), AtGRF1 (AT2G22840). The GenBank accession numbers for tobacco Ng*TRF1*, and rice *RTBP1* are AF543195 and AF242298, respectively.

`

CHAPTER THREE

COMPARATIVE TRANSCRIPTOME PROFILING PROVIDES INSIGHTS INTO PLANT SALT TOLERANCE IN SEASHORE PASPALUM (*PASPALUM VAGINATUM*)

`

Abstract

Paspalum vaginatum, a halophytic warm-seasoned perennial grass, is tolerant of many environmental stresses, especially salt stress. Physiological analysis comparing highly (Supreme) and moderately (Parish) salinity-tolerant cultivars revealed that Supreme's higher salinity tolerance is associated with higher Na^+ and Ca^{2+} accumulation under normal conditions and further increase of Na^+ under salt-treated conditions (400 mM NaCl), possibly by vacuolar sequestration. Moreover, K^+ retention under salt treatment occurs in both cultivars, suggesting that it may be a conserved mechanism for prevention of Na^+ toxicity. We sequenced the transcriptome of the two cultivars under both normal and salt-treated conditions (400 mM NaCl) using RNA-seq. *De novo* assembly of about 153 million high-quality reads and identification of Open Reading Frames (ORFs) uncovered a total of 82,608 non-redundant unigenes, of which 3,250 genes were identified as transcription factors (TFs). Gene Ontology (GO) annotation revealed the presence of genes involved in diverse cellular processes in Seashore paspalum's transcriptome. Differential expression analysis identified a total of 828 and 2,222 genes that are responsive to high salinity for Supreme and Parish, respectively. GO enrichment analysis demonstrated that genes involved in "oxidation-reduction process" and "nucleic acid binding" are significantly associated with salinity tolerance in both cultivars. Interestingly, compared to Parish, a number of salt stress induced transcription factors are enriched and show higher abundance in Supreme under normal conditions, possibly due to enhanced Ca^{2+} signaling transduction out of Na^+ accumulation, which may be another contributor to Supreme's higher salinity tolerance. Our data provide valuable molecular resources for functional studies and developing strategies to engineer plant salinity tolerance.

`

Introduction

High salinity stress, which is one of the most severe environmental stresses, impairs crop production on at least 20% of the cultivated land worldwide (Rhoades and Loveday 1990). This problem becomes increasingly severe due to the rising sea level from global warming and inappropriate irrigation practice. Salt stress inflicts not only ionic stress but also osmotic stress on plants. As a consequence of these primary effects, secondary stresses such as oxidative stress often occur (Zhu 2001). To survive against these stresses, plants have evolved a complex of mechanisms involving multiple genes and strategies at physiological, molecular and metabolic levels (Gupta and Huang 2014). As high levels of cytosolic Na^+ are toxic to plants by interfering with cellular K^+/Na^+ homeostasis and inhibiting enzyme activities, plants utilize three major mechanisms to prevent excess Na^+ accumulation in the cytoplasm: restriction of Na^+ entry into the cells, exclusion of Na^+ out of the cells and compartmentalization of excessive Na^+ into the vacuoles. Two types of plasma membrane localized transporter HKT are important salt tolerance determinants by regulating transportation of Na^+ and K^+. The Class 1 HKT transporters mediate Na^+-selective transport. The Current model in *Arabidopsis* suggests that the Class 1 HKT transporter AtHKT1 plays an essential role in protecting leaf blades from excessive accumulation of Na^+ by unloading of Na^+ from the xylem sap (Davenport et al. 2007). The Class 2 HKT transporters are suggested to mediate both Na^+ and K^+ transport (Rubio, Gassmann, and Schroeder 1995). Study of a Class 2 HKT transporter OsHKT2;1 in rice demonstrated a fail-safe mechanism of Na^+ uptake under K^+ starved rice roots (Horie et al. 2007). The plasma membrane localized Na^+/H^+ transporter Salt Overly Sensitive 1 (SOS1) and the tonoplast localized Na^+/H^+ transporter NHX are another two important

`

determinants for maintaining low cytosolic Na^+ concentration in plant cells by exporting Na^+ out of the cell and sequestration of Na^+ into the vacuoles, respectively (Apse et al. 1999; Shi et al. 2000). To neutralize the negative effect of osmotic stress imposed by high concentration of salt, plants can accumulate compatible solutes (e.g. proline, glycine betaine, sugars, mannitol, myo-inositol) and proteins (e.g. Late-embryogenesis-abundant-proteins (LEAs) and dehydrins) for osmotic adjustment or other protective functions (Munns 2005b). Most types of abiotic stresses including salinity disrupt the balance of cellular metabolism, resulting in oxidative stress with elevated level of reactive oxygen species (ROS), such as the superoxide radical anion ($O_2^{\cdot -}$), hydrogen peroxide (H_2O_2), and hydroxyl radicals ($OH^{\cdot}$). The elevated level of ROS plays a dual role in the salinity responses of plants. On one hand, the enhanced production of ROS is toxic to plants as they can cause protein and membrane lipid peroxidation, and DNA and RNA damage (Tuteja 2007). To ensure survival, plants have developed two efficient antioxidant defense systems to work in concert for ROS scavenging, which include both enzymatic and non-enzymatic machinery. Major enzymatic components include catalase (CAT), superoxide dismutase (SOD), ascorbate peroxidase (APX), glutathione peroxidase (GPX) and dehydroascorbate reductase (DHAR) while non-enzymatic antioxidants include ascorbic acid (AA), glutathione (GSH), phenolic compounds (Gill and Tuteja 2010; Das and Roychoudhury 2014). On the other hand, ROS can also act as a pivotal signaling molecule to trigger tolerance against stress (Mittler et al. 2011). For example, loss-of-function of one of the NADPH oxidase members AtrbohF, which catalyzes the production of ROS in root vasculature systems, leads to salt hypersensitivity phenotype due to the elevated root-to-shoot delivery of soil Na^+ and consequently elevated shoot Na^+ levels (Jiang et al. 2012).

`

The plant kingdom has about 1% of plant species classified as halophytes that possess capacities for salt tolerance of around 200 mM NaCl or more as a result of evolutionary adaptation to their habitats (Flowers and Colmer 2008). The inherent potentiality of halophytes to counteract the negative impact of salinity stress makes it very interesting and promising to investigate the associated mechanisms. Seashore paspalum (*Paspalum vaginatum*) is a halophytic warm-season perennial grass of the *Poaceae* family, which is native to tropical and coastal regions worldwide and is among the most salinity-tolerant turfgrass species. Previous studies show that its superior salinity tolerance is attributed to high level of photosynthesis and shoot growth rate, and tissue water maintenance through osmotic adjustment (Lee, Carrow, and Duncan 2004; Liu et al. 2011). However, little is known about the molecular mechanisms underlying its high salinity tolerance and the limited genomic information of Seashore paspalum has impeded further investigation. A recent study using the combination of 2-DE and MS technologies linked ROS detoxification and ATP biosynthesis to the superior salinity tolerance in Seashore paspalum's roots (Liu et al. 2012). Another recent study using RNA-seq provided the global transcriptome data for the Seashore paspalum cultivar 'Adalady' for the first time (Jia et al. 2015). However, no study has reported how the different cultivars of Seashore paspalum with inherent variation in their capabilities of salt tolerance undergo dynamic change of ion accumulation and how they respond to salt stress globally at the transcriptome level. This will help us better understand plant salinity tolerance mechanism at the physiological and molecular level and identify salt stress-related genes for functional study and application in the future.

`

In this study, we monitored the dynamic change of Na^+, K^+ and Ca^{2+} accumulation before and after salt treatment comparing two cultivars of Seashore paspalum. One is called Supreme, which is the most salinity-tolerant cultivar of all commercially grown paspalums (http://georgiacultivars.com/cultivars/seaisle-supreme-paspalum). Another cultivar is called Parish, which is a moderately salinity-tolerant cultivar. We also applied RNA-seq analysis to reveal differences in gene expression between two cultivars under normal conditions and when they are exposed to salt stress. To our knowledge, this study provides the first transcriptome profile for Seashore paspalum under salt stress. By comparing ion dynamics and expression profiling data of the two cultivars under both non-stressed and salt-stressed conditions, this study provides a new insight into the physiological and molecular mechanisms of high salinity tolerance in halophytes and establish a solid foundation for future studies of genes involved in salinity tolerance.

Methods

Plant materials growth and treatment

Two cultivars of Seashore paspalum, Supreme and Parish were clonally propagated from the same number of tillers in pure sand for 8 weeks in 10 x 10 cm square containers. They were maintained in the growth room under 14 hours of photoperiod with 350 to 450 μmol m^{-2} s^{-1} illumination. Temperature and humidity were maintained at 25°C and 30% during the daytime and 17°C and 60% at night. For the morphological observation of plant performance under salt stress, Supreme and Parish were immersed in a 400 mM NaCl solution supplemented with 0.2 g/l water soluble fertilizer (20:10:20 nitrogen:phosphorus:potassium; Scotts). Twelve days after salt treatment, plants were recovered from salt stress by washing off NaCl and watering with 0.2 g/l water soluble

`

fertilizer every other day. Plants were photographed 8 days after recovery for documentation. To collect salt-treated samples for RNA-seq, salt treatment was performed by washing the sand off roots and dipping them in 400 mM NaCl solution supplemented with 0.2 g/l water soluble fertilizer for 1 hour.

Measurement of Na^+, K^+ and Ca^{2+} content

For Na^+, K^+ and Ca^{2+} content measurements, leaves from Supreme and Parish were collected before and after a 7-day treatment of 400 mM NaCl solution supplemented with 0.2 g/l water soluble fertilizer, and then dried for 48 hours at 80°C. Na^+, K^+ and Ca^{2+} content was determined based on previous protocols (Haynes 1980; Plank 1992).

RNA isolation and cDNA library preparation

One hundred milligrams of mixed tissue (leaf:stem:root =1:1:1) was collected immediately after treatment and ground into a fine power for RNA exaction using Trizol (Invitrogen) following the manufacturer's protocol. Total RNA was then treated with DNase to eliminate DNA contamination and purified using the RNeasy Mini Kit (Qiagen). Total RNA fractions with 260/280 absorbance of 2.0 and RNA integrity of 8.0 or higher were used for further experiments. cDNAs were then synthesized for RNA-seq library construction using the Illumina TruSeq® RNA Sample Preparation Kit with Oligo-dT beads capturing polyA tails. Eight cDNA libraries were constructed, which were divided into 4 groups with each of the group having two biological replicates: untreated Supreme (S_{normal}-1, S_{normal}-2), salt-treated Supreme (S_{salt}-1, S_{salt}-2), untreated Parish (P_{normal}-1, P_{normal}-2), and salt-treated Parish (P_{salt}-1, P_{salt}-2). RNA extraction and an additional 4 cDNA libraries were also constructed for drought-treated Supreme ($S_{drought}$-1, $S_{drought}$-2) and drought-treated Parish ($P_{drought}$-1, $P_{drought}$-2). The reads generated from these drought-

`

treated samples were included in the *de novo* transcriptome assembly to increase assembly continuity but were not used for other analyses in this paper.

Transcriptome sequencing and *de novo* assembly

Paired-end sequencing of cDNA libraries was performed using the HiSeq 2000 (Illumina Technologies) platform. The raw reads were evaluated for quality using FastQC (version: 0.11.3, http://www.bioinformatics.babraham.ac.uk/projects/fastqc/), and then trimmed to remove adapter sequences and low quality bases using Trimmomatic 0.32 (Bolger, Lohse, and Usadel 2014). The trimmed reads were used to generate a *de novo* assembly using Trinity (version: trinityRNA-seq-2.1.1) with default k-mer length of 25 (Grabherr et al. 2011).

ORF identification and sequence annotation

The next step in the pipeline is identifying potential protein coding genes by using TransDecoder (version: TransDecoder-2.0, http://transdecoder.github.io/). CD-HIT (version: cd-hit-v4.6.6) (Li and Godzik 2006) clustered the remaining genes with a sequence identity ≥ 95%. This generated a final set of 82,608 potential protein coding unigenes. To obtain sequence annotation, they were blasted against the NCBI non-redundant (nr) protein database by using NCBI-BLAST+ (version: ncbi-blast-2.3.0+) (Camacho et al. 2009) with an E-value cutoff of $1E^{-5}$ and putative GO terms were assigned by running Blast2GO software (version 3.3) (Conesa et al. 2005). Unigenes were blasted against the plant transcription factor database (PlantTFDB) (Jin et al. 2017; Jin et al. 2015) (http://planttfdb.cbi.pku.edu.cn/index.php?sp=Ath) with E-value cutoff of $1E^{-5}$ to identify transcription factors in Seashore paspalum's transcriptome. The blast results were then parsed by a Python script to count the number of unigenes that have at least one hit to the

`

putative transcription factors of *Arabidopsis* and *Oryza* in different transcription factor families.

Differential expression analysis

To identify differentially expressed genes, the trimmed reads from each sample were aligned to the 82,608 reference unigenes and an abundance estimation for each unigene in each sample was then calculated with RSEM software (version: RSEM-1.2.28) (Li and Dewey 2011). The expected counts generated by RSEM were then used as input for differential expression analysis using DEseq2 software (Love, Huber, and Anders 2014). Four comparisons were conducted: 1) untreated Supreme (S_{normal}) versus untreated Parish (P_{normal}), 2) salt-treated Supreme (S_{salt}) versus untreated Supreme (S_{normal}), 3) salt-treated Parish (P_{salt}) versus untreated Parish (P_{normal}), and 4) salt-treated Supreme (S_{salt}) versus salt-treated Parish (P_{salt}). Differentially expressed genes are defined by a $\log_2$ fold change (FC) ≥ 1.0 or ≤ -1.0, P value ≤ 0.01, and an adjusted P value ≤ 0.01. To determine the differentially expressed transcription factors, the generated lists of DEGs were overlapped with the potential transcription factors identified in Seashore paspalum's transcriptome described above using a R script, and where they intersected defined the differentially expressed transcription factors.

GO enrichment analysis

Given that Seashore paspalum does not have an official ontology, a custom annotation list was generated as described above. To find significantly enriched GO terms, we calculated the P value from a Fisher's exact test between the frequency of the GO terms for genes in the differentially expressed set and the custom annotation serving as our background by using a scipy.stats package in a Python script (Jones, Oliphant, and Peterson

`

2014). The P value threshold was set as $P \leq 0.05$. To account for multiple testing, we adjusted the P values using a R script and used the Bonferroni value ≤ 0.05.

qRT-PCR confirmation

RNA from each sample was used for cDNA biosynthesis using ProtoScript II Reverse Transcriptase (Biolabs), according to the manufacturer's protocols. Quantitative real-time PCR (qRT-PCR) was conducted using SYBR Green (Thermo Fisher) in Bio-Rad iQ5 real-time PCR system (Bio-Rad) with the following thermal cycling conditions: 2mins denaturation at 95℃, followed by 40 cycles of 95℃ denaturation for 20s, 62℃ annealing for 20s and 72℃ extension for 15s. The dissociation curve was then generated by gradually heating the amplicons from 55 to 95℃. Actin was used as endogenous control for data normalization. The relative gene expression changes were calculated based on the $2^{-\Delta\Delta CT}$ method (Livak and Schmittgen 2001). qRT-PCR was carried out in three technical and two biological replicates.

Results

Ion dynamics of Supreme and Parish under normal and salt-treated conditions

Seashore paspalum (*Paspalum vaginatum*) is a halophytic warm-season perennial grass. Many studies have shown that Seashore paspalum is among the most salinity-tolerant warm-season turfgrass species with a NaCl tolerance threshold of 474.0 mM (Liu et al. 2009). To study the mechanisms underlying Seashore paspalum's high salt tolerance, Supreme, which is the most salinity-tolerant cultivar of all commercially grown paspalums (http://georgiacultivars.com/cultivars/seaisle-supreme-paspalum), and Parish, which is a moderately salinity-tolerant cultivar were used for morphological, physiological and comparative transcriptomics studies. Firstly, we compared their morphological differences

`

in response to salt treatment. Supreme and Parish grown under the same conditions were exposed to 400 mM NaCl solution. After a 12-day treatment, chlorotic leaves were clearly observed in Parish while Supreme was not strongly affected, indicative of a more tolerant trait of Supreme than Parish (Figure 3.1B). Moreover, Supreme also has a better recovery capacity than Parish after salt treatment (Figure 3.1C). To reveal possible physiological mechanisms of differential performance of Supreme and Parish under salt stress, we measured their leaf ion contents under normal and salt-stressed conditions. Supreme has significantly higher Na^+ content than Parish under both conditions, whereas their K^+ contents are similar, and remain the same even upon exposure to salinity (Figure 3.1D, 3.1E). In addition, Supreme has significantly higher Ca^{2+} content than Parish under normal conditions, but their Ca^{2+} contents are similar after treatment with salt (Figure 3.1F). The demonstration of higher salt tolerance of Supreme and its physiological characteristics implies the importance of the associated genetic underpinnings.

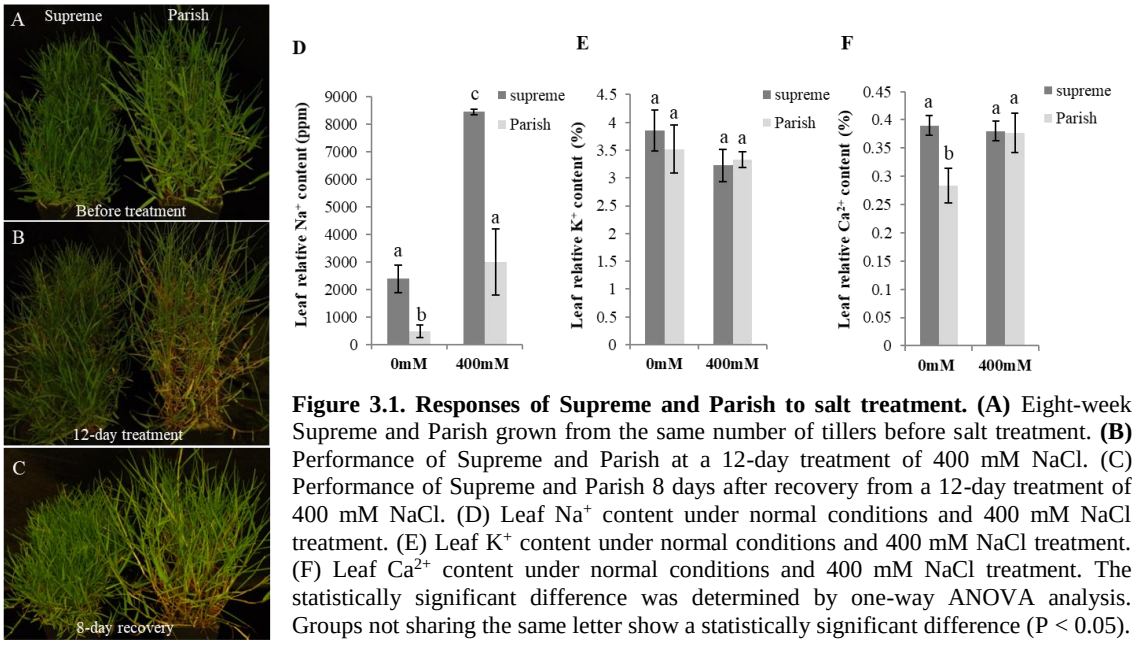

Figure 3.1. Responses of Supreme and Parish to salt treatment. (A) Eight-week Supreme and Parish grown from the same number of tillers before salt treatment. **(B)** Performance of Supreme and Parish at a 12-day treatment of 400 mM NaCl. (C) Performance of Supreme and Parish 8 days after recovery from a 12-day treatment of 400 mM NaCl. (D) Leaf Na^+ content under normal conditions and 400 mM NaCl treatment. (E) Leaf K^+ content under normal conditions and 400 mM NaCl treatment. (F) Leaf Ca^{2+} content under normal conditions and 400 mM NaCl treatment. The statistically significant difference was determined by one-way ANOVA analysis. Groups not sharing the same letter show a statistically significant difference ($P < 0.05$).

`

To characterize and compare the transcriptome response of Supreme and Parish under salt treatment, we treated plants with 400 mM NaCl for 1 hour. We use this condition because it was suggested that genes that rapidly changed expression upon salt stress should be important for salt tolerance (Taji et al. 2004). The following four types of samples were used for RNA-seq: untreated Supreme (S_{normal}-1, S_{normal}-2), salt-treated Supreme (S_{salt}-1, S_{salt}-2), untreated Parish (P_{normal}-1, P_{normal}-2) and salt-treated Parish (P_{salt}-1, P_{salt}-2). Illumina sequencing of indexed and pooled RNA with polyA tails generated a total of 80.29 million and 78.88 million paired-end reads with a single read length about 101bp for Supreme and Parish, respectively. The RNA-seq reads with quality scores were deposited in the NCBI Sequence Read Archive (SRA) with bioproject accession number PRJNA395934. An overview of the sequencing and assembly results are represented in Table 3.1. Among these raw reads, 95.89% and 95.77% remained after trimming for Supreme and Parish, respectively, which were then *de novo* assembled into one reference transcriptome using Trinity (version: trinityRNA-seq-2.1.1). *De novo* assembly of mixed trimmed reads generated 342,165 Trinity transcripts with an average length of 784 bp and N50 value of 1,339 bp, and a total of 244,926 Trinity genes with average length of 580 bp and N50 value of 761 bp. GC content, which is an important indicator of the gene and genomic composition as well as DNA stability is 49.7% in Seashore paspalum's transcriptome, which is similar to the transcriptome GC composition of other monocot plants such as rice (51.1%), *Triticum aestivum* (51.4%) (Kuhl et al. 2004; Goyal et al. 2016). In comparison with previously reported 32,603 Trinity genes from transcriptome analysis of Seashore paspalum's cultivar 'Adalady', this study has generated more Trinity gene

`

sequences, thus providing additional genomic resources that can be exploited for gene discovery and functional study (Jia et al. 2015).

Table 3.1. Summary of transcriptome sequencing and *de novo* assembly

Items	Supreme	Parish
Total raw reads	80,288,751	78,867,558
Total clean reads	76,986,554	75,528,530
Total Trinity transcripts	342,165	
Total Trinity genes	244,926	
Average transcript/gene length (bp)	783.7/580	
Transcript N50/gene N50 (bp)[a]	1,339/761	
Average GC content (%)	49.69	

[a] Transcript N50/gene N50 is defined as the length of the longest transcript/gene such that all transcripts/genes of the same or above that length compose at least 50% of the assembled base pairs.

ORF identification

169,391 ORFs (49.5% of all Trinity transcripts) were identified among 342,165 Trinity transcript sequences using TransDecoder (version: TransDecoder-2.0, http://transdecoder.github.io/) based on the following criteria: a minimum length of 100 amino acids ORF is found in a transcript sequence; an ORF with highest log-likelihood

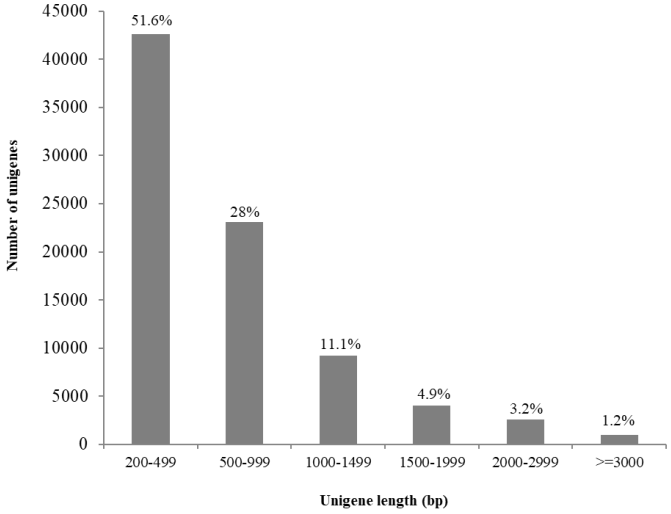

Figure 3.2. Size distribution of unigenes. Six groups of unigenes with different range of length were shown. The percentages of unigenes in each group out of the total unigenes (82,608) were indicated above each column.

`

score and greater than 0 is reported; if a shorter ORF is fully encapsulated by a longer ORF, the longer one is reported; any ORF that does not meet the above criteria but has homology to the UniProt and Protein family (Pfam) databases will also be retained. Using CD-HIT software (version: cd-hit-v4.6.6) (Li and Godzik 2006), the 169,391 ORFs were clustered into 82,608 unigenes. The length distribution of the unigenes is shown in Figure 3.2. Approximately 48.4% and 20.5% of the unigenes had a length >= 500bp and >= 1,000bp, respectively.

Functional annotation of Seashore paspalum's transcriptome

Homology-based functional annotation of the Seashore paspalum unigenes was then carried out. Distribution of the annotated unigenes in each database was shown in Table 3.2. 82,608 unigenes were blasted against the NCBI non-redundant (nr) protein database using Blastx with an E-value cutoff of $1E^{-5}$. 65,540 (79.3%) out of the 82608 unigenes showed homology to the nr protein sequences. E-value distribution of blast results was shown in Supplemental Figure B-1. The best blastx hits against the nr database were then imported to Blast2GO software (version 3.3) (Conesa et al. 2005) for gene ontology (GO) classification and the result was shown in Figure 3.3. Among 82,608 unigenes, 36,387 unigenes (44%) were successfully annotated with 16 GO terms (level 2) and classified into three ontologies: biological process (BP, Figure 3.3A), cellular component (CC, Figure 3.3B), and molecular function (MF, Figure 3.3C). Within the BP category, genes involved in metabolic process (16946), cellular response (14342), single-organism process (8922) and biological regulation (3787) are highly represented. The CP category mainly comprises genes involved in membrane (10287), cell (10050), cell part (9904),

`

membrane part (8528) and organelle (6716). Under MF, catalytic activity (15615) was the most abundant GO term, followed by binding (15411).

Table 3.2. Summary of annotation statistics of Seashore paspalum's transcriptome

Database	Unigenes having homologous sequence	
	Number	Hit (%)
nr	65540	79.3%
Interpro	32860	39.8%
GO	36387	44%
TF	3250	4%

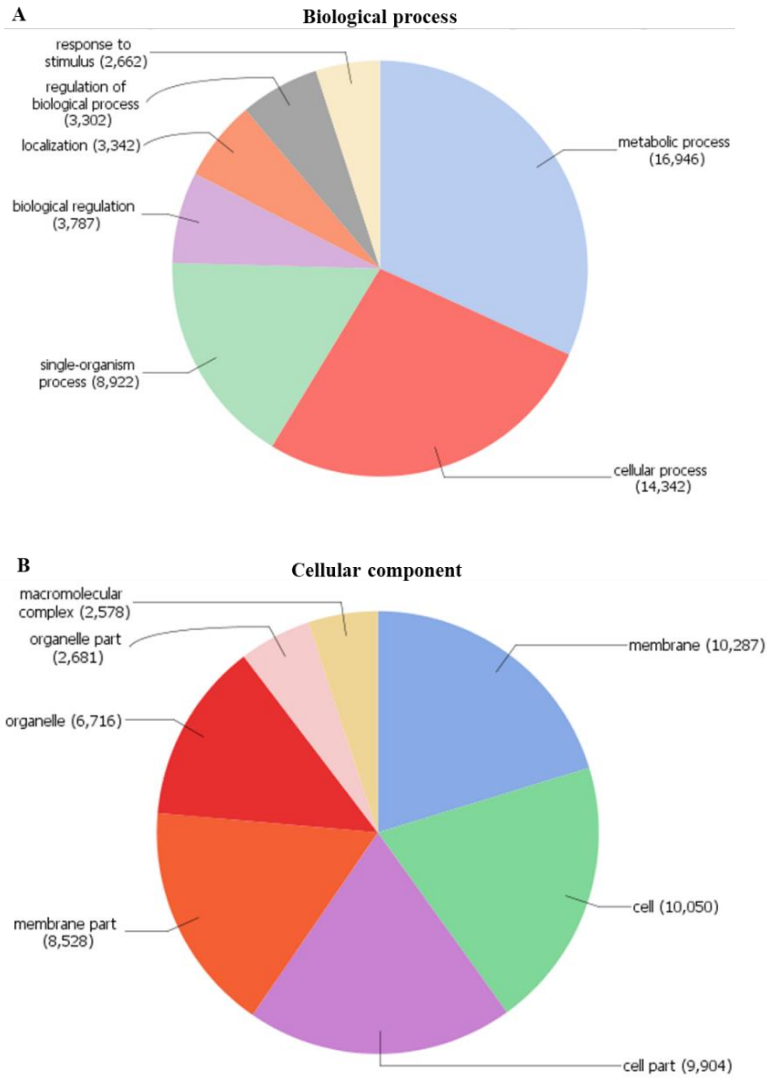

`

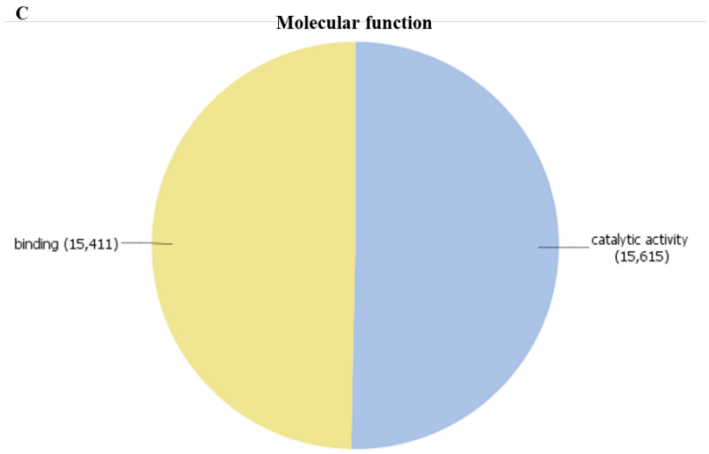

Figure 3.3. Pie chart representation of Seashore paspalum's transcriptome GO annotation on level 2. (A) Biological process; **(B)** Cellular component; **(C)** Molecular function. The number besides each GO term represents the number of sequences belonging to it.

To compare the gene repertoire of Supreme paspalum to other plant species, we aligned the unigenes against the nr protein database and performed the species distribution of the unigenes using Blast2GO software. As shown in Supplemental Figure B-2, the five top-hit species that best match the sequences of Supreme paspalum unigenes are *Setaria italica*, *Sorghum bicolor*, *Zea mays*, *Oryza sativa Japonica* Group and *Brachypodium distachyon*, all of which belong to the *Poaceae* family.

Identification of transcription factors in Seashore paspalum's transcriptome

Transcription factors (TFs) play a vital role in regulating plant stress response as important regulatory elements. To identify potential TFs in the Seashore paspalum's transcriptome, 82,608 unigenes were searched against the PlantTFDB (Jin et al. 2017; Jin et al. 2015) using Blastx with E-value cutoff of $1E^{-5}$. There are 3,250 transcripts that have at least one hit to the *Arabidopsis* and *Oryza* TFs, representing about 4% of the total unigenes and covering 68 putative TF families (Supplemental Table S1). The TF gene families with ten or more unigenes identified in the Supreme Paspalum transcriptome are

`

presented in Figure 3.4, among which the five most abundant categories are Myb (419), followed by WRKY (370), G2-like (268), bZIP (240), and bHLH (185).

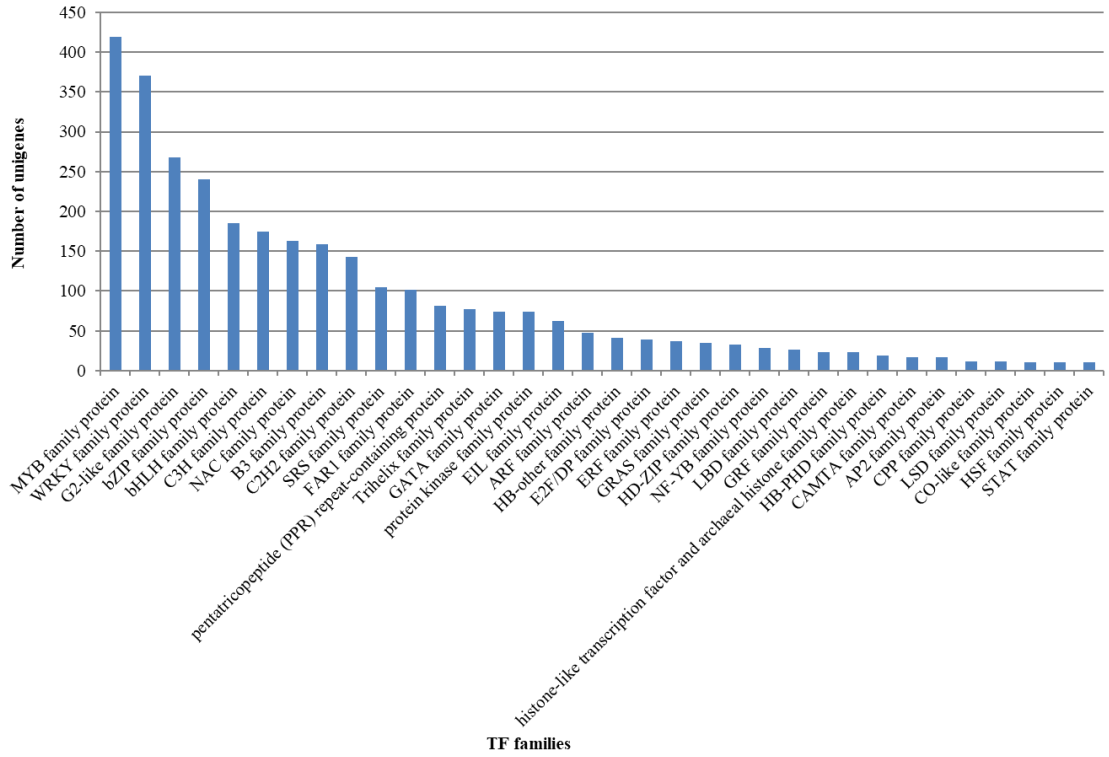

Figure 3.4. Distribution of transcription factors (TFs) in Seashore paspalum's transcriptome. A total of 3,250 TF unigenes were identified by blastx against *Arabidopsis* and rice TF database with a E-value cutoff of $1E^{-5}$. 34 TF families with ten or more unigenes were plotted.

Differentially expression analysis for Supreme and Parish under salt treatment

To compare gene expression levels in the control and salt-treated samples, the trimmed reads in each library were mapped to the 82,608 reference unigenes and the abundance of each unigene in different libraries was estimated using the RSEM software (version: RSEM-1.2.28) (Li and Dewey 2011). The expected count data produced by RSEM was used to identify DEGs with DEseq2 software (Love, Huber, and Anders 2014). To test reproducibility among two biological replicates, a MDS plot (Figure 3.5) was generated for the control and salt-treated samples of Supreme and Parish. The fact that our biological replicates cluster so closely to each other on an ordination plot demonstrates

`

their low inter-sample variability and therefore makes them generalizable to the overall population. Two comparisons were conducted: salt-treated Supreme versus untreated Supreme and salt-treated Parish versus untreated Parish. DEGs are defined by a P value ≤ 0.01, an adjusted P value ≤ 0.01 and $\log_2$ fold change (FC) ≥ 1.0 or ≤ -1.0. As shown in Figure 3.6A, a total of 828 unigenes were differentially expressed for salt-treated Supreme while 2,222 unigenes were differentially expressed for salt-treated Parish. 34 and 107 DEGs were identified to be potential transcription factors for Supreme and Parish, respectively (Figure 3.6B). Overlapping of two DEGs lists generated 231 unigenes that were commonly regulated by salt in both plants, out of which 12 unigenes were potential transcription factors (Figure 3.6A and 3.6B). The common regulated transcription factors in both cultivars under salt treatment are listed in Supplemental Table 2. We also confirmed the DEGs by qRT-PCR, indicating that our RNA-seq data and differential expression analysis were reliable in this study.

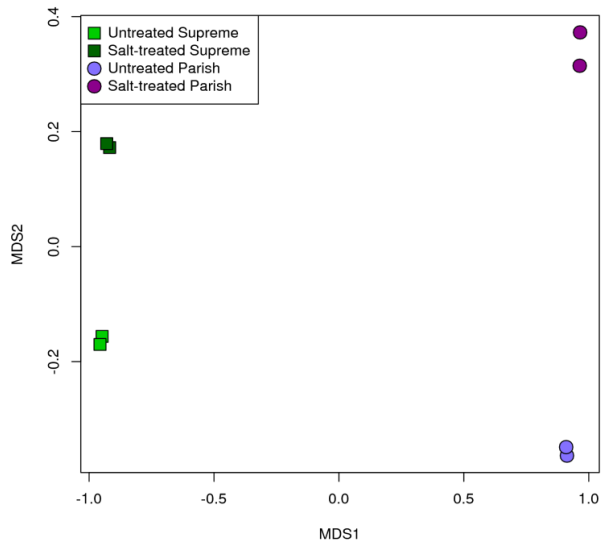

Figure 3.5. MDS plot showing reproducibility among two biological replicates of our RNA-seq samples. The MDS plot was generated by using the filtered and normalized expected counts generated by RSEM to ordinate samples in multidimensional space based on differences in expression values. The close clustering of biological replicates indicates a high degree of consistency across all genes.

`

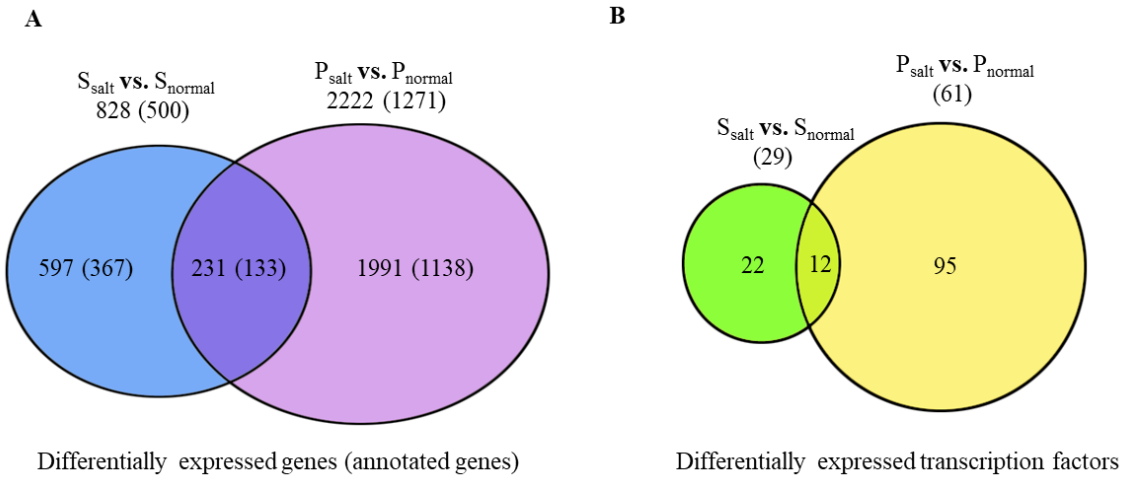

Figure 3.6. Venn diagram showing the number of common and specific DEGs with 2-fold change or above for Supreme and Parish under salt treatment. The number of common and specific DEGs **(A)** and transcription factors **(B)** with 2-fold change or above, P value ≤ 0.01, and adjusted P value ≤ 0.01 were shown in the overlapping and non-overlapping regions, respectively. Numbers within parentheses represent DEGs that have assigned GO terms. S_{normal}: untreated Supreme; S_{salt}: salt-treated Supreme; P_{normal}: untreated Parish; P_{salt}: salt-treated Parish.

Gene enrichment analysis of DEGs identified in Supreme and Parish under salt treatment

To inspect the biological relevance of DEGs, GO terms were assigned using Blast2GO. Five-hundred out of 828 DEGs (60.4%) were annotated for Supreme while 1,271 out of 2,222 DEGs (57.2%) were annotated for Parish (Figure 3.6A). GO enrichment analysis was then conducted to extract the over-represented GO terms that are significantly associated with the identified DEGs in Supreme and Parish under salt treatment, respectively. As shown in Figure 3.7A, genes that are up-regulated in salt-treated Supreme are involved in "oxidation-reduction process" and "nucleic acid binding" while genes that are down-regulated in salt-treated Supreme are involved in "regulation of transcription", "transcription, DNA-templated", "defense response" and "transcription factor activity". GO functional enrichment analysis of DEGs in salt-treated Parish revealed that they are

`

involved in much broader processes (Figure 3.7B). Many biological processes that are associated with salt response are induced in Parish, such as “oxidation-reduction process”, “cellular oxidant detoxification”, “response to oxidative stress”. Interestingly, “oxidation-reduction process” and “nucleic acid binding” are the most significantly enriched GO terms in the Biological Process (BP) category and Molecular Function (MF) category, respectively for up-regulated genes in both Supreme and Parish, implying their importance in salt tolerance in both cultivars. DEGs involved in “oxidation-reduction process” and “nucleic acid binding” are listed in Table 3.3 and Table 3.4, respectively.

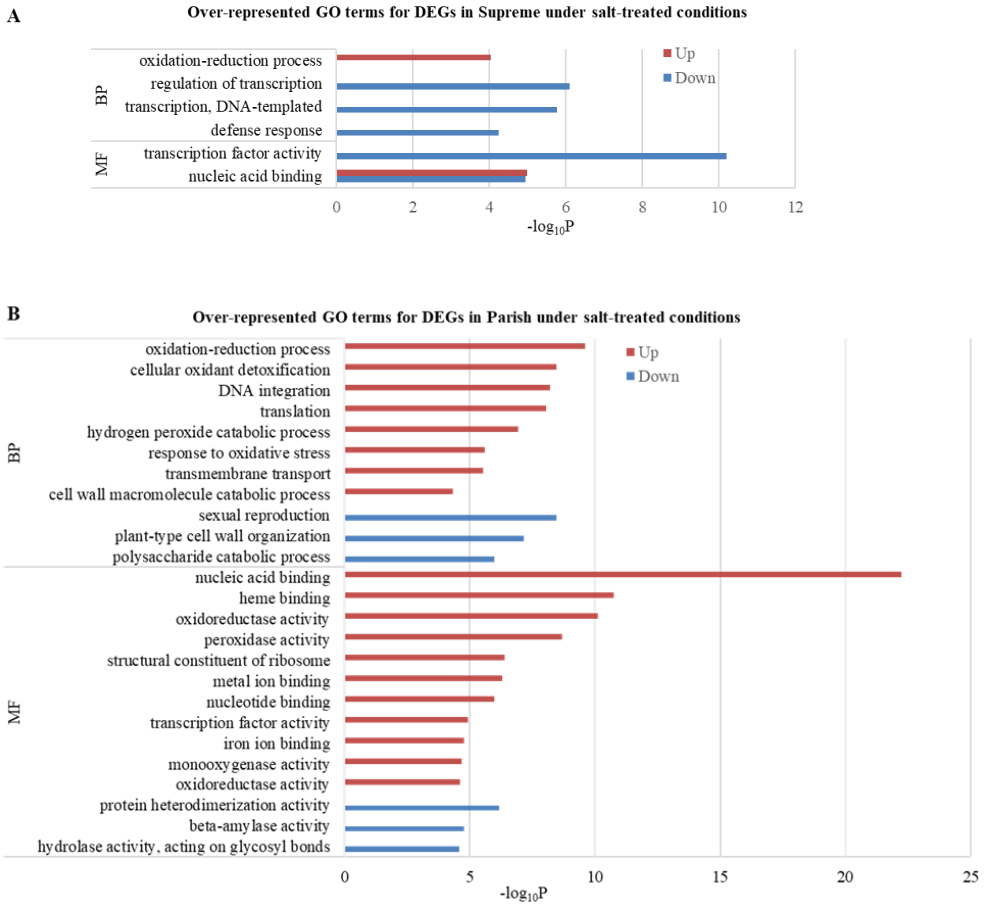

Figure 3.7. Functional enrichment analysis for DEGs identified in salt-treated Supreme and Parish, respectively. The y-axis shows significantly enriched gene ontology (GO) terms ($P \leq 0.05$, Bonferroni ≤ 0.05) in two categories, Biological Process (BP) and Molecular Function (MF). The x-axis shows the $-\log_{10}P$ values of these terms. Red bars, up-regulated genes; blue bars, down-regulated genes.

`

Table 3.3A. DEGs involved in "oxidation-reduction process" in salt-treated Supreme

Gene_ID	Description	Log_2FC	P value	Adjusted P value
m.219752	alcohol dehydrogenase [Aureimonas sp. Leaf324]	10.06	5.68E-12	9.88E-10
m.162586	dimeric dihydrodiol dehydrogenase, putative [Phytophthora infestans T30-4]	8.99	3.19E-09	3.25E-07
m.198035	Alternative oxidase [Phytophthora nicotianae]	8.93	1.67E-09	1.8E-07
m.57181	bifunctional acetaldehyde-CoA/alcohol dehydrogenase [Thermosynechococcus sp. NK55a]	8.81	3.25E-09	3.3E-07
m.77775	hypothetical protein PHYSODRAFT_358973 [Phytophthora sojae]	8.68	6.43E-09	6.17E-07
m.254086	hypothetical protein L915_21056 [Phytophthora parasitica]	8.63	1.1E-08	9.95E-07
m.321045	6-phosphogluconate dehydrogenase (decarboxylating), partial [Phytophthora parasitica]	8.51	1.94E-08	1.64E-06
m.181937	hypothetical protein PHYSODRAFT_305881 [Phytophthora sojae]	8.35	2.68E-08	2.17E-06
m.203632	peroxiredoxin [Aphanomyces invadans]	8.12	1.01E-07	7.26E-06
m.294690	succinate dehydrogenase, cytochrome b556 subunit [Aphanomyces astaci]	7.98	1.97E-07	0.0000131
m.39608	hypothetical protein PHYSODRAFT_352121 [Phytophthora sojae]	7.94	2.56E-07	0.0000167
m.138453	pyruvate dehydrogenase (acetyl-transferring) E1 component, alpha subunit [Aphanomyces astaci]	7.90	0.0000002	0.0000133
m.37144	unnamed protein product [Albugo laibachii Nc14]	7.82	4.23E-07	0.0000262
m.16736	hypothetical protein PHYSODRAFT_283992 [Phytophthora sojae]	7.72	9.29E-07	0.0000528
m.37206	NADH dehydrogenase flavoprotein 1, mitochondrial precursor [Phytophthora infestans T30-4]	7.69	9.66E-07	0.0000545
m.99482	unnamed protein product [Albugo laibachii Nc14]	7.67	6.53E-07	0.0000383
m.183628	glutathione-disulfide reductase [Aphanomyces astaci]	7.64	1.39E-06	0.0000749
m.129505	hypothetical protein SORBIDRAFT_05g000680 [Sorghum bicolor]	7.47	1.11E-06	0.0000619
m.106518	glyceraldehyde-3-phosphate dehydrogenase, type I, partial [Phytophthora parasitica]	7.45	2.76E-06	0.0001386
m.121913	hypothetical protein PHYSODRAFT_285408 [Phytophthora sojae]	7.39	0.0000242	0.000937
m.39609	hypothetical protein PPTG_09100 [Phytophthora parasitica INRA-310]	7.37	0.0000078	0.0003505
m.272094	succinate dehydrogenase [ubiquinone] iron-sulfur subunit [Saprolegnia diclina VS20]	7.19	7.58E-06	0.0003423
m.272278	manganese superoxide dismutase putative [Albugo laibachii Nc14]	7.12	0.0000324	0.0012105
m.181668	isocitrate dehydrogenase, NADP-dependent [Phytophthora parasitica P1976]	6.88	0.0000468	0.0016592
m.225391	enoyl-ACP reductase [Pedosphaera parvula]	6.72	0.0001661	0.0049238
m.181849	hypothetical protein H310_08590 [Aphanomyces invadans]	6.61	0.0001954	0.0056474
m.112242	hypothetical protein F442_14819 [Phytophthora parasitica P10297]	6.61	0.0001636	0.0048601
m.273529	hypothetical protein BATDEDRAFT_10803 [Batrachochytrium dendrobatidis JAM81]	6.58	0.0001378	0.004218
m.264186	PREDICTED: cytochrome P450 71D8-like [Setaria italica]	3.33	2.18E-06	0.0001116
m.26238	PREDICTED: DIBOA-glucoside dioxygenase BX6-like [Setaria italica]	2.91	2.67E-14	6.33E-12
m.188036	hypothetical protein SORBIDRAFT_05g022340 [Sorghum bicolor]	2.87	1.31E-13	2.85E-11
m.52678	PREDICTED: peroxidase 2-like [Zea mays]	2.58	4.5E-13	9.29E-11
m.137462	hypothetical protein BRADI_4g09040 [Brachypodium distachyon]	2.53	3.41E-14	7.95E-12
m.105343	hypothetical protein SORBIDRAFT_01g007240 [Sorghum bicolor]	2.52	2.77E-19	1.31E-16
m.244824	PREDICTED: thioredoxin M-type, chloroplastic-like [Setaria italica]	2.39	1.2E-09	1.34E-07
m.237571	PREDICTED: peroxidase 2-like [Setaria italica]	2.23	0.0000136	0.0005707
m.266076	hypothetical protein SORBIDRAFT_07g001280 [Sorghum bicolor]	2.01	1.36E-08	0.0000012
m.150499	aldehyde dehydrogenase 5 [Zea mays]	1.96	7.18E-13	1.44E-10
m.126273	PREDICTED: peroxidase 57-like [Setaria italica]	1.96	0.0003207	0.0085632
m.107171	replicase [Lolium latent virus]	1.83	1.28E-10	1.75E-08

`

m.64522	hypothetical protein SORBIDRAFT_03g034400 [Sorghum bicolor]	1.77	2.33E-12	4.35E-10
m.245096	PREDICTED: peroxidase 1 [Setaria italica]	1.76	3.19E-12	5.82E-10
m.206325	uncharacterized protein LOC107522037 [Zea mays]	1.74	0.0002303	0.0064728
m.108821	PREDICTED: peroxidase 2 [Setaria italica]	1.73	1.27E-06	0.0000693
m.245166	PREDICTED: cytochrome P450 78A9-like [Setaria italica]	1.68	2.24E-14	5.4E-12
m.14787	uncharacterized protein LOC100283169 [Zea mays]	1.66	1.85E-45	7.65E-42
m.285938	PREDICTED: peroxidase 72-like [Setaria italica]	1.57	4.93E-09	4.83E-07
m.29517	PREDICTED: plant cysteine oxidase 2-like [Setaria italica]	1.51	7.8E-08	5.75E-06
m.151533	PREDICTED: cytochrome P450 CYP72A219-like [Setaria italica]	1.50	0.0001813	0.0053016
m.122847	hypothetical protein SORBIDRAFT_10g006050 [Sorghum bicolor]	1.47	0.0000608	0.0020866
m.29512	PREDICTED: plant cysteine oxidase 2-like [Setaria italica]	1.45	4.64E-15	1.2E-12
m.29518	PREDICTED: plant cysteine oxidase 2-like [Setaria italica]	1.38	8.63E-09	8.01E-07
m.150497	hypothetical protein SETIT_000898mg [Setaria italica]	1.31	0.0002972	0.0080241
m.34834	siroheme uroporphyrinogen methyltransferase 1 [Zea mays]	1.21	6.87E-10	8.12E-08
m.239595	hypothetical protein SORBIDRAFT_04g034160 [Sorghum bicolor]	1.18	1.49E-45	6.76E-42
m.218596	PREDICTED: peroxidase 2-like [Setaria italica]	1.13	1.63E-12	3.08E-10
m.83369	PREDICTED: geraniol 8-hydroxylase-like [Setaria italica]	1.11	4.55E-08	3.53E-06
m.206977	uncharacterized protein LOC100273624 [Zea mays]	1.05	0.0000361	0.0013296
m.203926	hypothetical protein SORBIDRAFT_02g034370 [Sorghum bicolor]	1.02	6.22E-36	1.29E-32

Table 3.3B. DEGs involved in "oxidation-reduction process" in salt-treated Parish

Gene_ID	Description	Log_2FC	P value	Adjusted P value
m.282685	hypothetical protein SORBIDRAFT_05g003100 [Sorghum bicolor]	4.38	7.78E-19	4.77E-17
m.282690	PREDICTED: cytochrome P450 94C1-like [Setaria italica]	4.17	3.08E-30	3.97E-28
m.198771	putative cytochrome P450 superfamily protein, partial [Zea mays]	4.01	0.0006585	0.004989
m.74203	PsbA (chloroplast) [Bambusa oldhamii]	3.87	0.0000939	0.0008965
m.267635	hypothetical protein SORBIDRAFT_05g003100 [Sorghum bicolor]	3.84	3.61E-15	1.56E-13
m.187403	PREDICTED: 2'-deoxymugineic-acid 2'-dioxygenase-like [Setaria italica]	3.78	1.6E-91	2.19E-88
m.283169	polyphenol oxidase [Setaria italica]	3.66	0.0010859	0.0077061
m.204080	hypothetical protein SORBIDRAFT_01g030560 [Sorghum bicolor]	3.44	6.3E-11	1.69E-09
m.154967	PREDICTED: cytochrome P450 734A6-like [Setaria italica]	3.30	6.18E-23	5.02E-21
m.176435	cytochrome P450 94C1-like [Zea mays]	3.20	1.03E-06	0.0000151
m.44266	hypothetical protein SORBIDRAFT_09g021040 [Sorghum bicolor]	3.12	0.000592	0.0045424
m.17513	PREDICTED: cytochrome P450 734A5-like [Setaria italica]	3.11	5.83E-06	0.0000728
m.26238	PREDICTED: DIBOA-glucoside dioxygenase BX6-like [Setaria italica]	3.05	7.45E-11	1.98E-09
m.137462	hypothetical protein BRADI_4g09040 [Brachypodium distachyon]	2.93	1.36E-08	2.64E-07

`

m.282702	PREDICTED: cytochrome P450 94C1-like [Setaria italica]	2.88	0.000011	0.0001303
m.174331	NADH dehydrogenase subunit 5 (mitochondrion) [Bambusa oldhamii]	2.86	0.0005402	0.0041928
m.88361	PREDICTED: peroxidase 5-like [Zea mays]	2.83	0.0014216	0.0097072
m.59079	PREDICTED: peroxidase 9-like [Setaria italica]	2.81	0.0003372	0.0027726
m.61296	PREDICTED: putative cytochrome P450 superfamily protein isoform X1 [Zea mays]	2.81	0.0012673	0.0087922
m.64522	hypothetical protein SORBIDRAFT_03g034400 [Sorghum bicolor]	2.79	3.03E-20	1.99E-18
m.127911	PREDICTED: proline dehydrogenase 2, mitochondrial-like [Setaria italica]	2.74	2.89E-145	1.72E-141
m.219069	PREDICTED: L-ascorbate oxidase homolog [Setaria italica]	2.71	0.0000372	0.0003882
m.4981	PREDICTED: peroxidase 25 [Setaria italica]	2.71	1.86E-06	0.0000256
m.66489	PREDICTED: nitrate reductase [NADH] [Setaria italica]	2.71	1.75E-255	6.23E-251
m.204071	hypothetical protein SORBIDRAFT_01g030560 [Sorghum bicolor]	2.63	1.95E-32	2.9E-30
m.266076	hypothetical protein SORBIDRAFT_07g001280 [Sorghum bicolor]	2.61	9.94E-14	3.65E-12
m.188036	hypothetical protein SORBIDRAFT_05g022340 [Sorghum bicolor]	2.56	1.82E-06	0.0000251
m.237571	PREDICTED: peroxidase 2-like [Setaria italica]	2.55	6.86E-06	0.0000845
m.113717	PREDICTED: abscisic acid 8'-hydroxylase 3 [Setaria italica]	2.55	3.54E-30	4.53E-28
m.282695	hypothetical protein SORBIDRAFT_05g003100 [Sorghum bicolor]	2.50	9.65E-15	4.03E-13
m.280138	hypothetical protein SORBIDRAFT_01g001160 [Sorghum bicolor]	2.48	3.07E-14	1.2E-12
m.267641	hypothetical protein SORBIDRAFT_08g003110 [Sorghum bicolor]	2.48	7.06E-28	7.79E-26
m.154930	hypothetical protein SORBIDRAFT_02g040500 [Sorghum bicolor]	2.47	2.13E-38	4.25E-36
m.34834	siroheme uroporphyrinogen methyltransferase 1 [Zea mays]	2.47	1.02E-38	2.09E-36
m.160156	predicted protein [Hordeum vulgare subsp. vulgare]	2.38	5.21E-06	0.0000656
m.126273	PREDICTED: peroxidase 57-like [Setaria italica]	2.35	0.0006227	0.0047469
m.245166	PREDICTED: cytochrome P450 78A9-like [Setaria italica]	2.33	1.63E-20	1.09E-18
m.113905	PREDICTED: probable lipoxygenase 8, chloroplastic [Setaria italica]	2.30	2.32E-13	8.16E-12
m.66495	AChain A, Structural Studies On Corn Nitrate Reductase: Refined Structure Of The Cytochrome B Reductase Fragment At 2.5 Angstroms, Its Adp Complex And An Active Site Mutant And Modeling Of The Cytochrome B Domain	2.26	5.39E-38	1.05E-35
m.198183	PREDICTED: cytochrome P450 72A15-like [Setaria italica]	2.25	3.86E-17	2.06E-15
m.239595	hypothetical protein SORBIDRAFT_04g034160 [Sorghum bicolor]	2.24	2.4E-195	4.26E-191

`

m.52678	PREDICTED: peroxidase 2-like [Zea mays]	2.23	4.6E-11	1.25E-09
m.62488	Cytochrome P450 99A2 [Aegilops tauschii]	2.22	1.28E-54	5.13E-52
m.47963	unknown [Zea mays]	2.20	4.43E-43	1.09E-40
m.127929	PREDICTED: proline dehydrogenase 2, mitochondrial-like [Setaria italica]	2.17	0.0004364	0.0034659
m.50105	PREDICTED: HIPL1 protein-like [Setaria italica]	2.15	0.0007468	0.0055631
m.127936	hypothetical protein SETIT_035342mg [Setaria italica]	2.11	1.89E-08	3.6E-07
m.94094	hypothetical protein SETIT_029527mg [Setaria italica]	2.10	6.58E-09	1.35E-07
m.139442	hypothetical protein SORBIDRAFT_09g021040 [Sorghum bicolor]	2.09	0.0002488	0.0021221
m.26615	putative cinnamyl-alcohol dehydrogenase family protein [Zea mays]	2.06	1.42E-08	2.75E-07
m.129962	PREDICTED: abscisic acid 8'-hydroxylase 1 [Setaria italica]	2.03	1.94E-75	1.87E-72
m.51271	PREDICTED: uncharacterized protein LOC100381459 isoform X1 [Zea mays]	2.03	0.0001361	0.0012449
m.23307	PREDICTED: cationic peroxidase 1-like [Setaria italica]	1.97	1.26E-21	9.17E-20
m.22083	PREDICTED: cytochrome P450 714C2-like isoform X1 [Brachypodium distachyon]	1.95	1.7E-27	1.83E-25
m.173810	taxane 10-beta-hydroxylase [Zea mays]	1.94	0.0006829	0.005154
m.307652	hypothetical protein SORBIDRAFT_02g023150 [Sorghum bicolor]	1.94	1.65E-06	0.0000229
m.151533	PREDICTED: cytochrome P450 CYP72A219-like [Setaria italica]	1.91	3.27E-06	0.0000429
m.285938	PREDICTED: peroxidase 72-like [Setaria italica]	1.89	2.31E-11	6.58E-10
m.51257	PREDICTED: respiratory burst oxidase homolog protein B-like [Setaria italica]	1.86	0.0000325	0.0003442
m.29512	PREDICTED: plant cysteine oxidase 2-like [Setaria italica]	1.86	6.74E-32	9.75E-30
m.8466	gibberellin 2-beta-dioxygenase [Zea mays]	1.84	1.06E-10	2.76E-09
m.150499	aldehyde dehydrogenase 5 [Zea mays]	1.78	2.74E-09	5.93E-08
m.26622	putative cinnamyl-alcohol dehydrogenase family protein [Zea mays]	1.78	0.000054	0.0005445
m.206985	PREDICTED: tropinone reductase homolog At2g29170-like [Setaria italica]	1.78	0.0005698	0.0043875
m.26185	hypothetical protein SORBIDRAFT_04g030310 [Sorghum bicolor]	1.78	1.85E-12	5.9E-11
m.23347	PREDICTED: peroxidase 4-like [Setaria italica]	1.77	3.94E-48	1.22E-45
m.83369	PREDICTED: geraniol 8-hydroxylase-like [Setaria italica]	1.77	7.78E-27	8.02E-25
m.280133	hypothetical protein SORBIDRAFT_01g001160 [Sorghum bicolor]	1.76	0.000027	0.0002903
m.174651	hypothetical protein SORBIDRAFT_02g040520 [Sorghum bicolor]	1.73	3.22E-13	1.11E-11

`

m.29517	PREDICTED: plant cysteine oxidase 2-like [Setaria italica]	1.72	8.64E-10	2.01E-08
m.198787	PREDICTED: cytochrome P450 93A2-like [Zea mays]	1.71	2.8E-08	5.19E-07
m.226980	uncharacterized protein LOC100217119 [Zea mays]	1.70	8.78E-108	1.95E-104
m.198335	PREDICTED: 1-aminocyclopropane-1-carboxylate oxidase 1 isoform X1 [Zea mays]	1.69	0.0003365	0.0027675
m.173438	PREDICTED: cytochrome P450 86A1 [Setaria italica]	1.68	5.77E-17	3.01E-15
m.187858	PREDICTED: laccase-10-like [Setaria italica]	1.66	0.000157	0.0014156
m.29518	PREDICTED: plant cysteine oxidase 2-like [Setaria italica]	1.66	5.93E-12	1.8E-10
m.94079	PREDICTED: flavin-containing monooxygenase FMO GS-OX-like 8 [Setaria italica]	1.59	0.0000572	0.0005741
m.113684	PREDICTED: stearoyl-[acyl-carrier-protein] 9-desaturase 1, chloroplastic [Setaria italica]	1.58	1.45E-13	5.22E-12
m.248182	hypothetical protein SORBIDRAFT_04g017460 [Sorghum bicolor]	1.57	1.27E-06	0.0000181
m.239478	hypothetical protein SORBIDRAFT_06g018040 [Sorghum bicolor]	1.56	2.43E-72	2.16E-69
m.248363	PREDICTED: polyphenol oxidase I, chloroplastic-like [Zea mays]	1.56	2.52E-16	1.23E-14
m.147368	PREDICTED: thioredoxin H4-2 [Setaria italica]	1.55	1.54E-12	4.96E-11
m.41429	PREDICTED: flavonol synthase/flavanone 3-hydroxylase [Oryza sativa Japonica Group]	1.55	2.28E-55	9.45E-53
m.248170	hypothetical protein OsI_07154 [Oryza sativa Indica Group]	1.55	1.72E-09	3.85E-08
m.56310	hypothetical protein SORBIDRAFT_01g030560 [Sorghum bicolor]	1.54	1.02E-38	2.09E-36
m.206977	uncharacterized protein LOC100273624 [Zea mays]	1.54	1.03E-06	0.0000151
m.41405	PREDICTED: 1-aminocyclopropane-1-carboxylate oxidase 5-like [Setaria italica]	1.53	1.55E-43	3.94E-41
m.226420	PREDICTED: monothiol glutaredoxin-S2 [Setaria italica]	1.48	0.0010347	0.0073781
m.83127	flavoprotein wrbA [Zea mays]	1.48	4.6E-23	3.76E-21
m.98338	PREDICTED: peroxidase 45-like [Setaria italica]	1.47	1.86E-07	3.08E-06
m.307657	hypothetical protein SORBIDRAFT_02g023150 [Sorghum bicolor]	1.46	0.0007168	0.0053697
m.23335	PREDICTED: peroxidase 4-like [Setaria italica]	1.46	2.8E-46	8.15E-44
m.18004	putative laccase precursor [Zea mays]	1.45	1.1E-17	6.12E-16
m.301900	PREDICTED: L-gulonolactone oxidase-like [Zea mays]	1.44	5.43E-06	0.0000682
m.303894	respiratory burst oxidase protein D variant alpha [Zea mays]	1.44	4.41E-08	7.99E-07
m.196099	hypothetical protein SORBIDRAFT_07g024030 [Sorghum bicolor]	1.43	6.19E-06	0.0000769
m.96471	uncharacterized protein LOC100381459 [Zea mays]	1.43	0.0004642	0.0036608

`

m.185746	PREDICTED: gibberellin 2-beta-dioxygenase 8-like [Setaria italica]	1.42	2.13E-06	0.000029
m.98344	PREDICTED: peroxidase 45-like [Setaria italica]	1.42	0.000001	0.0000146
m.41409	PREDICTED: 1-aminocyclopropane-1-carboxylate oxidase 5-like [Setaria italica]	1.40	4.14E-62	2.68E-59
m.56113	ascorbate-specific transmembrane electron transporter 1 [Zea mays]	1.39	3.27E-24	2.84E-22
m.299765	PREDICTED: cytochrome P450 CYP72A219-like [Setaria italica]	1.38	2.22E-13	7.82E-12
m.158584	PREDICTED: glutamate dehydrogenase 2-like [Setaria italica]	1.35	4.49E-06	0.0000572
m.40826	catalase [Saccharum hybrid cultivar NCo 376]	1.34	3.14E-13	1.09E-11
m.143013	unknown [Zea mays]	1.34	1.52E-50	5.26E-48
m.279952	PREDICTED: uncharacterized oxidoreductase At1g06690, chloroplastic-like [Setaria italica]	1.31	2.03E-38	4.08E-36
m.225221	PREDICTED: laccase-10-like [Setaria italica]	1.30	0.0000589	0.0005889
m.291116	hypothetical protein SORBIDRAFT_07g024230 [Sorghum bicolor]	1.29	4.2E-09	8.85E-08
m.303872	respiratory burst oxidase protein D variant alpha [Zea mays]	1.28	4.07E-57	1.88E-54
m.98341	hypothetical protein SORBIDRAFT_01g007230 [Sorghum bicolor]	1.27	0.0000163	0.0001846
m.265977	NAD(P)H-dependent oxidoreductase [Zea mays]	1.27	1.01E-11	3.01E-10
m.255862	PREDICTED: peroxidase 16-like [Setaria italica]	1.26	8.32E-10	1.94E-08
m.248186	hypothetical protein SORBIDRAFT_04g017460 [Sorghum bicolor]	1.26	1.68E-09	3.76E-08
m.141480	PREDICTED: glyceraldehyde-3-phosphate dehydrogenase A, chloroplastic [Setaria italica]	1.26	2.64E-22	2.04E-20
m.91343	PREDICTED: probable phospholipid hydroperoxide glutathione peroxidase [Setaria italica]	1.25	0.0001214	0.0011261
m.190058	unknown [Zea mays]	1.24	0.0001114	0.0010438
m.136651	ALDR_HORVURecName: Full=Aldose reductase; Short=AR; AltName: Full=Aldehyde reductase	1.24	0.0001501	0.0013606
m.309440	peroxidase 24 precursor [Zea mays]	1.23	2.45E-25	2.3E-23
m.141474	glyceraldehyde-3-phosphate dehydrogenase A, chloroplastic precursor [Zea mays]	1.22	1.05E-48	3.27E-46
m.41396	PREDICTED: flavanone 3-dioxygenase-like [Setaria italica]	1.21	1.46E-16	7.32E-15
m.140358	PREDICTED: malate dehydrogenase, chloroplastic-like [Setaria italica]	1.21	3.44E-33	5.31E-31
m.95209	PREDICTED: putative respiratory burst oxidase homolog protein H [Setaria italica]	1.21	2.06E-15	9.18E-14
m.303885	PREDICTED: respiratory burst oxidase homolog protein B [Setaria italica]	1.20	3.91E-14	1.51E-12
m.95198	PREDICTED: putative respiratory burst oxidase homolog protein H [Setaria italica]	1.20	5.27E-31	7.16E-29
m.154951	hypothetical protein SORBIDRAFT_02g040490 [Sorghum bicolor]	1.19	0.000688	0.0051867

`

m.2413	hypothetical protein SORBIDRAFT_03g036760 [Sorghum bicolor]	1.19	1.09E-13	3.97E-12
m.139906	PREDICTED: flavonoid 3'-monooxygenase-like [Setaria italica]	1.18	1.94E-08	3.69E-07
m.307287	hypothetical protein SORBIDRAFT_10g022440 [Sorghum bicolor]	1.17	9.76E-06	0.0001165
m.300523	hypothetical protein SORBIDRAFT_07g022650 [Sorghum bicolor]	1.17	6.47E-06	0.00008
m.276373	hypothetical protein SORBIDRAFT_05g001000 [Sorghum bicolor]	1.13	1.02E-25	9.81E-24
m.188251	PREDICTED: plant cysteine oxidase 5-like [Setaria italica]	1.12	1.96E-15	8.79E-14
m.199448	hypothetical protein SORBIDRAFT_02g040190 [Sorghum bicolor]	1.12	5.61E-11	1.51E-09
m.72825	PREDICTED: flavonol synthase/flavanone 3-hydroxylase-like [Zea mays]	1.12	1.61E-30	2.13E-28
m.299275	uncharacterized protein LOC100281213 [Zea mays]	1.11	7.97E-24	6.81E-22
m.187156	hypothetical protein SORBI_001G062300 [Sorghum bicolor]	1.11	4.84E-30	6.17E-28
m.41447	PREDICTED: flavanone 3-dioxygenase-like [Setaria italica]	1.09	6.07E-17	3.15E-15
m.203926	hypothetical protein SORBIDRAFT_02g034370 [Sorghum bicolor]	1.09	8.06E-42	1.87E-39
m.14298	PREDICTED: extradiol ring-cleavage dioxygenase-like [Zea mays]	1.08	1.28E-20	8.67E-19
m.27825	hypothetical protein SETIT_019843mg, partial [Setaria italica]	1.08	0.0003571	0.0029166
m.150415	PREDICTED: peroxidase 11 [Setaria italica]	1.08	1.15E-21	8.45E-20
m.5429	acc oxidase [Zea mays]	1.06	0.0000828	0.0008019
m.124640	hypothetical protein SORBIDRAFT_06g032450 [Sorghum bicolor]	1.06	5.95E-69	4.81E-66
m.216101	hypothetical protein SORBIDRAFT_02g036650 [Sorghum bicolor]	1.06	3.93E-06	0.0000507
m.266697	hypothetical protein SORBIDRAFT_10g006650 [Sorghum bicolor]	1.03	2.58E-13	9.05E-12
m.145682	PREDICTED: peroxidase 21 [Setaria italica]	1.03	0.0000589	0.0005895
m.18076	gibberellin 2-beta-dioxygenase [Saccharum hybrid cultivar R570]	1.02	0.0000265	0.0002856
m.232330	PREDICTED: fatty acid desaturase DES2 [Setaria italica]	1.02	7.88E-27	8.1E-25
m.83132	flavoprotein wrbA [Zea mays]	1.02	9.21E-06	0.0001105
m.41387	PREDICTED: flavanone 3-dioxygenase-like [Setaria italica]	1.01	7.1E-16	3.3E-14
m.226979	uncharacterized protein LOC100217119 [Zea mays]	1.01	1.62E-08	3.11E-07

`

Table 3.4A. DEGs with "nucleic acid binding activity" in salt-treated Supreme

Gene_ID	Description	Log_2FC	P value	Adjusted P value
m.268973	splicing factor putative [Albugo laibachii Nc14]	10.39	9.13E-13	1.8E-10
m.95962	hypothetical protein L917_04771 [Phytophthora parasitica]	7.20	0.000178281	0.005223068
m.326868	hypothetical protein L915_18980 [Phytophthora parasitica]	6.97	0.000044	0.001570743
m.319487	DEAD-box ATP-dependent RNA helicase 56 [Aphanomyces invadans] *	6.92	0.0000824	0.002708217
m.71991	hypothetical protein SETIT_017165mg [Setaria italica]	5.72	0.000218737	0.006232131

Table 3.4B. DEGs with "nucleic acid binding activity" in salt-treated Parish

Gene_ID	Description	Log_2FC	P value	Adjusted P value
m.73458	PREDICTED: endonuclease 2-like [Setaria italica]	1.26	0.000978368	0.007035904
m.226928	TPA: hypothetical protein ZEAMMB73_851898 [Zea mays]	1.66	5.60E-07	8.62E-06
m.292931	PREDICTED: uncharacterized protein LOC101753419 [Setaria italica]	1.72	1.42E-09	3.20E-08
m.159032	AF466646_7putative polyprotein [Zea mays]	1.77	1.42E-08	2.76E-07
m.292921	PREDICTED: uncharacterized protein LOC101753419 [Setaria italica]	1.78	9.77E-67	7.24E-64

Salt stress induced genes shows higher expression in Supreme than in Parish under normal conditions

Although Supreme has fewer genes that are responsive to salt treatment than Parish, Supreme exhibits much higher tolerance than Parish. It is possible that Supreme may have a higher expression of salt stress induced genes than Parish under normal conditions that may or may not be induced upon salt treatment, and therefore may be more prepared when exposed to salinity. To test this hypothesis, we selected 202 genes based on the following criteria: 1) salt-induced genes in Parish; 2) higher expression in Supreme than in Parish under normal condition; 3) not changed or further induced in Supreme under salt treatment. To get insight into the biological meanings of these genes, we conducted GO enrichment

`

analysis and found the following over-represented GO terms: “proline catabolic process”, “transcription factor activity”, “proline dehydrogenase activity” and “monooxygenase activity” (Figure 3.8). We then further examined genes with “transcription factor activity” (Table 3.5). It is interesting that many of these transcription factors have been associated with salt tolerance in the previous studies, such as dehydration-responsive element-binding (DREB) proteins, ethylene-responsive transcription factors (ERFs), and WRKY transcription factors (Wang et al. 2016).

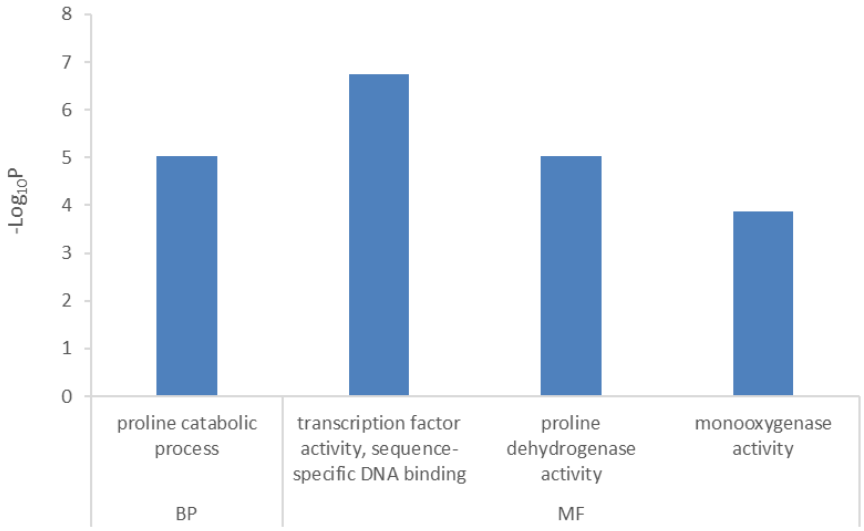

Figure 3.8. Functional enrichment analysis for salt-induced genes that show higher expression in Supreme than in Parish under normal conditions. The x-axis shows significantly enriched gene ontology (GO) terms ($P < 0.05$, Bonferroni < 0.05) in two categories, Biological Process (BP) and Molecular Function (MF). The y-axis shows the $-\log_{10}P$ values of these terms.

`

Table 3.5. Summary of salt-induced transcription factors that are enriched among genes showing higher expression in Supreme than in Parish under normal conditions

Gene_ID	Description	Log_2FC (S_{normal}/P_{normal})	Log_2FC (S_{salt}/S_{normal})	Log_2FC (P_{salt}/P_{normal})
m.108243	hypothetical protein [Paspalum vaginatum]	2.26	NA[a]	1.95
m.237095	hypothetical protein SORBIDRAFT_02g026630 [Sorghum bicolor]	2.27	NA	3.54
m.114339	hypothetical protein SORBIDRAFT_03g034670 [Sorghum bicolor]	9.36	NA	7.50
m.43990	hypothetical protein SORBIDRAFT_03g038210 [Sorghum bicolor]	1.49	NA	2.06
m.108223	hypothetical protein SORBIDRAFT_04g031960 [Sorghum bicolor]	1.97	NA	2.02
m.285764	hypothetical protein SORBIDRAFT_06g025900 [Sorghum bicolor]	3.56	NA	4.76
m.133559	PREDICTED: AP2-like ethylene-responsive transcription factor AIL5 [Setaria italica]	1.82	NA	1.51
m.108267	PREDICTED: dehydration-responsive element-binding protein 1A-like [Setaria italica]	1.81	NA	2.44
m.85022	PREDICTED: dehydration-responsive element-binding protein 1E [Setaria italica]	2.73	NA	3.88
m.26812	PREDICTED: dehydration-responsive element-binding protein 1H-like [Setaria italica]	2.72	1.01	4.46
m.84649	PREDICTED: ethylene-responsive transcription factor 2 [Setaria italica]	1.07	NA	1.00
m.204461	PREDICTED: ethylene-responsive transcription factor ERF027-like [Setaria italica]	1.22	NA	1.67
m.73960	PREDICTED: ethylene-responsive transcription factor ERF109-like [Setaria italica]	1.84	NA	3.03
m.195857	PREDICTED: homeobox-leucine zipper protein HOX25-like [Setaria italica]	1.30	NA	1.08
m.60871	PREDICTED: probable WRKY transcription factor 4 [Setaria italica]	1.21	NA	2.28
m.264805	PREDICTED: probable WRKY transcription factor 41 isoform X2 [Zea mays]	2.23	NA	1.78
m.298519	PREDICTED: probable WRKY transcription factor 70 [Setaria italica]	1.23	NA	1.28
m.160848	PREDICTED: transcription factor HBP-1b(c1)-like [Setaria italica]	1.23	NA	1.51
m.73865	PREDICTED: WRKY transcription factor 18-like [Setaria italica]	1.55	NA	3.24
m.263026	PREDICTED: zinc finger protein ZAT9 [Brachypodium distachyon]	1.17	NA	1.54
m.264779	TPA: putative WRKY DNA-binding domain superfamily protein [Zea mays]	1.04	NA	1.61

[a]NA: not applicable. Expression change that didn't pass the DEGs analysis statistics (2-fold change or above, P value ≤ 0.01, and adjusted P value ≤ 0.01) is annotated as NA.

The possible role of vacuolar Na^+/H^+ antiporters and proton pump in conferring salt tolerance in Supreme

As Supreme accumulated more Na^+ and showed higher salt tolerance than Parish, we speculated that the former may have developed a strong capacity to sequestrate excessive Na^+ into the vacuole through vacuolar Na^+/H^+ antiporters, thus maintaining high

`

osmotic pressure to facilitate water uptake and protecting the cytoplasm from Na^+ toxicity. To test our hypothesis, we identified a total of seven presumable Na^+/H^+ antiporters (m.194123, m.133530, m.194121, m.194125, m.207121, m.28253, m.170234) in Seashore paspalum's transcriptome, two of which, m.133530 and m.170234, have homology to *Zea mays* vacuolar NHX3 and NHX4, respectively by BLAST search in NCBI (Table 3.6A). We performed differential expression analysis for these putative Na^+/H^+ antiporters with the following four comparisons: S_{normal} vs. P_{normal}, S_{salt} vs. S_{normal}, P_{salt} vs. P_{normal}, S_{salt} vs. P_{salt}. For the two presumable Na^+/H^+ antiporters m.133530 and m.170234, the expression level of m.133530 did not show significant changes between the two cultivars under both normal and salt-treated conditions while the expression level of m.170234 is significantly higher in Parish than in Supreme under normal conditions (Table 3.6A). Among the remaining five putative Na^+/H^+ antiporters, m.194123 showed a significantly higher expression level in Supreme than in Parish under both normal and salt-treated conditions while m.194121 showed a significantly higher expression level in Parish than in Supreme under salt-treated conditions (Table 3.6A).

As vacuolar Na^+/H^+ antiporters are empowered by the electrochemical gradient created by H^+-ATPases and H^+-pyrophosphatases (H^+-PPases) (Roy, Negrão, and Tester 2014), we also identified eleven H^+-ATPases and four H^+-PPases in Seashore paspalum's transcriptome, which are shown in Table 3.6B and Table 3.6C, respectively. None of the H^+-ATPases showed differential expression (Table 3.6B). Interestingly, all of the four vacuolar H^+-PPases showed lower expression level in Supreme than in Parish under normal conditions, especially for one of the vacuolar H^+-PPase m.112845 (Table 3.6C). However, m.112845 was induced by about 1024 times ($FC=2^{10.28}$) in Supreme under salt treatment,

`

suggesting a possible role in facilitating Na^+ sequestration under high salinity and conferring salinity tolerance in Supreme (Table 3.6C).

Table 3.6A. Summary of possible Na^+/H^+ antiporters in Seashore paspalum's transcriptome and their expression change under different comparisons. DEGs (2-fold change or above, P value ≤ 0.01, and adjusted P value ≤ 0.01) are in the orange background.

Gene_ID	Description	Log_2FC (S_{normal}/P_{normal})	Log_2FC (S_{salt}/S_{normal})	Log_2FC (P_{salt}/P_{normal})	Log_2FC (S_{salt}/P_{salt})
m.194123	PREDICTED: sodium/hydrogen exchanger 2-like [Setaria italica]	8.88	-0.22	-1.09	9.74
m.133530*	sodium/hydrogen exchanger [Zea mays]	0.49	0.02	-0.07	0.58
m.194121	PREDICTED: sodium/hydrogen exchanger 2-like [Setaria italica]	-0.01	-0.97	0.17	-1.15
m.194125	PREDICTED: sodium/hydrogen exchanger 2-like [Setaria italica]	0.25	-0.43	0.3	-0.49
m.207121	PREDICTED: sodium/hydrogen exchanger 6-like [Setaria italica]	0.55	-0.1	-0.1	0.55
m.28253	PREDICTED: sodium/hydrogen exchanger 8 [Setaria italica]	0.52	0.09	-0.3	0.92
m.170234*	PREDICTED: sodium/hydrogen exchanger 2 [Setaria italica]	-1.1	-0.1	-0.37	-0.83

* m.133530 and m.170234 have homology to Zea mays vacuolar NHX3 and NHX4, respectively.

Table 3.6B. Summary of possible vacuolar H^+-ATPases in Seashore paspalum's transcriptome and their expression change under different comparisons. Note that vacuolar H^+-ATPases are not differentially expressed for different comparisons indicated below.

Gene_ID	Description	Log_2FC (S_{normal}/P_{normal})	Log_2FC (S_{salt}/S_{normal})	Log_2FC (P_{salt}/P_{normal})	Log_2FC ($S_{salt}P_{salt}$)
m.102654	PREDICTED: V-type proton ATPase catalytic subunit A [Brachypodium distachyon]	0.16	0.46	-0.07	0.69
m.116106	PREDICTED: V-type proton ATPase subunit F-like [Setaria italica]	-0.22	0.04	0.15	-0.33
m.117254	Vacuolar proton pump 16 kDa proteolipid subunit	-0.23	0.15	-0.08	-0.01
m.117255	PREDICTED: V-type proton ATPase 16 kDa proteolipid subunit [Oryza brachyantha]	-0.19	0.26	0.19	-0.12
m.117270	PREDICTED: V-type proton ATPase 16 kDa proteolipid subunit [Oryza brachyantha]	-0.51	0.27	0.16	-0.39
m.173282	PREDICTED: V-type proton ATPase subunit a1 [Setaria italica]	0.21	0.06	0.02	0.25
m.190922	PREDICTED: V-type proton ATPase subunit E [Setaria italica]	-0.73	0.47	0.68	-0.94
m.23021	putative ATPase, V1 complex, subunit A protein [Zea mays]	0.29	-0.08	0.34	-0.12
m.230918	PREDICTED: V-type proton ATPase subunit G1-like [Oryza brachyantha]	-0.58	0.13	0.18	-0.62
m.232963	PREDICTED: V-type proton ATPase subunit a3-like [Setaria italica]	-0.38	0.24	0.17	-0.32
m.279500	V-type proton ATPase subunit E-like [Zea mays]	-0.27	0.20	0.12	-0.19

`

Table 3.6C. Summary of possible vacuolar H^+-PPases in Seashore paspalum's transcriptome and their expression change under different comparisons. DEGs (2-fold change or above, P value ≤ 0.01, and adjusted P value ≤ 0.01) are in the orange background.

Gene_ID	Description	Log_2FC (S_{normal}/P_{normal})	Log_2FC (S_{salt}/S_{normal})	Log_2FC (P_{salt}/P_{normal})	Log_2FC ($S_{salt}P_{salt}$)
m.112845	V-type H(+)-translocating pyrophosphatase [Aphanomyces invadans]	-8.48	10.28	0.69	1.12
m.73322	PREDICTED: pyrophosphate-energized vacuolar membrane proton pump-like [Setaria italica]	-1.68	-0.94	0.30	-2.92
m.88459	PREDICTED: pyrophosphate-energized vacuolar membrane proton pump-like [Setaria italica]	-1.83	-1.16	0.30	-3.29
m.95345	PREDICTED: pyrophosphate-energized vacuolar membrane proton pump-like isoform X1 [Setaria italica]	-2.20	1.11	0.43	-1.52

Discussion

Supreme takes advantage of Na^+ accumulation for improved salt tolerance

It becomes evident that the mechanisms that contribute to high salt-tolerance in halophytes are conserved to those known in glycophytes although some halophytes have evolved special adaptive mechanisms such as salt glands to actively excrete salts (Zhang and Shi 2013). However, halophytes may possess unique genomic structure (e.g. a higher gene copy number and altered promoter sequences), and subtle gene regulation at the transcription and protein levels that leads to their better adaption to high salinity in the environment (Kosová, Prášil, and Vítámvás 2013).

In our study, we investigated the mechanisms underlying salt tolerance in a halophyte called Seashore paspalum by comparing two cultivars: Supreme (high salt-tolerance) and Parish (moderate salt-tolerance) at physiological and transcriptome levels under both non-treated and salt-treated conditions (400 mM NaCl). Measurement of Na^+ content suggests that Na^+ accumulation under both normal and salt-treated conditions is a key mechanism underlying Supreme's high salinity tolerance (Figure 1D). Na^+ accumulation by Supreme under salt treatment is not surprising as previous studies suggest

`

that this is a common mechanism for both halophyte and glycophyte under salt stress to facilitate water uptake (Xu et al. 2016). However, the Seashore paspalum genotype, Supreme takes full advantage of this mechanism by accumulating Na^+ in a significantly higher level than Parish under normal conditions, which may be evolved as a protective mechanism for osmotic adjustment to counteract high levels of Na^+ in the surrounding environment.

We suggest that further increased Na^+ in Supreme under salt-treated conditions is sequestrated into the vacuole to prevent its toxicity to the cytoplasm. Na^+ sequestration into the vacuole takes place by the operation of vacuolar Na^+/H^+ antiporters (NHXs) in concert with two proton pumps H^+-ATPases and H^+-PPases. Genes involved in Na^+ sequestration are promising candidate genes to engineer crops for salinity tolerance. Several salinity tolerant plants have been successfully developed by overexpression of either NHXs or H^+-PPases (e.g. AVP1) (Roy, Negrão, and Tester 2014). In our study, we identified at least two possible vacuolar Na^+/H^+ antiporters (NHXs), namely m.133530 and m.170234 (Table 3.6A). Of the remaining five NHXs, m.194123 exhibits dramatically higher expression in Supreme than in Parish under both normal and salt-treated conditions, raising the question of whether or not m.194123 functions as a vacuolar Na^+/H^+ antiporter. We also identified four H^+-PPases, namely m.112845, m.73322, m.88459 and m.95345, of which m.112845 was highly induced by salt treatment in Supreme despite its lower expression than Parish under normal conditions (Table 3.6C). The function and activity of these NHXs and H^+-PPases are all worth further examination.

`

Elevated expression of salt stress induced transcription factors in Supreme under normal conditions, possibly due to enhanced Ca^{2+} signaling, is another contributor to Supreme's higher salt tolerance

As a terminal transducer of the salt stress signaling pathway, transcription factors (TFs) can directly regulate the expression of an array of downstream stress-responsive genes through interaction with the specific cis-acting elements in their promoter region. In our study, we found that an array of salt stress induced transcription factors showed higher expression level in Supreme than in Parish under normal conditions (Table 3.5). Some of these transcription factors are associated with salt stress response, including dehydration-responsive element-binding (DREB) proteins, ethylene-responsive transcription factors and WRKY transcription factors (Wang et al. 2016). This result is consistent with previous study of transcriptomic variation of three different ecotypes of *Arabidopsis* (Col, Ler, and Sha) in response to salt stress, in which it was found that there existed extensive differences in gene expression between the salt-tolerant ecotype Sha and the other two relatively salt-sensitive ecotypes Col and Ler for salt stress related TFs, such as heat shock TFs (HSF) under normal conditions (Wang et al. 2013). It is possible that the elevated expression of salt stress induced TFs in Supreme under normal conditions contributes to its higher salt-tolerance and this mechanism may be conserved between different salt-tolerant plant species.

Ca^{2+} is a very important second messenger in response to a wide range of external stimuli, including salt stress. High salinity causes a rapid and transient increase in cytosolic Ca^{2+}, which is further decoded by Calcineurin B-like protein (CBL)-CBL-interacting protein kinase (CIPK) complex to initiate a phosphorylation/dephosphorylation cascade,

`

resulting in regulation of multiple stress-responsive genes and ultimately leading to phenotypic response of stress tolerance directly or indirectly (Mahajan, Pandey, and Tuteja 2008). Higher Ca^{2+} accumulation in Supreme (possibly triggered by Na^+ accumulation) than in Parish under normal conditions may account for the elevated expression of salt stress responsive TFs in Supreme through high Na^+-triggered Ca^{2+} signaling pathway (Figure 3.1F). Supporting this hypothesis, salt-treated Parish accumulated Na^+ and Ca^{2+} to a level that is comparable to the Na^+ and Ca^{2+} content in non-treated Supreme, which coincides with the induction of many salt stress responsive TFs.

Intracellular K^+ retention under high salinity may contribute to salinity tolerance in both cultivars

K^+ uptake at the root-soil interface is mainly mediated by high affinity uptake transporters (μM range) and low affinity uptake transporters (mM range). While the former uptake mechanism is performed by members of the KT/HAK/KUP family such as high affinity potassium transporter 5 (HAK5) and potassium uptake transporter 7 (KUP7), the latter uptake mechanism is achieved by K^+ channels of the Shaker family, such as Arabidopsis K^+ transporter (AKT1) (Assaha et al. 2017). Xylem K^+ loading from the root is carried out by stelar K^+ outward rectifying channels (SKORs) and KUP7 in *Arabidopsis* (Demidchik 2014) while K^+ transport across the vascular bundle to mesophyll cells in the shoot has not been clearly elucidated so far. Under salt stress, high levels of Na^+ often inhibit K^+ uptake and induce K^+ efflux in both root and leaf cells due to Na^+-induced plasma membrane (PM) depolarization and a consequential inhibition of K^+ uptake channels and activation of K^+ efflux channels such as K^+ outward rectifying channels (KORs) and nonselective cation channels (NSCCs). Thus, K^+ deficiency often occurs

`

under salt stress, which results in growth inhibition (Mian et al. 2011; Assaha et al. 2017). The capacity to retain intracellular K^+, which counteracts the toxic effect of excessive Na^+, was regarded as equally important mechanism to the regulation of toxic Na^+ accumulation for salt stress tolerance (Janicka-Russak and Kabała 2015). In our study, both Supreme and Parish maintained a stable K^+ level after salt treatment, suggesting that K^+ retention, possibly by maintaining negative membrane potential may play a critical role for salinity tolerance in both cultivars. An important question to be addressed in the future is how Supreme and Parish alleviate Na^+-induced PM depolarization to maintain negative membrane potential for K^+ retention under salt conditions. Moreover, we identified a total of 18 putative potassium transporters in Seashore paspalum's transcriptome, of which m.149226 is a high affinity potassium transporter and m.6215 is a predicted low affinity uptake channel AKT2 (Table 3.7). Further examination of their roles in potassium uptake and translocation is recommended.

Table 3.7. Summary of possible K^+ transporters in Seashore paspalum's transcriptome and their expression change under different conditions. DEGs (2-fold change or above, P value ⩽ 0.01, and adjusted P value ⩽ 0.01) are in the orange background.

Gene_ID	Description	Log_2FC (S_{normal}/P_{normal})	Log_2FC (S_{salt}/S_{normal})	Log_2FC (P_{salt}/P_{normal})	Log_2FC (S_{salt}/P_{salt})
m.124553	PREDICTED: potassium transporter 10-like [Setaria italica]	0.56	0.00	0.82	-0.27
m.149226*	high-affinity potassium transporter [Phragmites australis]	-0.85	2.86	1.26	0.75
m.167648	PREDICTED: potassium channel KOR1 [Setaria italica]	-1.29	1.39	1.27	-1.17
m.169812	potassium transporter [Phragmites australis]	-1.12	-0.28	0.19	-1.59
m.169813	potassium transporter [Phragmites australis]	0.97	-0.85	-0.24	0.36
m.177897	PREDICTED: potassium transporter 1-like [Setaria italica]	0.00	2.08	0.86	1.23
m.210030	PREDICTED: potassium transporter 25 [Setaria italica]	-1.54	-0.46	-0.12	-1.88
m.222898	Putative potassium transporter 14 [Aegilops tauschii]	-0.86	-0.08	0.21	-1.15
m.259914	PREDICTED: two-pore potassium channel 2-like [Setaria italica]	-1.47	0.50	-0.70	-0.28
m.261833	potassium channel [Saccharum hybrid cultivar]	1.32	-0.35	0.65	0.32
m.268433	PREDICTED: probable potassium transporter 11 [Setaria italica]	-1.16	-0.26	0.41	-1.82
m.307318	potassium transporter [Phragmites australis]	0.06	-0.37	0.26	-0.57
m.307324	PREDICTED: probable potassium transporter 9 [Setaria italica]	1.08	0.31	2.00	-0.62
m.58659	PREDICTED: probable potassium transporter 11 [Setaria italica]	-0.66	0.10	-0.06	-0.49
m.5987	PREDICTED: potassium transporter 22-like [Setaria italica]	-0.25	-0.75	-0.12	-0.87
m.6215*	PREDICTED: potassium channel AKT2 [Setaria italica]	1.10	-0.38	0.45	0.27
m.77121	PREDICTED: potassium transporter 24-like [Setaria italica]	0.04	-0.13	0.26	-0.35
m.79462	PREDICTED: probable potassium transporter 16 [Setaria italica]	-1.82	0.43	0.08	-1.48

* m.149226 and m.6215 are transporters known for potassium uptake.

`

Oxidation-reduction regulation and nucleic acid binding activity under high salinity may be other important factors for salinity tolerance in both cultivars

Salt stress can lead to the accumulation of ROS, causing oxidative stress to the plants. The oxidation-reduction process is critical for salinity tolerance in plants as it is involved in scavenging ROS and maintaining oxidation-reduction homeostasis. In our study, "oxidation-reduction process" is the most significantly enriched GO term in the BP category for both Supreme and Parish up-regulated genes under salt treatment (Figure 3.7), which indicates that this process may play an important role in salt tolerance in both cultivars. This result is consistent with previous transcriptome profiling study in a halophyte, ice plant (*Mesembryanthemum crystallinum*) under high salinity, suggesting that oxidation-reduction may be a conserved mechanism conveying salt tolerance (Tsukagoshi et al. 2015). Accordingly, several oxidoreductase genes such as glutathione-disulfide reductase (GSR), superoxide dismutase (SOD), aldehyde dehydrogenase (ALDHs), and peroxidases are upregulated in Supreme (Table 3.3A) while more oxidoreductase genes including ALDHs and peroxidases are upregulated in Parish under salt treatment (Table 3.3B).

"Nucleic acid binding" is the most significantly enriched GO term in the MF category for both Supreme and Parish up-regulated genes under salt treatment, suggesting that this process may also play a crucial role in salt tolerance in both cultivars. In Supreme, a DEAD-box ATP-dependent RNA helicase gene (m.319487) was upregulated over 100-fold ($FC=2^{6.92}$) under high salinity conditions (Table 3.4A), implying a possible role in salinity tolerance. DEAD-box RNA helicases are regarded as RNA chaperones as these proteins can unwind misfolded RNAs with non-functional secondary structures for correct

`

folding using energy derived from ATP hydrolysis, ensuring the translation initiation inhibited by stress to proceed (Tuteja 2007; Owttrim 2006). Overexpression of an *Apocynum venetum* DEAD-box helicase 1 (*AvDH1*) in cotton under CaMV 35S promoter confers salinity tolerance and increasing crop productivity in saline fields (Chen et al. 2016). Expression of a putative DEAD-Box RNA helicase gene *SlDEAD31* in tomato was induced by heat, cold, and dehydration. Transgenic tomato plants overexpressing *SlDEAD31* significantly improved salt tolerance and slightly improved drought resistance compared to wild-type plants (Zhu et al. 2015). It will be interesting to overexpress the salt stress induced DEAD-box RNA helicase identified in Supreme in model species such as *Arabidopsis* to test whether it confers salinity tolerance.

Based on our results, we proposed a hypothetical model depicting the mechanisms underlying Supreme's high salt tolerance (Figure 11). We suggest that Na^+ accumulation under normal conditions and the resulting osmotic adjustment and the expression of salt stress responsive transcription factors induced by Ca^{2+} signaling pathway, possibly due to Na^+ accumulation under normal conditions, are two important protective mechanisms that are responsible for the higher salinity tolerance observed in Supreme. In addition, K^+ retention, strong oxidation-reduction processes, and nucleic acid binding activities under high salinity conditions are three contributors to the salinity tolerance in both cultivars. Ion transporters, including NHXs coupled with H^+-PPases and K^+ uptake transporters, salt stress responsive transcription factors, oxidoreductases and the salt stress induced DEAD-box RNA helicase identified in Supreme in this study can be used as candidate genes for

`

functional studies and potential targets to engineer plants for enhanced salinity tolerance, opening new avenues for future research.

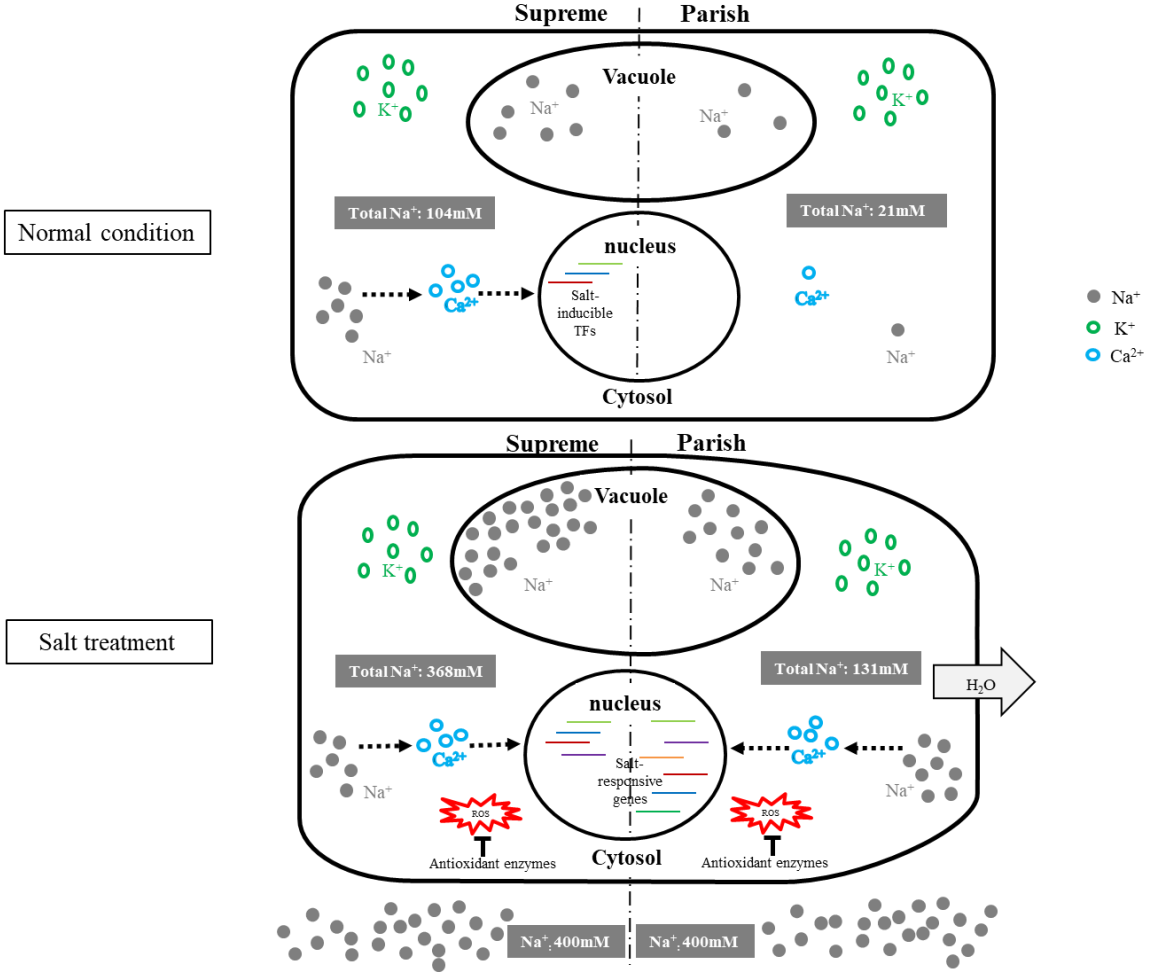

Figure 3.9. A schematic model for the salinity tolerance mechanisms in Supreme versus the salinity tolerance mechanisms in Parish. Numbers indicated are intracellular and extracellular Na^+ concentrations. ROS detoxification and maintaining K^+ uptake under salt stress are two common mechanisms for salinity tolerance in both cultivars. High Na^+ levels in Supreme under normal and salt-treated conditions lower the water potential, preventing water loss. Moreover, an array of salt stress inducible transcription factors is highly expressed in Supreme under normal conditions, possibly induced by the Ca^{2+} signaling pathway due to Na^+ accumulation under normal conditions, making Supreme prepared for salt stress.

`

CHAPTER FOUR

CONCLUSIONS AND FUTURE PERSPECTIVES

`

The genetic basis that dictates plant size and shape and how plants respond to environmental stresses given their sessile life style has fascinated scientists for many years. In context of the rapidly rising world population and climate change such as global warming and a resulting sea level rise, getting a deep understanding of the underlying mechanisms governing plant growth and stress response are important for implementing feasible and sustainable strategies to address these challenges.

Plant organ development to a specific size and shape is controlled by two cellular processes, cell proliferation and cell expansion. The current biological approach to study plant development has leveraged the power of *Arabidopsis* as a model system because of its simple life style and annotated genome sequence. Studies of single gene function by forward or reverse genetics progressing to studies of pathways and interaction/regulatory networks largely expanded our knowledge of the genetic control of organ size and shape in plants. However, a complete picture of how plants integrate different developmental pathways to a central growth mechanism, especially for the process of cell expansion is still poorly understood. To this end, my first project identified a novel Myb-like family protein named Development Related Myb-like1 (DRMY1) which is essential for cell expansion. We proposed a hypothetical mechanism of its action: DRMY1, possibly through forming a complex with other transcription factors as a trans-regulatory module, may regulate cell expansion directly through regulating cell wall biosynthesis/remodeling and ribosome biogenesis. Moreover, DRMY1 may also be a point of crosstalk between ethylene and ABA signaling pathways and control cell expansion indirectly through regulating the expression of genes in these two pathways. Interestingly, DRMY1 also regulates a variety of genes in response to a broad range of environmental stresses. A

`

number of questions still remain to be addressed in the future. Which downstream genes are directly regulated by DRMY1 among the DEGs identified by RNAseq? What is the binding sequence of DRMY1? What are the interaction partners of DRMY1? Does DRMY1 play a role in plant response to environmental stresses? If it does, could it also be an integration point of growth and defense signaling pathways to balance the growth-defense tradeoff?

Soil salinity is a major abiotic stress affecting crop productivity. It was estimated that 20 % of the world's irrigated land is affected by salinity (Rhoades and Loveday 1990). Plant species vary in the level to which they tolerate salt-affected soils. Halophytes are plants that can develop and reproduce in the environmental conditions where the concentration of NaCl is around 200 mM NaCl or more as a result of evolutionary adaptation to their habitats (Flowers and Colmer 2008). The inherent capability of these fascinating plants to withstand high salinity makes it interesting to understand the associated mechanisms. Moreover, the salt-tolerant genes identified are very promising candidate genes for functional study and developing novel strategies for engineering crops to improve their salinity tolerance. In our study, we investigated the mechanisms of plant salt tolerance in Supreme, the most salt-tolerant cultivar of a halophytic warm-seasoned perennial grass, Seashore paspalum, at the physiological and transcriptomic levels by comparative study with another cultivar Parish, which possesses moderate salinity tolerance. Our data suggests that Na^+ accumulation under normal conditions and the resulting osmotic adjustment and the expression of salt stress responsive transcription factors induced by Ca^{2+} signaling pathway, possibly due to Na^+ accumulation under normal conditions, are two important protective mechanisms that are responsible for higher salinity

`

tolerance in Supreme. In addition, K^+ retention, strong oxidation-reduction processes and nucleic acid binding activities under high salinity conditions are three contributors to the salinity tolerance in both cultivars. As Na^+ accumulation and K^+ retention are two major mechanisms for salinity tolerance, our major focus in the future will be cloning the vacuolar Na^+/H^+ antiporters along with H^+-PPases and K^+ uptake transporters using Rapid Amplification of cDNA Ends (RACE) and testing their functions by overexpression in *Arabidopsis.* Moreover, the salt stress responsive transcription factors, oxidoreductases and the salt stress induced DEAD-box RNA helicase identified in Supreme are also worth further examination in *Arabidopsis*. We hope to engineer crop species for enhanced salinity tolerance in the future if the candidate genes are verified to contribute to salt tolerance in *Arabidopsis*.

`

APPENDICES

`

APPENDIX A

SUPPORTING MATERIAL FOR CHAPTER TWO

Supplemental Table A-1: Primers for gene cloning and PCR analyses

Primer name	Sequence (5' to 3')	Purpose
SALK_012746_PCR_LP	CGCAACAGCTTCCGTTACTAC	Selection for *drmy1* homozygous T-DNA insertion mutant
SALK_012746_PCR_RP	TTTCACACTCTCCTCCTCTCG	Selection for *drmy1* homozygous T-DNA insertion mutant
SALK_113831_PCR_LP	AGGGTTCTCAGGAACCATCAG	Selection for *dp1* homozygous T-DNA insertion mutant
SALK_113831_PCR_RP	ATGACGTCGTTGGCATAAGAC	Selection for *dp1* homozygous T-DNA insertion mutant
DRMY1_CDS_BamH 1_F	CGGATCCATGGTTGATAACAGTAACAATAAGAAG	Cloning of *DRMY1* coding sequence with stop codon
DRMY1_CDS_BamH1_R	AGGATCCCTACAACTCCTTCAGTCCGGTCC	Cloning of *DRMY1* coding sequence with stop codon
DRMY1_CDS-stopcodon_BamH 1_F	CGGATCCATGGTTGATAACAGTAACAATAAGAAG	Cloning of *DRMY1* coding sequence without stop codon in frame upstream of GFP
DRMY1_CDS-stopcodon_BamH 1_R	CGGATCCTCCCACCGCTAAAGATAATGC	Cloning of *DRMY1* coding sequence without stop codon in frame upstream of GFP
DRMY1_Genomic_AgeI_F1	GCATACCGGTGACTGATCGAGTCAATGTTAC	Cloning of *DRMY1* genomic DNA
DRMY1_Genomic_ R1	TGGCGATGTCTGCTTCACTGATG	Cloning of *DRMY1* genomic DNA

`

DRMY1_Genomic_ F2	CAGTGAAGCAGACATCGCCACTC	Cloning of *DRMY1* genomic DNA
DRMY1_Genomic_ R2	CCTTGATGGTACCGGATGAC	Cloning of *DRMY1* genomic DNA
DRMY1_Genomic_F3	GTCATCCGGTACCATCAAGG	Cloning of *DRMY1* genomic DNA
DRMY1_Genomic_AgeI _R5	GCATACCGGTGGTTAGGGTGAAATTTGCAG	Cloning of *DRMY1* genomic DNA
AtGRF1_CDS_F2_NdeI	CATATG CCCATGGGAAAAATCTCTGA	Cloning of *GRF1* coding sequence
AtGRF1_CDS_R2_PstI	CTGCAG TTTTTGTTTTCGCAATTGTCC	Cloning of *GRF1* coding sequence
DRMY1_RT_F	AGAATGCTGTTTCTGCGTTG	RT-PCR
DRMY1_RT_R	TCAGCCTTTGGTGCTGATAG	RT-PCR
DP1_RT_LP	TTAGAGGAGAGAGAACCGCC	RT-PCR
DP1_RT_RP	ACAGCAAGCTCCACTTCCAG	RT-PCR
DRMY1_qPCR_LP3	GCAACACTTCCGCCAAATAAA	qRT-PCR
DRMY1_qPCR_RP3	TAGGCATAAGGCTAGGAGGAG	qRT-PCR
ERF11_qPCR_F	GCCCACTGCTTGAGTT	qRT-PCR
ERF11_qPCR_R	ACACGTCGTCCTTCAT	qRT-PCR
ERF5_qPCR_F	CGGAATTATGTGACTGGGATTTAAC	qRT-PCR
ERF5_qPCR_R	ACAACGGTCAACTGGGAATAA	qRT-PCR
ERF4_qPCR_F	AGATTCGTTACAGAGGCGTTAG	qRT-PCR
ERF4_qPCR_R	CTCTTCAGCCGTATCGAAAGT	qRT-PCR
ERF6_qPCR_F	CGAGGATCAAAGGCGATTCT	qRT-PCR
ERF6_qPCR_R	CCGTCTCTCTTCCGTTTGTT	qRT-PCR

`

AT4G28140_qPCR_F	TGTGAATAAGGAAAGCGAGCTGC	qRT-PCR
AT4G28140_qPCR_R	GGCTGTGGCGTTTCAGGTTC	qRT-PCR
AT1G64380_qPCR_F	ACGACAACTACTACTGCGGTTAC	qRT-PCR
AT1G64380_qPCR_R	GCAAGAACTTCCCAAATCAGCT	qRT-PCR
WAK-like 2_qPCR_F	TAGGACGCAACCAGTGTAAAG	qRT-PCR
WAK-like 2_qPCR_R	AGCAACAGTGCTGAACCTATAA	qRT-PCR
Pectate lyase 9_qPCR_F	GACCACAACTCGCTCTCTAAC	qRT-PCR
Pectate lyase 9_qPCR_R	CCCTAGCAACATCACCTCATC	qRT-PCR
GATL10_qPCR_F	GCGATGGAGAGAAGGAGATTAC	qRT-PCR
GATL10_qPCR_R	TCACCACCAAACACTAGAAGAA	qRT-PCR
GATL2_qPCR_F	CAAACCCTTCTCTCTCCATCAC	qRT-PCR
GATL2_qPCR_R	ATCTCCTTCTCGCCATTTCTTT	qRT-PCR
EXT4_qPCR_F	ACCATTCTCCTCCTCCTCCA	qRT-PCR
EXT4_qPCR_R	ATGAAGGGATCACACTCATTAACA	qRT-PCR
PP2CA_qPCR_F	CGTCGGTTTGTGGTAGAAGA	qRT-PCR
PP2CA_qPCR_R	CCGTCAAAGACACCGTAGAA	qRT-PCR

`

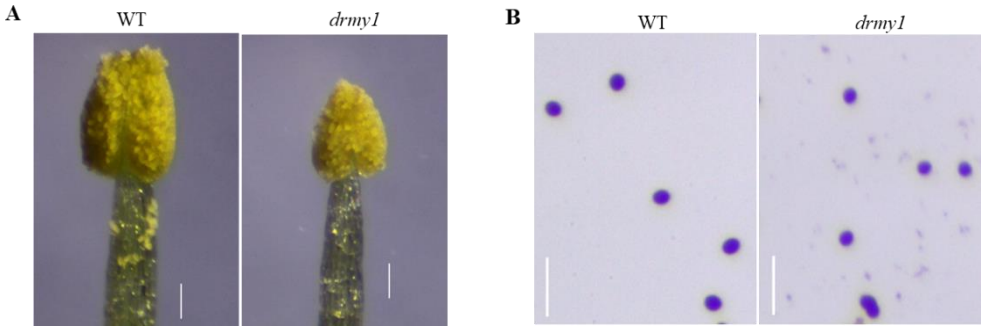

Supplemental Figure A-1. Anther dehiscence and pollen viability of WT and the *drmy1* mutant. (A) Anther dehiscence is normal in both genotypes. Bars, 0.1 mm. (B) I_2-KI staining of mature pollen grains collected from WT and the *drmy1* mutant. Bars, 0.1 mm.

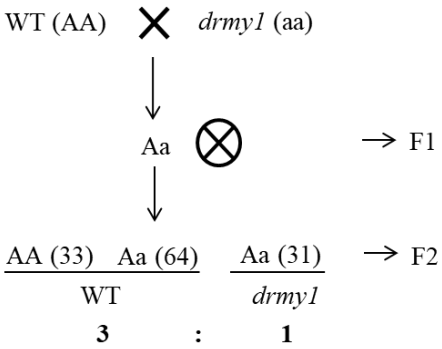

Supplemental Figure A-2. Co-segregation analysis of the *drmy1* mutant. A schematic diagram showing the co-segregation analysis procedure and the segregation ratio of 3:1 (97:31, P>0.8, Student's T-test) in F2 plants.

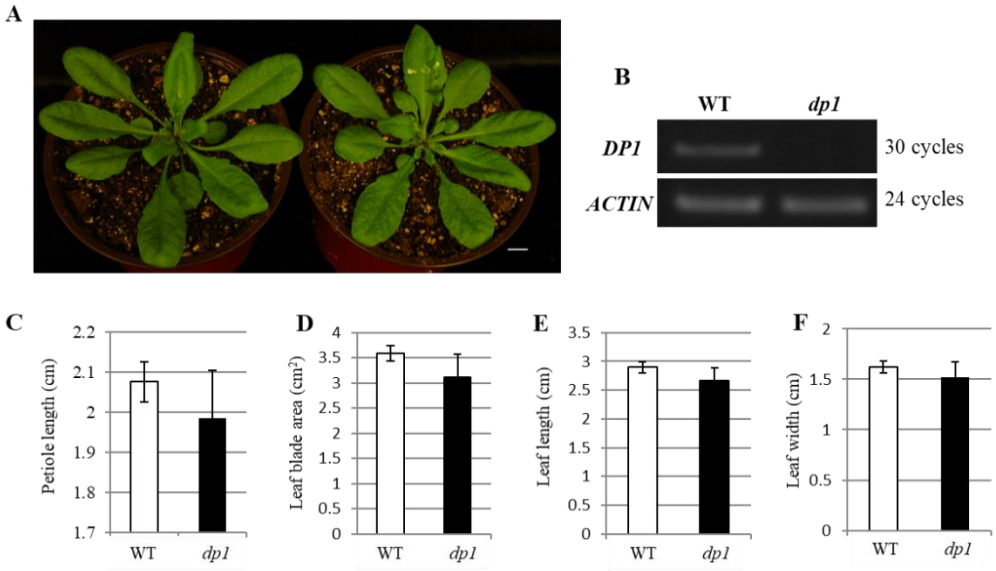

Supplemental Figure A-3. Leaf morphology of WT and the *dp1* mutant. (A) 28-d-old plants of WT (left) and the *dp1* mutant (SALK_113831C, right). Bar, 2 cm. (B) RT-PCR analysis of *DP1* expression in WT and the *dp1* mutant. *AtACTIN2* was used as an endogenous gene. Leaf parameters of fully expanded fifth leaf in WT and the *dp1* mutant: (C) Petiole length, (D) Leaf blade area, (E) Leaf blade length, and (F) Leaf blade width. At least five leaves for each genotype were used for measurement. Error bars indicate SD. No significant difference was found between of WT and the *dp1* mutant in different leaf parameters.

`

Supplemental Figure A-4. Phenotype of the *drmy1* mutant and the *drmy1* mutant carrying *35S-DRMY1-GFP*. The introduction of *35S-DRMY1-GFP* into the *drmy1* mutant background rescued the mutant phenotype, indicating that *DRMY1-GFP* is functional.

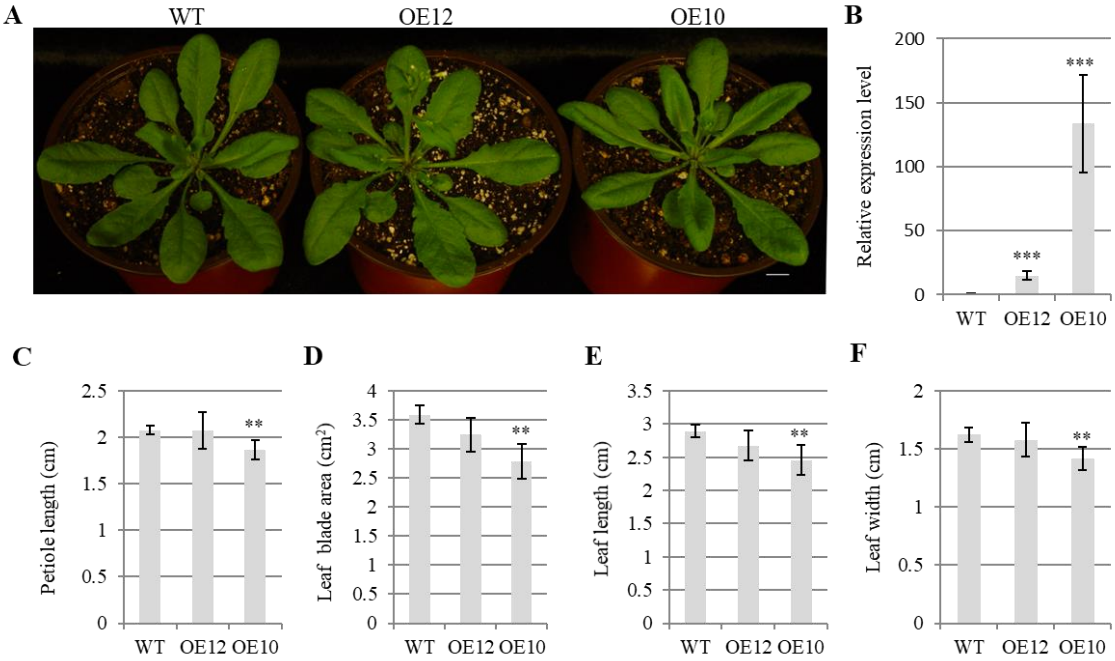

Supplemental Figure A-5. Leaf morphology of WT and *35S-DRMY1* overexpression transgenic plants. (A) 28-d-old plants of WT (left) and the *35S-DRMY1* overexpression transgenic line 12 (middle) and line 10 (right). Bar, 2 cm. (B) qRT-PCR analysis of *DRMY1* expression in WT and two transgenic lines with two biological replicates (three technical replicates each). *AtACTIN2* was used as an endogenous control. Leaf parameters of fully expanded fifth leaf in WT and two transgenic lines: (C) Petiole length, (D) Leaf blade area, (E) Leaf blade length, and (F) Leaf blade width. At least five leaves for each genotype were used for measurement. Error bars indicate SD. Asterisks represent statistically significant differences calculated by Student's t-test (*, $P < 0.05$; **, $P < 0.01$; ***, $P < 0.001$).

`

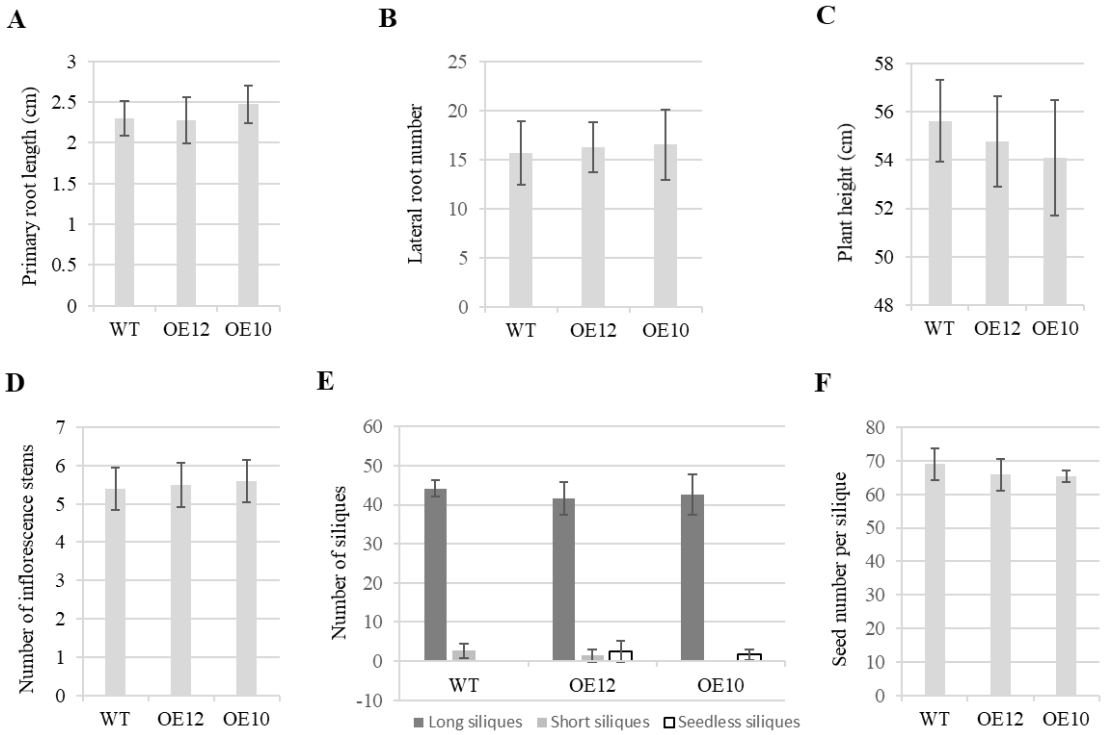

Supplemental Figure A-6. Phenotype of root, stem and seed production in WT and *35S-DRMY1* overexpression transgenic plants. (A) 1-week-old primary root length (n=16). (B) 10-day-old lateral root number (n=13). (C) 7-week-old plant height (n=6). (D) Number of inflorescence stems (n=5). (E) Number of siliques in the main inflorescence stem (n=5). (F) Average number of seeds per long silique (n=9). Error bars indicate SD.

`

APPENDIX B

SUPPORTING MATERIAL FOR CHAPTER THREE

Supplemental Table B-1: Transcription factors of different families in Seashore paspalum's transcriptome

Family	Number of genes
MYB family protein	419
WRKY family protein	370
G2-like family protein	268
bZIP family protein	240
bHLH family protein	185
C3H family protein	175
NAC family protein	163
B3 family protein	159
C2H2 family protein	143
SRS family protein	105
FAR1 family protein	102
pentatricopeptide (PPR) repeat-containing protein	81
Trihelix family protein	77
GATA family protein	74
protein kinase family protein	74
EIL family protein	62
ARF family protein	47
HB-other family protein	41
E2F/DP family protein	39
ERF family protein	37
GRAS family protein	35
HD-ZIP family protein	33
NF-YB family protein	28
LBD family protein	26
GRF family protein	23
histone-like transcription factor and archaeal histone family protein	23
HB-PHD family protein	19
CAMTA family protein	17
AP2 family protein	17
CPP family protein	12
LSD family protein	11
CO-like family protein	10
HSF family protein	10
STAT family protein	10
ZF-HD family protein	9
alpha/beta hydrolase fold, putative	8
BES1 family protein	8
WD-40 repeat family protein	8

`

MIKC family protein	7
Nin-like family protein	7
NF-YA family protein	6
RIPER7 - Ripening-related family protein precursor	6
GeBP family protein	5
LFY family protein	5
S1Fa-like family protein	5
TCP family transcription factor, putative	5
AP2 domain containing protein	4
NF-YC family protein	4
helix-loop-helix DNA-binding domain containing protein	3
SBP family protein	3
AGAMOUS-like 26	2
ARR-B family protein	2
BEE 3, putative, expressed	2
Dof family protein	2
APRATAXIN-like	1
auxin response factor 19, putative	1
auxin response factor 9	1
B-box type zinc finger protein with CCT domain	1
BBR-BPC family protein	1
CCT/B-box zinc finger protein, putative	1
DUF260 domain containing protein, putative	1
ethylene response factor 110	1
homeobox associated leucine zipper, putative	1
no apical meristem protein, putative, expressed	1
nuclear transcription factor Y subunit, putative	1
pathogenesis related homeodomain protein A	1
two-component response regulator, putative	1
zinc finger C-x8-C-x5-C-x3-H type family protein	1
Total	**3250**

`

Supplemental Table B-2: Summary of possible transcription factors that are commonly regulated by Supreme and Parish under salt-treated conditions

Gene_ID	Hit description	Log_2FC (S_{salt}/S_{normal})	Log_2FC (P_{salt}/P_{normal})
m.52678	Oryza sativa Indica Group MYB_related family protein	2.6	2.2
m.237571	Oryza sativa Indica Group MYB_related family protein	2.2	2.6
m.48837	Oryza barthii GATA family protein	2.1	1.8
m.167648	Oryza barthii C3H family protein	1.4	1.3
m.88900	Oryza sativa Indica Group WRKY family protein	1.2	1.4
m.96240	Oryza barthii G2-like family protein	1.0	1.0
m.54046	Oryza punctata G2-like family protein	-1.1	-1.0
m.32600	Oryza sativa Indica Group MYB family protein	-1.1	1.1
m.181019	Oryza punctata bZIP family protein	-1.2	-1.3
m.65089	Oryza sativa Japonica Group histone-like transcription factor	-1.9	-3.0
m.43705	Arabidopsis lyrata C3H family protein	-2.5	1.4
m.80449	Oryza barthii SRS family protein	-2.9	-1.7

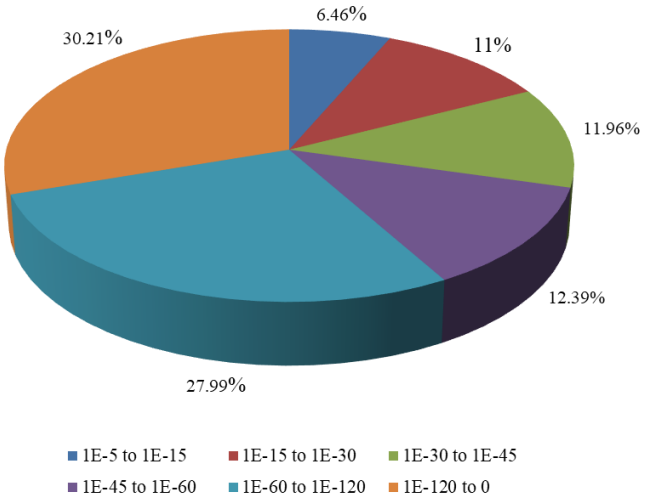

Supplemental Figure B-1. E-value distribution of the Blastx hits against the nr protein database with a E-value cutoff of $1E^{-5}$.

`

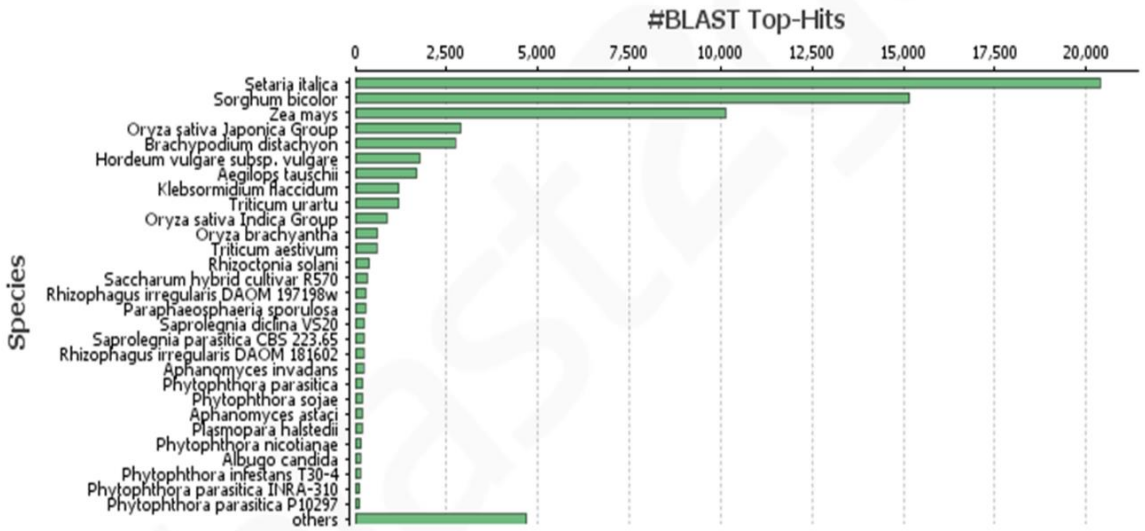

Supplemental Figure B-2. Species distribution of the top blast hits for each unigene with a E-value cutoff of 1E^{-5}. 82,608 unigenes in Seashore paspalum's transcriptome were blasted against the NCBI non-redundant (nr) protein database using Blastx with an E-value cutoff of 1E^{-5}. The best blastx hits were then imported to Blast2GO software to generate the species distribution diagram.

`

REFERENCES

Achard, Patrick, Hui Cheng, Liesbeth De Grauwe, Jan Decat, Hermien Schoutteten, Thomas Moritz, Dominique Van Der Straeten, Jinrong Peng, and Nicholas P Harberd. 2006. 'Integration of plant responses to environmentally activated phytohormonal signals', Science, 311: 91-94.

Agatep, Ronald, Robert D Kirkpatrick, Debra L Parchaliuk, Robin A Woods, and R Daniel Gietz. 1998. 'Transformation of Saccharomyces cerevisiae by the lithium acetate/single-stranded carrier DNA/polyethylene glycol protocol', Technical Tips Online, 3: 133-37.

Alabadí, David, Marcelo J Yanovsky, Paloma Más, Stacey L Harmer, and Steve A Kay. 2002. 'Critical role for CCA1 and LHY in maintaining circadian rhythmicity in Arabidopsis', Current Biology, 12: 757-61.

Ambawat, Supriya, Poonam Sharma, Neelam R Yadav, and Ram C Yadav. 2013. 'MYB transcription factor genes as regulators for plant responses: an overview', Physiology and Molecular Biology of Plants, 19: 307-21.

Apse, Maris P, Gilad S Aharon, Wayne A Snedden, and Eduardo Blumwald. 1999. 'Salt tolerance conferred by overexpression of a vacuolar Na+/H+ antiport in Arabidopsis', Science, 285: 1256-58.

Apweiler, Rolf, Amos Bairoch, Cathy H Wu, Winona C Barker, Brigitte Boeckmann, Serenella Ferro, Elisabeth Gasteiger, Hongzhan Huang, Rodrigo Lopez, and Michele Magrane. 2004. 'UniProt: the universal protein knowledgebase', Nucleic Acids Research, 32: D115-D19.

Assaha, Dekoum VM, Akihiro Ueda, Hirofumi Saneoka, Rashid Al-Yahyai, and Mahmoud W Yaish. 2017. 'The Role of Na+ and K+ Transporters in Salt Stress Adaptation in Glycophytes', Frontiers in Physiology, 8: 509.

Banerjee, Aditya, and Aryadeep Roychoudhury. 2015. 'WRKY proteins: signaling and regulation of expression during abiotic stress responses', The Scientific World Journal, 2015.

Baranowskij, Nadja, Claus Frohberg, Salome Prat, and Lothar Willmitzer. 1994. 'A novel DNA binding protein with homology to Myb oncoproteins containing only one repeat can function as a transcriptional activator', The EMBO Journal, 13: 5383.

Barragán, Verónica, Eduardo O Leidi, Zaida Andrés, Lourdes Rubio, Anna De Luca, José A Fernández, Beatriz Cubero, and José M Pardo. 2012. 'Ion exchangers NHX1 and NHX2 mediate active potassium uptake into vacuoles to regulate cell turgor and stomatal function in Arabidopsis', The Plant Cell, 24: 1127-42.

`

Barrero, José María, Pedro Piqueras, Miguel González-Guzmán, Ramón Serrano, Pedro L Rodríguez, María Rosa Ponce, and José Luis Micol. 2005. 'A mutational analysis of the ABA1 gene of Arabidopsis thaliana highlights the involvement of ABA in vegetative development', Journal of Experimental Botany, 56: 2071-83.

Bartels, Dorothea, and Ramanjulu Sunkar. 2005. 'Drought and salt tolerance in plants', Critical Reviews in Plant Sciences, 24: 23-58.

Bassil, Elias, Masa-aki Ohto, Tomoya Esumi, Hiromi Tajima, Zhu Zhu, Olivier Cagnac, Mark Belmonte, Zvi Peleg, Toshio Yamaguchi, and Eduardo Blumwald. 2011. 'The Arabidopsis intracellular Na+/H+ antiporters NHX5 and NHX6 are endosome associated and necessary for plant growth and development', The Plant Cell, 23: 224-39.

Beemster, Gerrit TS, Kristof De Vusser, Evelien De Tavernier, Kirsten De Bock, and Dirk Inzé. 2002. 'Variation in growth rate between Arabidopsis ecotypes is correlated with cell division and A-type cyclin-dependent kinase activity', Plant Physiology, 129: 854-64.

Berckmans, Barbara, and Lieven De Veylder. 2009. 'Transcriptional control of the cell cycle', Current Opinion in Plant Biology, 12: 599-605.

Bolger, Anthony M, Marc Lohse, and Bjoern Usadel. 2014. 'Trimmomatic: a flexible trimmer for Illumina sequence data', Bioinformatics: btu170.

Bose, Jayakumar, Ana Rodrigo-Moreno, and Sergey Shabala. 2014. 'ROS homeostasis in halophytes in the context of salinity stress tolerance', Journal of Experimental Botany, 65: 1241-57.

Boudolf, V., T. Lammens, J. Boruc, J. Van Leene, H. Van Den Daele, S. Maes, G. Van Isterdael, E. Russinova, E. Kondorosi, E. Witters, G. De Jaeger, D. Inze, and L. De Veylder. 2009. 'CDKB1;1 forms a functional complex with CYCA2;3 to suppress endocycle onset', Plant Physiology, 150: 1482-93.

Breuer, C., T. Ishida, and K. Sugimoto. 2010. 'Developmental control of endocycles and cell growth in plants', Current Opinion in Plant Biology, 13: 654-60.

Breuer, C., A. Kawamura, T. Ichikawa, R. Tominaga-Wada, T. Wada, Y. Kondou, S. Muto, M. Matsui, and K. Sugimoto. 2009. 'The trihelix transcription factor GTL1 regulates ploidy-dependent cell growth in the Arabidopsis trichome', The Plant Cell, 21: 2307-22.

Breuer, Christian, Kengo Morohashi, Ayako Kawamura, Naoki Takahashi, Takashi Ishida, Masaaki Umeda, Erich Grotewold, and Keiko Sugimoto. 2012. 'Transcriptional repression of the APC/C activator CCS52A1 promotes active termination of cell growth', The EMBO Journal, 31: 4488-501.

`

Breuer, Christian, Nicola J Stacey, Christopher E West, Yunde Zhao, Joanne Chory, Hirokazu Tsukaya, Yoshitaka Azumi, Anthony Maxwell, Keith Roberts, and Keiko Sugimoto-Shirasu. 2007. 'BIN4, a novel component of the plant DNA topoisomerase VI complex, is required for endoreduplication in Arabidopsis', The Plant Cell, 19: 3655-68.

Byrne, Mary E. 2009. 'A role for the ribosome in development', Trends in Plant Science, 14: 512-19.

Caesar, Katharina, Kirstin Elgass, Zhonghua Chen, Peter Huppenberger, Janika Witthöft, Frank Schleifenbaum, Michael R Blatt, Claudia Oecking, and Klaus Harter. 2011. 'A fast brassinolide-regulated response pathway in the plasma membrane of Arabidopsis thaliana', The Plant Journal, 66: 528-40.

Caldana, Camila, Yan Li, Andrea Leisse, Yi Zhang, Lisa Bartholomaeus, Alisdair R Fernie, Lothar Willmitzer, and Patrick Giavalisco. 2013. 'Systemic analysis of inducible target of rapamycin mutants reveal a general metabolic switch controlling growth in Arabidopsis thaliana', The Plant Journal, 73: 897-909.

Camacho, Christiam, George Coulouris, Vahram Avagyan, Ning Ma, Jason Papadopoulos, Kevin Bealer, and Thomas L Madden. 2009. 'BLAST+: architecture and applications', BMC Bioinformatics, 10: 421.

Chaiwanon, Juthamas, Wenfei Wang, Jia-Ying Zhu, Eunkyoo Oh, and Zhi-Yong Wang. 2016. 'Information integration and communication in plant growth regulation', Cell, 164: 1257-68.

Chaves, M. M., J. Flexas, and C. Pinheiro. 2009. 'Photosynthesis under drought and salt stress: regulation mechanisms from whole plant to cell', Annals of Botany, 103: 551-60.

Chen, Jie, Sibao Wan, Huaihua Liu, Shuli Fan, Yujuan Zhang, Wei Wang, Minxuan Xia, Rui Yuan, Fenni Deng, and Fafu Shen. 2016. 'Overexpression of an Apocynum venetum DEAD-box helicase gene (AvDH1) in cotton confers salinity tolerance and increases yield in a saline field', Frontiers in Plant Science, 6: 1227.

Cheng, Wan-Hsing, Akira Endo, Li Zhou, Jessica Penney, Huei-Chi Chen, Analilia Arroyo, Patricia Leon, Eiji Nambara, Tadao Asami, and Mitsunori Seo. 2002. 'A unique short-chain dehydrogenase/reductase in Arabidopsis glucose signaling and abscisic acid biosynthesis and functions', The Plant Cell, 14: 2723-43.

Cho, Hyung-Taeg, and Daniel J Cosgrove. 2000. 'Altered expression of expansin modulates leaf growth and pedicel abscission in Arabidopsis thaliana', Proceedings of the National Academy of Sciences of USA, 97: 9783-88.

Churchman, Michelle L, Matthew L Brown, Naohiro Kato, Viktor Kirik, Martin Hülskamp, Dirk Inzé, Lieven De Veylder, Jason D Walker, Zhengui Zheng, and David G

Oppenheimer. 2006. 'SIAMESE, a plant-specific cell cycle regulator, controls endoreplication onset in Arabidopsis thaliana', The Plant Cell, 18: 3145-57.

Claeys, Hannes, Aleksandra Skirycz, Katrien Maleux, and Dirk Inzé. 2012. 'DELLA signaling mediates stress-induced cell differentiation in Arabidopsis leaves through modulation of anaphase-promoting complex/cyclosome activity', Plant Physiology, 159: 739-47.

Cleland, Robert E. 2010. 'Auxin and cell elongation.' in, Plant Hormones (Springer).

Clough, Steven J, and Andrew F Bent. 1998. 'Floral dip: a simplified method forAgrobacterium-mediated transformation ofArabidopsis thaliana', The Plant Journal, 16: 735-43.

Clouse, Steven D, Mark Langford, and Trevor C McMorris. 1996. 'A brassinosteroid-insensitive mutant in Arabidopsis thaliana exhibits multiple defects in growth and development', Plant Physiology, 111: 671-78.

Conesa, Ana, Stefan Götz, Juan Miguel García-Gómez, Javier Terol, Manuel Talón, and Montserrat Robles. 2005. 'Blast2GO: a universal tool for annotation, visualization and analysis in functional genomics research', Bioinformatics, 21: 3674-76.

Consortium, UniProt. 2017. 'UniProt: the universal protein knowledgebase', Nucleic Acids Research, 45: D158-D69.

Corpet, Florence. 1988. 'Multiple sequence alignment with hierarchical clustering', Nucleic Acids Research, 16: 10881-90.

Cosgrove, Daniel Cosgrove. 2012. 'Comparative structure and biomechanics of plant primary and secondary cell walls', Frontiers in Plant Science, 3: 204.

Cosgrove, Daniel J. 1993. 'How do plant cell walls extend?', Plant Physiology, 102: 1.

———. 2005. 'Growth of the plant cell wall', Nature Reviews Molecular Cell Biology, 6: 850-61.

———. 2014. 'The Plant Cell Growth and Elongation', eLS.

Das, Kaushik, and Aryadeep Roychoudhury. 2014. 'Reactive oxygen species (ROS) and response of antioxidants as ROS-scavengers during environmental stress in plants', Frontiers in Environmental Science, 2: 53.

Dassanayake, Maheshi, Dong-Ha Oh, Jeffrey S Haas, Alvaro Hernandez, Hyewon Hong, Shahjahan Ali, Dae-Jin Yun, Ray A Bressan, Jian-Kang Zhu, and Hans J Bohnert. 2011. 'The genome of the extremophile crucifer Thellungiella parvula', Nature Genetics, 43: 913-18.

Davenport, Romola Jane, ALICIA MUÑOZ-MAYOR, Deepa Jha, Pauline Adobea Essah, ANA Rus, and Mark Tester. 2007. 'The Na+ transporter AtHKT1; 1 controls

retrieval of Na+ from the xylem in Arabidopsis', Plant, Cell & Environment, 30: 497-507.

De Cnodder, Tinne, Kris Vissenberg, Dominique Van Der Straeten, and J-P Verbelen. 2005. 'Regulation of cell length in the Arabidopsis thaliana root by the ethylene precursor 1-aminocyclopropane-1-carboxylic acid: a matter of apoplastic reactions', New Phytologist, 168: 541-50.

De Schutter, Kristof, Jérôme Joubès, Toon Cools, Aurine Verkest, Florence Corellou, Elena Babiychuk, Els Van Der Schueren, Tom Beeckman, Sergeï Kushnir, and Dirk Inze. 2007. 'Arabidopsis WEE1 kinase controls cell cycle arrest in response to activation of the DNA integrity checkpoint', The Plant Cell, 19: 211-25.

De Veylder, L., J. C. Larkin, and A. Schnittger. 2011. 'Molecular control and function of endoreplication in development and physiology', Trends in Plant Science, 16: 624-34.

De Veylder, Lieven, Tom Beeckman, Gerrit TS Beemster, Luc Krols, Franky Terras, Isabelle Landrieu, Els Van Der Schueren, Sara Maes, Mirande Naudts, and Dirk Inzé. 2001. 'Functional analysis of cyclin-dependent kinase inhibitors of Arabidopsis', The Plant Cell, 13: 1653-68.

Deinlein, U., A. B. Stephan, T. Horie, W. Luo, G. Xu, and J. I. Schroeder. 2014. 'Plant salt-tolerance mechanisms', Trends Plant Science, 19: 371-9.

Del Pozo, Juan Carlos, Maria Beatrice Boniotti, and Crisanto Gutierrez. 2002. 'Arabidopsis E2Fc functions in cell division and is degraded by the ubiquitin-SCFAtSKP2 pathway in response to light', The Plant Cell, 14: 3057-71.

Demidchik, Vadim. 2014. 'Mechanisms and physiological roles of K+ efflux from root cells', Journal of Plant Physiology, 171: 696-707.

Demidchik, Vadim, and Frans JM Maathuis. 2007. 'Physiological roles of nonselective cation channels in plants: from salt stress to signalling and development', New Phytologist, 175: 387-404.

Demidchik, Vadim, Zhonglin Shang, Ryoung Shin, Renato Colaço, Anuphon Laohavisit, Sergey Shabala, and Julia M Davies. 2011. 'Receptor-like activity evoked by extracellular ADP in Arabidopsis root epidermal plasma membrane', Plant Physiology, 156: 1375-85.

Demidchik, Vadim, and Mark Tester. 2002. 'Sodium fluxes through nonselective cation channels in the plasma membrane of protoplasts from Arabidopsis roots', Plant Physiology, 128: 379-87.

Deprost, Dorothee, Lei Yao, Rodnay Sormani, Manon Moreau, Guillaume Leterreux, Maryse Nicolaï, Magali Bedu, Christophe Robaglia, and Christian Meyer. 2007.

'The Arabidopsis TOR kinase links plant growth, yield, stress resistance and mRNA translation', EMBO Reports, 8: 864-70.

Dewitte, Walter, Simon Scofield, Annette A Alcasabas, Spencer C Maughan, Margit Menges, Nils Braun, Carl Collins, Jeroen Nieuwland, Els Prinsen, and Venkatesan Sundaresan. 2007. 'Arabidopsis CYCD3 D-type cyclins link cell proliferation and endocycles and are rate-limiting for cytokinin responses', Proceedings of the National Academy of Sciences of USA, 104: 14537-42.

Diet, Anouck, Bruce Link, Georg J Seifert, Barbara Schellenberg, Ulrich Wagner, Markus Pauly, Wolf-Dieter Reiter, and Christoph Ringli. 2006. 'The Arabidopsis root hair cell wall formation mutant lrx1 is suppressed by mutations in the RHM1 gene encoding a UDP-L-rhamnose synthase', The Plant Cell, 18: 1630-41.

Du, Hai, Yong-Bin Wang, Yi Xie, Zhe Liang, San-Jie Jiang, Shuang-Shuang Zhang, Yu-Bi Huang, and Yi-Xiong Tang. 2013. 'Genome-wide identification and evolutionary and expression analyses of MYB-related genes in land plants', DNA Research, 20: 437-48.

Dubois, Marieke, Aleksandra Skirycz, Hannes Claeys, Katrien Maleux, Stijn Dhondt, Stefanie De Bodt, Robin Vanden Bossche, Liesbeth De Milde, Takeshi Yoshizumi, and Minami Matsui. 2013. 'ETHYLENE RESPONSE FACTOR6 acts as a central regulator of leaf growth under water-limiting conditions in Arabidopsis', Plant Physiology, 162: 319-32.

Dubois, Marieke, Lisa Van den Broeck, Hannes Claeys, Kaatje Van Vlierberghe, Minami Matsui, and Dirk Inzé. 2015. 'The ETHYLENE RESPONSE FACTORs ERF6 and ERF11 antagonistically regulate mannitol-induced growth inhibition in Arabidopsis', Plant Physiology: pp. 00335.2015.

Dubos, Christian, Ralf Stracke, Erich Grotewold, Bernd Weisshaar, Cathie Martin, and Loïc Lepiniec. 2010. 'MYB transcription factors in Arabidopsis', Trends in Plant Science, 15: 573-81.

Dubouzet, Joseph G, Yoh Sakuma, Yusuke Ito, Mie Kasuga, Emilyn G Dubouzet, Setsuko Miura, Motoaki Seki, Kazuo Shinozaki, and Kazuko Yamaguchi-Shinozaki. 2003. 'OsDREB genes in rice, Oryza sativa L., encode transcription activators that function in drought-, high-salt-and cold-responsive gene expression', The Plant Journal, 33: 751-63.

Elleman, Carole J, Clare E Willson, RH Sarker, and HG Dickinson. 1988. 'Interaction between the pollen tube and stigmatic cell wall following pollination in Brassica oleracea', New Phytologist, 109: 111-17.

Eloy, Nubia B, Marcelo de Freitas Lima, Daniël Van Damme, Hannes Vanhaeren, Nathalie Gonzalez, Liesbeth De Milde, Adriana S Hemerly, Gerrit TS Beemster, Dirk Inzé,

and Paulo CG Ferreira. 2011. 'The APC/C subunit 10 plays an essential role in cell proliferation during leaf development', The Plant Journal, 68: 351-63.

Ferjani, Ali, Gorou Horiguchi, Satoshi Yano, and Hirokazu Tsukaya. 2007. 'Analysis of leaf development in fugu mutants of Arabidopsis reveals three compensation modes that modulate cell expansion in determinate organs', Plant Physiology, 144: 988-99.

Ferjani, Ali, Kazuki Ishikawa, Mariko Asaoka, Masanori Ishida, Gorou Horiguchi, Masayoshi Maeshima, and Hirokazu Tsukaya. 2013. 'Class III compensation, represented by KRP2 overexpression, depends on V-ATPase activity in proliferative cells', Plant Signaling & Behavior, 8: e27204.

Flowers, Timothy J, and Timothy D Colmer. 2008. 'Salinity tolerance in halophytes', New Phytologist, 179: 945-63.

Foster, Cliff E, Tina M Martin, and Markus Pauly. 2010a. 'Comprehensive compositional analysis of plant cell walls (lignocellulosic biomass) part I: lignin', JoVE (Journal of Visualized Experiments): e1745-e45.

———. 2010b. 'Comprehensive compositional analysis of plant cell walls (lignocellulosic biomass) part II: carbohydrates', JoVE (Journal of Visualized Experiments): e1837-e37.

Francis, Dennis. 2007. 'The plant cell cycle− 15 years on', New Phytologist, 174: 261-78.

Fu, Xiangdong, Donald E Richards, Barbara Fleck, Daoxin Xie, Nicolas Burton, and Nicholas P Harberd. 2004. 'The Arabidopsis mutant sleepy1gar2-1 protein promotes plant growth by increasing the affinity of the SCFSLY1 E3 ubiquitin ligase for DELLA protein substrates', The Plant Cell, 16: 1406-18.

Fujikura, Ushio, Gorou Horiguchi, María Rosa Ponce, José Luis Micol, and Hirokazu Tsukaya. 2009. 'Coordination of cell proliferation and cell expansion mediated by ribosome-related processes in the leaves of Arabidopsis thaliana', The Plant Journal, 59: 499-508.

Fujita, Yasunari, Miki Fujita, Kazuo Shinozaki, and Kazuko Yamaguchi-Shinozaki. 2011. 'ABA-mediated transcriptional regulation in response to osmotic stress in plants', Journal of Plant Research, 124: 509-25.

Fukushima, Romualdo S, and Ronald D Hatfield. 2004. 'Comparison of the acetyl bromide spectrophotometric method with other analytical lignin methods for determining lignin concentration in forage samples', Journal of Agricultural and Food Chemistry, 52: 3713-20.

Gaamouche, Tarik, Carmem-Lara de O Manes, Dorota Kwiatkowska, Barbara Berckmans, Rachel Koumproglou, Sara Maes, Tom Beeckman, Teva Vernoux, John H Doonan, and Jan Traas. 2010. 'Cyclin-dependent kinase activity maintains the shoot apical meristem cells in an undifferentiated state', The Plant Journal, 64: 26-37.

`

Geitmann, Anja. 2010. 'Mechanical modeling and structural analysis of the primary plant cell wall', Current Opinion in Plant Biology, 13: 693-99.

Gill, Sarvajeet Singh, and Narendra Tuteja. 2010. 'Reactive oxygen species and antioxidant machinery in abiotic stress tolerance in crop plants', Plant Physiology and Biochemistry, 48: 909-30.

Golldack, Dortje, Chao Li, Harikrishnan Mohan, and Nina Probst. 2014. 'Tolerance to drought and salt stress in plants: unraveling the signaling networks', Abiotic Stress: Molecular Genetics and Genomics: 15.

Gonzalez, Nathalie, Hannes Vanhaeren, and Dirk Inzé. 2012. 'Leaf size control: complex coordination of cell division and expansion', Trends in Plant Science, 17: 332-40.

Goujon, Mickael, Hamish McWilliam, Weizhong Li, Franck Valentin, Silvano Squizzato, Juri Paern, and Rodrigo Lopez. 2010. 'A new bioinformatics analysis tools framework at EMBL–EBI', Nucleic Acids Research, 38: W695-W99.

Goyal, Etika, Singh K Amit, Ravi S Singh, Ajay K Mahato, Suresh Chand, and Kumar Kanika. 2016. 'Transcriptome profiling of the salt-stress response in Triticum aestivum cv. Kharchia Local', Scientific Reports, 6.

Grabherr, Manfred G, Brian J Haas, Moran Yassour, Joshua Z Levin, Dawn A Thompson, Ido Amit, Xian Adiconis, Lin Fan, Raktima Raychowdhury, and Qiandong Zeng. 2011. 'Full-length transcriptome assembly from RNA-Seq data without a reference genome', Nature Biotechnology, 29: 644-52.

Guo, Lin, Haibian Yang, Xiaoyan Zhang, and Shuhua Yang. 2013. 'Lipid transfer protein 3 as a target of MYB96 mediates freezing and drought stress in Arabidopsis', Journal of Experimental Botany, 64: 1755-67.

Gupta, Bhaskar, and Bingru Huang. 2014. 'Mechanism of salinity tolerance in plants: physiological, biochemical, and molecular characterization', International Journal of Genomics, 2014.

Haga, Nozomi, Kiichi Kato, Masatake Murase, Satoshi Araki, Minoru Kubo, Taku Demura, Kaoru Suzuki, Isabel Müller, Ute Voß, and Gerd Jürgens. 2007. 'R1R2R3-Myb proteins positively regulate cytokinesis through activation of KNOLLE transcription in Arabidopsis thaliana', Development, 134: 1101-10.

Hamant, Olivier, and Jan Traas. 2010. 'The mechanics behind plant development', New Phytologist, 185: 369-85.

Harman-Ware, Anne E, Cliff Foster, Renee M Happs, Crissa Doeppke, Kristoffer Meunier, Jackson Gehan, Fengxia Yue, Fachuang Lu, and Mark Davis. 2016. 'Quantitative Analysis of Lignin Monomers by a Thioacidolysis Method Tailored for Higher-Throughput Analysis', Biotechnology Journal.

`

Hartung, Frank, Karel J Angelis, Armin Meister, Ingo Schubert, Michael Melzer, and Holger Puchta. 2002. 'An archaebacterial topoisomerase homolog not present in other eukaryotes is indispensable for cell proliferation of plants', Current Biology, 12: 1787-91.

Haynes, RJ. 1980. 'A comparison of two modified Kjeldahl digestion techniques for multi-element plant analysis with conventional wet and dry ashing methods', Communications in Soil Science & Plant Analysis, 11: 459-67.

Hepworth, Jo, and Michael Lenhard. 2014. 'Regulation of plant lateral-organ growth by modulating cell number and size', Current Opinion in Plant Biology, 17: 36-42.

Hjellström, Mattias, Anna SB Olsson, Peter Engström, and EM Söderman. 2003. 'Constitutive expression of the water deficit-inducible homeobox gene ATHB7 in transgenic Arabidopsis causes a suppression of stem elongation growth', Plant, Cell & Environment, 26: 1127-36.

Horie, T., A. Costa, T. H. Kim, M. J. Han, R. Horie, H. Y. Leung, A. Miyao, H. Hirochika, G. An, and J. I. Schroeder. 2007. 'Rice OsHKT2;1 transporter mediates large Na+ influx component into K+-starved roots for growth', The EMBO Journal, 26: 3003-14.

Horie, Tomoaki, Felix Hauser, and Julian I Schroeder. 2009. 'HKT transporter-mediated salinity resistance mechanisms in Arabidopsis and monocot crop plants', Trends in Plant Science, 14: 660-68.

Horie, Tomoaki, Jo Motoda, Masahiro Kubo, Hua Yang, Kinya Yoda, Rie Horie, Wai-Yin Chan, Ho-Yin Leung, Kazumi Hattori, and Mami Konomi. 2005. 'Enhanced salt tolerance mediated by AtHKT1 transporter-induced Na+ unloading from xylem vessels to xylem parenchyma cells', The Plant Journal, 44: 928-38.

Horiguchi, Gorou, Gyung-Tae Kim, and Hirokazu Tsukaya. 2005. 'The transcription factor AtGRF5 and the transcription coactivator AN3 regulate cell proliferation in leaf primordia of Arabidopsis thaliana', The Plant Journal, 43: 68-78.

Horiguchi, Gorou, Almudena Mollá-Morales, José Manuel Pérez-Pérez, Kouji Kojima, Pedro Robles, María Rosa Ponce, José Luis Micol, and Hirokazu Tsukaya. 2011. 'Differential contributions of ribosomal protein genes to Arabidopsis thaliana leaf development', The Plant Journal, 65: 724-36.

Horiguchi, Gorou, and Hirokazu Tsukaya. 2011. 'Organ size regulation in plants: insights from compensation', Frontiers in Plant Science, 2.

Hu, Yuxin, Huay Mei Poh, and Nam-Hai Chua. 2006. 'The Arabidopsis ARGOS-LIKE gene regulates cell expansion during organ growth', The Plant Journal, 47: 1-9.

`

Humplík, Jan F, Véronique Bergougnoux, and Elizabeth Van Volkenburgh. 2017. 'To Stimulate or Inhibit? That Is the Question for the Function of Abscisic Acid', Trends in Plant Science, 22: 830-41.

Hur, Yoon-Sun, Ji-Hyun Um, Sunghan Kim, Kyunga Kim, Hee-Jung Park, Jong-Seok Lim, Woo-Young Kim, Sang Eun Jun, Eun Kyung Yoon, and Jun Lim. 2015. 'Arabidopsis thaliana homeobox 12 (ATHB12), a homeodomain-leucine zipper protein, regulates leaf growth by promoting cell expansion and endoreduplication', New Phytologist, 205: 316-28.

Hwang, Moo Gak, In Kwon Chung, Bin Goo Kang, and Myeon Haeng Cho. 2001. 'Sequence-specific binding property of Arabidopsis thaliana telomeric DNA binding protein 1 (AtTBP1)', FEBS Letters, 503: 35-40.

Inzé, Dirk, and Lieven De Veylder. 2006. 'Cell cycle regulation in plant development 1', Annual Review of Genetics, 40: 77-105.

Ishida, Takashi, Sumiko Adachi, Mika Yoshimura, Kohei Shimizu, Masaaki Umeda, and Keiko Sugimoto. 2010. 'Auxin modulates the transition from the mitotic cycle to the endocycle in Arabidopsis', Development, 137: 63-71.

Ito, Masaki, Satoshi Araki, Sachihiro Matsunaga, Takashi Itoh, Ryuichi Nishihama, Yasunori Machida, John H Doonan, and Akira Watanabe. 2001. 'G2/M-phase–specific transcription during the plant cell cycle is mediated by c-Myb–like transcription factors', The Plant Cell, 13: 1891-905.

Jacob, Tobias, Sian Ritchie, Sarah M Assmann, and Simon Gilroy. 1999. 'Abscisic acid signal transduction in guard cells is mediated by phospholipase D activity', Proceedings of the National Academy of Sciences of USA, 96: 12192-97.

Janicka-Russak, Małgorzata, and Katarzyna Kabała. 2015. 'The role of plasma membrane H+-ATPase in salinity stress of plants.' in, Progress in Botany (Springer).

Jia, Xinping, Yanming Deng, Xiaobo Sun, Lijian Liang, and Xiaoqing Ye. 2015. 'Characterization of the global transcriptome using Illumina sequencing and novel microsatellite marker information in seashore paspalum', Genes & Genomics, 37: 77-86.

Jiang, Caifu, Eric J Belfield, Aziz Mithani, Anne Visscher, Jiannis Ragoussis, Richard Mott, J Andrew C Smith, and Nicholas P Harberd. 2012. 'ROS-mediated vascular homeostatic control of root-to-shoot soil Na delivery in Arabidopsis', The EMBO Journal, 31: 4359-70.

Jin, J., K. He, X. Tang, Z. Li, L. Lv, Y. Zhao, J. Luo, and G. Gao. 2015. 'An Arabidopsis Transcriptional Regulatory Map Reveals Distinct Functional and Evolutionary Features of Novel Transcription Factors', Molecular Biology and Evolution, 32: 1767-73.

`

Jin, J., F. Tian, D. C. Yang, Y. Q. Meng, L. Kong, J. Luo, and G. Gao. 2017. 'PlantTFDB 4.0: toward a central hub for transcription factors and regulatory interactions in plants', Nucleic Acids Research, 45: D1040-D45.

Jones, Eric, Travis Oliphant, and Pearu Peterson. 2014. '{SciPy}: open source scientific tools for {Python}'.

Joshi, Rohit, Shabir H Wani, Balwant Singh, Abhishek Bohra, Zahoor A Dar, Ajaz A Lone, Ashwani Pareek, and Sneh L Singla-Pareek. 2016. 'Transcription factors and plants response to drought stress: current understanding and future directions', Frontiers in Plant Science, 7.

Kalve, Shweta, Dirk De Vos, and Gerrit TS Beemster. 2014. 'Leaf development: a cellular perspective', Frontiers in Plant Science, 5.

Karamysheva, Zemfira N, Yulia V Surovtseva, Laurent Vespa, Eugene V Shakirov, and Dorothy E Shippen. 2004. 'A C-terminal Myb extension domain defines a novel family of double-strand telomeric DNA-binding proteins in Arabidopsis', Journal of Biological Chemistry, 279: 47799-807.

Katiyar, Amit, Shuchi Smita, Sangram Keshari Lenka, Ravi Rajwanshi, Viswanathan Chinnusamy, and Kailash Chander Bansal. 2012. 'Genome-wide classification and expression analysis of MYB transcription factor families in rice and Arabidopsis', BMC Genomics, 13: 1.

Kawade, Kensuke, Gorou Horiguchi, and Hirokazu Tsukaya. 2010. 'Non-cell-autonomously coordinated organ size regulation in leaf development', Development, 137: 4221-27.

Kieber, Joseph J, Madge Rothenberg, Gregg Roman, Kenneth A Feldmann, and Joseph R Ecker. 1993. 'CTR1, a negative regulator of the ethylene response pathway in Arabidopsis, encodes a member of the raf family of protein kinases', Cell, 72: 427-41.

Kim, Gyung-Tae, Shozo Fujioka, Toshiaki Kozuka, Frans E Tax, Suguru Takatsuto, Shigeo Yoshida, and Hirokazu Tsukaya. 2005. 'CYP90C1 and CYP90D1 are involved in different steps in the brassinosteroid biosynthesis pathway in Arabidopsis thaliana', The Plant Journal, 41: 710-21.

Kim, Gyung-Tae, Keiko Shoda, Tomohiko Tsuge, Kiu-Hyung Cho, Hirofumi Uchimiya, Ryusuke Yokoyama, Kazuhiko Nishitani, and Hirokazu Tsukaya. 2002. 'The ANGUSTIFOLIA gene of Arabidopsis, a plant CtBP gene, regulates leaf-cell expansion, the arrangement of cortical microtubules in leaf cells and expression of a gene involved in cell-wall formation', The EMBO Journal, 21: 1267-79.

Kim, June-Sik, Junya Mizoi, Takuya Yoshida, Yasunari Fujita, Jun Nakajima, Teppei Ohori, Daisuke Todaka, Kazuo Nakashima, Takashi Hirayama, and Kazuo Shinozaki. 2011. 'An ABRE promoter sequence is involved in osmotic stress-

responsive expression of the DREB2A gene, which encodes a transcription factor regulating drought-inducible genes in Arabidopsis', Plant and Cell Physiology, 52: 2136-46.

Kirik, Viktor, Andrea Schrader, Joachim F Uhrig, and Martin Hulskamp. 2007. 'MIDGET unravels functions of the Arabidopsis topoisomerase VI complex in DNA endoreduplication, chromatin condensation, and transcriptional silencing', The Plant Cell, 19: 3100-10.

Knight, Heather, Anthony J Trewavas, and Marc R Knight. 1997. 'Calcium signalling in Arabidopsis thaliana responding to drought and salinity', The Plant Journal, 12: 1067-78.

Komaki, S., and K. Sugimoto. 2012. 'Control of the The Plant Cell Cycle by Developmental and Environmental Cues', Plant and Cell Physiology, 53: 953-64.

Kosová, Klára, Ilja T Prášil, and Pavel Vítámvás. 2013. 'Protein contribution to plant salinity response and tolerance acquisition', International Journal of Molecular Sciences, 14: 6757-89.

Kowles, Richard V, and Ronald L Phillips. 1985. 'DNA amplification patterns in maize endosperm nuclei during kernel development', Proceedings of the National Academy of Sciences of USA, 82: 7010-14.

Kuhl, Joseph C, Foo Cheung, Qiaoping Yuan, William Martin, Yayeh Zewdie, John McCallum, Andrew Catanach, Paul Rutherford, Kenneth C Sink, and Maria Jenderek. 2004. 'A unique set of 11,008 onion expressed sequence tags reveals expressed sequence and genomic differences between the monocot orders Asparagales and Poales', The Plant Cell, 16: 114-25.

Kumari, Sumita, Vaishali Panjabi nee Sabharwal, Hemant R Kushwaha, Sudhir K Sopory, Sneh L Singla-Pareek, and Ashwani Pareek. 2009. 'Transcriptome map for seedling stage specific salinity stress response indicates a specific set of genes as candidate for saline tolerance in Oryza sativa L', Functional & Integrative Genomics, 9: 109.

Kwon, Ye Rim, Hee Jin Lee, Kyoung Heon Kim, Suk-Whan Hong, Sung Joon Lee, and Hojoung Lee. 2008. 'Ectopic expression of Expansin3 or Expansinβ1 causes enhanced hormone and salt stress sensitivity in Arabidopsis', Biotechnology Letters, 30: 1281-88.

Lata, Charu, and Manoj Prasad. 2011. 'Role of DREBs in regulation of abiotic stress responses in plants', Journal of Experimental Botany, 62: 4731-48.

Lee, Geungjoo, Robert N Carrow, and Ronny R Duncan. 2004. 'Photosynthetic responses to salinity stress of halophytic seashore paspalum ecotypes', Plant Science, 166: 1417-25.

`

Lee, Sun-ji, Jung-youn Kang, Hee-Jin Park, Myoung Duck Kim, Min Seok Bae, Hyung-in Choi, and Soo Young Kim. 2010. 'DREB2C interacts with ABF2, a bZIP protein regulating abscisic acid-responsive gene expression, and its overexpression affects abscisic acid sensitivity', Plant Physiology, 153: 716-27.

Leiber, Ruth-Maria, Florian John, Yves Verhertbruggen, Anouck Diet, J Paul Knox, and Christoph Ringli. 2010. 'The TOR pathway modulates the structure of cell walls in Arabidopsis', The Plant Cell, 22: 1898-908.

Leidi, Eduardo O, Verónica Barragán, Lourdes Rubio, Abdelaziz El-Hamdaoui, M Teresa Ruiz, Beatriz Cubero, José A Fernández, Ray A Bressan, Paul M Hasegawa, and Francisco J Quintero. 2010. 'The AtNHX1 exchanger mediates potassium compartmentation in vacuoles of transgenic tomato', The Plant Journal, 61: 495-506.

Lescot, Magali, Patrice Déhais, Gert Thijs, Kathleen Marchal, Yves Moreau, Yves Van de Peer, Pierre Rouzé, and Stephane Rombauts. 2002. 'PlantCARE, a database of plant cis-acting regulatory elements and a portal to tools for in silico analysis of promoter sequences', Nucleic Acids Research, 30: 325-27.

Li, Bo, and Colin N Dewey. 2011. 'RSEM: accurate transcript quantification from RNA-Seq data with or without a reference genome', BMC Bioinformatics, 12: 323.

Li, Chaonan, Carl K-Y Ng, and Liu-Min Fan. 2015. 'MYB transcription factors, active players in abiotic stress signaling', Environmental and Experimental Botany, 114: 80-91.

Li, Weizhong, and Adam Godzik. 2006. 'Cd-hit: a fast program for clustering and comparing large sets of protein or nucleotide sequences', Bioinformatics, 22: 1658-59.

Liszkay, A, and P Schopfer. 2003. "Plasma membrane-generated superoxide anion radicals and peroxidase-generated hydroxyl radicals may be involved in the growth of coleoptiles." In Free Radical Research, 26-27. TAYLOR & FRANCIS LTD 4 PARK SQUARE, MILTON PARK, ABINGDON OX14 4RN, OXON, ENGLAND.

Liu, Qiang, Mie Kasuga, Yoh Sakuma, Hiroshi Abe, Setsuko Miura, Kazuko Yamaguchi-Shinozaki, and Kazuo Shinozaki. 1998. 'Two transcription factors, DREB1 and DREB2, with an EREBP/AP2 DNA binding domain separate two cellular signal transduction pathways in drought-and low-temperature-responsive gene expression, respectively, in Arabidopsis', The Plant Cell Online, 10: 1391-406.

Liu, Y, F Cheng, Q Wang, Y Hu, and Z Wang. 2009. 'Salinity stress responses and-thresholds in four warm-season turfgrasses', Acta Pharmaceutica Sinica, 18: 192-9.

Liu, Yiming, Hongmei Du, Xiaoxia He, Bingru Huang, and Zhaolong Wang. 2012. 'Identification of differentially expressed salt-responsive proteins in roots of two

perennial grass species contrasting in salinity tolerance', Journal of Plant Physiology, 169: 117-26.

Liu, Yiming, Hongmei Du, Kai Wang, Bingru Huang, and Zhaolong Wang. 2011. 'Differential photosynthetic responses to salinity stress between two perennial grass species contrasting in salinity tolerance', HortScience, 46: 311-16.

Livak, Kenneth J, and Thomas D Schmittgen. 2001. 'Analysis of relative gene expression data using real-time quantitative PCR and the 2− ΔΔCT method', Methods, 25: 402-08.

Lodeyro, Anabella Fernanda, and Néstor Carrillo. 2015. 'Salt Stress in Higher Plants: Mechanisms of Toxicity and Defensive Responses.' in, Stress Responses in Plants (Springer).

Love, Michael I, Wolfgang Huber, and Simon Anders. 2014. 'Moderated estimation of fold change and dispersion for RNA-seq data with DESeq2', Genome Biology, 15: 550.

Lu, Dandan, Ting Wang, Staffan Persson, Bernd Mueller-Roeber, and Jos HM Schippers. 2014. 'Transcriptional control of ROS homeostasis by KUODA1 regulates cell expansion during leaf development', Nature Communications, 5.

Ma, Yue, Izabela Szostkiewicz, Arthur Korte, Danièle Moes, Yi Yang, Alexander Christmann, and Erwin Grill. 2009. 'Regulators of PP2C phosphatase activity function as abscisic acid sensors', Science, 324: 1064-68.

Maggio, Albino, Paul M Hasegawa, Ray A Bressan, M Federica Consiglio, and Robert J Joly. 2001. 'Unravelling the functional relationship between root anatomy and stress tolerance', Functional Plant Biology, 28: 999-1004.

Magyar, Zoltán, Lieven De Veylder, Ana Atanassova, László Bakó, Dirk Inzé, and László Bögre. 2005. 'The role of the Arabidopsis E2FB transcription factor in regulating auxin-dependent cell division', The Plant Cell, 17: 2527-41.

Mahajan, Shilpi, Girdhar K Pandey, and Narendra Tuteja. 2008. 'Calcium-and salt-stress signaling in plants: shedding light on SOS pathway', Archives of Biochemistry and Biophysics, 471: 146-58.

Manik, SM, Sujuan Shi, Jingjing Mao, Lianhong Dong, Yulong Su, Qian Wang, and Haobao Liu. 2015. 'The calcium sensor CBL-CIPK is involved in plant's response to abiotic stresses', International Journal of Genomics, 2015.

Marchler-Bauer, Aron, Shennan Lu, John B Anderson, Farideh Chitsaz, Myra K Derbyshire, Carol DeWeese-Scott, Jessica H Fong, Lewis Y Geer, Renata C Geer, and Noreen R Gonzales. 2011. 'CDD: a Conserved Domain Database for the functional annotation of proteins', Nucleic Acids Research, 39: D225-D29.

Mariconti, Luisa, Barbara Pellegrini, Rita Cantoni, Rebecca Stevens, Catherine Bergounioux, Rino Cella, and Diego Albani. 2002. 'The E2F Family of

Transcription Factors from Arabidopsis thaliana NOVEL AND CONSERVED COMPONENTS OF THE RETINOBLASTOMA/E2F PATHWAY IN PLANTS', Journal of Biological Chemistry, 277: 9911-19.

Mäser, Pascal, Brendan Eckelman, Rama Vaidyanathan, Tomoaki Horie, David J Fairbairn, Masahiro Kubo, Mutsumi Yamagami, Katsushi Yamaguchi, Mikio Nishimura, and Nobuyuki Uozumi. 2002. 'Altered shoot/root Na+ distribution and bifurcating salt sensitivity in Arabidopsis by genetic disruption of the Na+ transporter AtHKT1', FEBS Letters, 531: 157-61.

Mian, A., R. J. Oomen, S. Isayenkov, H. Sentenac, F. J. Maathuis, and A. A. Very. 2011. 'Over-expression of an Na+-and K+-permeable HKT transporter in barley improves salt tolerance', Plant Journal, 68: 468-79.

Micol, José Luis. 2009. 'Leaf development: time to turn over a new leaf?', Current Opinion in Plant Biology, 12: 9-16.

Mittler, Ron, Sandy Vanderauwera, Nobuhiro Suzuki, Gad Miller, Vanesa B Tognetti, Klaas Vandepoele, Marty Gollery, Vladimir Shulaev, and Frank Van Breusegem. 2011. 'ROS signaling: the new wave?', Trends in Plant Science, 16: 300-09.

Mizoguchi, Tsuyoshi, Kay Wheatley, Yoshie Hanzawa, Louisa Wright, Mutsuko Mizoguchi, Hae-Ryong Song, Isabelle A Carré, and George Coupland. 2002. 'LHY and CCA1 are partially redundant genes required to maintain circadian rhythms in Arabidopsis', Developmental Cell, 2: 629-41.

Mizukami, Yukiko, and Robert L Fischer. 2000. 'Plant organ size control: AINTEGUMENTA regulates growth and cell numbers during organogenesis', Proceedings of the National Academy of Sciences of USA, 97: 942-47.

Møller, Inge S, Matthew Gilliham, Deepa Jha, Gwenda M Mayo, Stuart J Roy, Juliet C Coates, Jim Haseloff, and Mark Tester. 2009. 'Shoot Na+ exclusion and increased salinity tolerance engineered by cell type–specific alteration of Na+ transport in Arabidopsis', The Plant Cell, 21: 2163-78.

Munns, R. 2005a. 'Genes and salt tolerance: bringing them together', New Phytologist, 167: 645-63.

Munns, Rana. 2005b. 'Genes and salt tolerance: bringing them together', New Phytologist, 167: 645-63.

Munns, Rana, and Mark Tester. 2008. 'Mechanisms of salinity tolerance', Annual Review of Plant Biology, 59: 651-81.

Nakashima, Kazuo, and Kazuko Yamaguchi-Shinozaki. 2013. 'ABA signaling in stress-response and seed development', Plant Cell Reports, 32: 959-70.

Nicol, Frédéric, Isabelle His, Alain Jauneau, Samantha Vernhettes, Hervé Canut, and Herman Höfte. 1998. 'A plasma membrane-bound putative endo-1, 4-β-d-glucanase

is required for normal wall assembly and cell elongation in Arabidopsis', The EMBO Journal, 17: 5563-76.

Ogata, Kazuhiro, Souichi Morikawa, Haruki Nakamura, Ai Sekikawa, Taiko Inoue, Hiroko Kanai, Akinori Sarai, Shunsuke Ishii, and Yoshifumi Nishimura. 1994. 'Solution structure of a specific DNA complex of the Myb DNA-binding domain with cooperative recognition helices', Cell, 79: 639-48.

Owttrim, George W. 2006. 'RNA helicases and abiotic stress', Nucleic Acids Research, 34: 3220-30.

Pang, Qiuying, Sixue Chen, Shaojun Dai, Yazhou Chen, Yang Wang, and Xiufeng Yan. 2010. 'Comparative proteomics of salt tolerance in Arabidopsis thaliana and Thellungiella halophila', Journal of Proteome Research, 9: 2584-99.

Paredez, Alexander R, Christopher R Somerville, and David W Ehrhardt. 2006. 'Visualization of cellulose synthase demonstrates functional association with microtubules', Science, 312: 1491-95.

Park, Sang-Youl, Pauline Fung, Noriyuki Nishimura, Davin R Jensen, Hiroaki Fujii, Yang Zhao, Shelley Lumba, Julia Santiago, Americo Rodrigues, and F Chow Tsz-fung. 2009. 'Abscisic acid inhibits type 2C protein phosphatases via the PYR/PYL family of START proteins', Science, 324: 1068-71.

Pei, Haixia, Nan Ma, Ji Tian, Jing Luo, Jiwei Chen, Jing Li, Yi Zheng, Xiang Chen, Zhangjun Fei, and Junping Gao. 2013. 'An NAC transcription factor controls ethylene-regulated cell expansion in flower petals', Plant Physiology, 163: 775-91.

Pesch, Martina, and Martin Hülskamp. 2011. 'Role of TRIPTYCHON in trichome patterning in Arabidopsis', BMC Plant Biology, 11: 1.

Pinon, Violaine, J Peter Etchells, Pascale Rossignol, Sarah A Collier, Juana M Arroyo, Robert A Martienssen, and Mary E Byrne. 2008. 'Three PIGGYBACK genes that specifically influence leaf patterning encode ribosomal proteins', Development, 135: 1315-24.

Plank, C Owen. 1992. 'Plant analysis reference procedures for the southern region of the United States', Southern Cooperative Series Bulletin (USA).

Pottosin, Igor, and Oxana Dobrovinskaya. 2014. 'Non-selective cation channels in plasma and vacuolar membranes and their contribution to K+ transport', Journal of Plant Physiology, 171: 732-42.

Powell, A. E., and M. Lenhard. 2012. 'Control of Organ Size in Plants', Current Biology, 22: R360-R67.

Qin, Zhixiang, Xiao Zhang, Xiaoran Zhang, Guanping Feng, and Yuxin Hu. 2014. 'The Arabidopsis ORGAN SIZE RELATED 2 is involved in regulation of cell expansion during organ growth', BMC Plant Biology, 14: 349.

`

Qiu-Fang, Zhang, Li Yuan-Yuan, Pang Cai-Hong, Lu Cong-Ming, and Wang Bao-Shan. 2005. 'NaCl enhances thylakoid-bound SOD activity in the leaves of C 3 halophyte Suaeda salsa L', Plant Science, 168: 423-30.

Qiu, Nianwei, Min Chen, Jianrong Guo, Huayin Bao, Xiuling Ma, and Baoshan Wang. 2007. 'Coordinate up-regulation of VH+-ATPase and vacuolar Na+/H+ antiporter as a response to NaCl treatment in a C 3 halophyte Suaeda salsa', Plant Science, 172: 1218-25.

Qiu, Quan-Sheng, Yan Guo, Margaret A Dietrich, Karen S Schumaker, and Jian-Kang Zhu. 2002. 'Regulation of SOS1, a plasma membrane Na+/H+ exchanger in Arabidopsis thaliana, by SOS2 and SOS3', Proceedings of the National Academy of Sciences of USA, 99: 8436-41.

Ren, Hong, Aaron Santner, Juan Carlos del Pozo, James AH Murray, and Mark Estelle. 2008. 'Degradation of the cyclin-dependent kinase inhibitor KRP1 is regulated by two different ubiquitin E3 ligases', The Plant Journal, 53: 705-16.

Rexin, Daniel, Christian Meyer, Christophe Robaglia, and Bruce Veit. 2015. 'TOR signalling in plants', Biochemical Journal, 470: 1-14.

Rhoades, JD, and J Loveday. 1990. 'Salinity in irrigated agriculture', Agronomy: 1089-142.

Riechmann, Jose Luis, and Elliot M Meyerowitz. 1998. 'The AP2/EREBP family of plant transcription factors', Biological Chemistry, 379: 633-46.

Rojas, Cristian Antonio, Nubia Barbosa Eloy, Marcelo de Freitas Lima, Roberta Lopes Rodrigues, Luciana Ozório Franco, Kristiina Himanen, Gerrit TS Beemster, Adriana Silva Hemerly, and Paulo Cavalcanti Gomes Ferreira. 2009. 'Overexpression of the Arabidopsis anaphase promoting complex subunit CDC27a increases growth rate and organ size', Plant Molecular Biology, 71: 307-18.

Rossignol, P, R Stevens, C Perennes, S Jasinski, R Cella, D Tremousaygue, and C Bergounioux. 2002. 'AtE2F-a and AtDP-a, members of the E2F family of transcription factors, induce Arabidopsis leaf cells to re-enter S phase', Molecular Genetics and Genomics, 266: 995-1003.

Roy, Stuart J, Sónia Negrão, and Mark Tester. 2014. 'Salt resistant crop plants', Current Opinion in Biotechnology, 26: 115-24.

Rubio, F., W. Gassmann, and J. I. Schroeder. 1995. 'Sodium-driven potassium uptake by the plant potassium transporter HKT1 and mutations conferring salt tolerance', Science, 270: 1660-3.

Růžička, Kamil, Karin Ljung, Steffen Vanneste, Radka Podhorská, Tom Beeckman, Jiří Friml, and Eva Benková. 2007. 'Ethylene regulates root growth through effects on auxin biosynthesis and transport-dependent auxin distribution', The Plant Cell, 19: 2197-212.

`

Sablowski, Robert, and Marcelo Carnier Dornelas. 2014. 'Interplay between cell growth and cell cycle in plants', Journal of Experimental Botany, 65: 2703-14.

Sakuma, Yoh, Qiang Liu, Joseph G Dubouzet, Hiroshi Abe, Kazuo Shinozaki, and Kazuko Yamaguchi-Shinozaki. 2002. 'DNA-binding specificity of the ERF/AP2 domain of Arabidopsis DREBs, transcription factors involved in dehydration-and cold-inducible gene expression', Biochemical and Biophysical Research Communications, 290: 998-1009.

Sakuma, Yoh, Kyonoshin Maruyama, Yuriko Osakabe, Feng Qin, Motoaki Seki, Kazuo Shinozaki, and Kazuko Yamaguchi-Shinozaki. 2006. 'Functional analysis of an Arabidopsis transcription factor, DREB2A, involved in drought-responsive gene expression', The Plant Cell, 18: 1292-309.

Saladié, Montserrat, Jocelyn KC Rose, Daniel J Cosgrove, and Carmen Catalá. 2006. 'Characterization of a new xyloglucan endotransglucosylase/hydrolase (XTH) from ripening tomato fruit and implications for the diverse modes of enzymic action', The Plant Journal, 47: 282-95.

Schachtman, Daniel P, and Julian I Schroeder. 1994. 'Structure and transport mechanism of a high-affinity potassium uptake transporter from higher plants', Nature, 370: 655-58.

Schaffer, Robert, Nicola Ramsay, Alon Samach, Sally Corden, Joanna Putterill, Isabelle A Carré, and George Coupland. 1998. 'The late elongated hypocotyl mutation of Arabidopsis disrupts circadian rhythms and the photoperiodic control of flowering', Cell, 93: 1219-29.

Schepetilnikov, Mikhail, Maria Dimitrova, Eder Mancera-Martínez, Angèle Geldreich, Mario Keller, and Lyubov A Ryabova. 2013. 'TOR and S6K1 promote translation reinitiation of uORF-containing mRNAs via phosphorylation of eIF3h', The EMBO Journal, 32: 1087-102.

Schopfer, Peter, Anja Liszkay, Michael Bechtold, Gitta Frahry, and Andrea Wagner. 2002. 'Evidence that hydroxyl radicals mediate auxin-induced extension growth', Planta, 214: 821-28.

Schrumpfová, Petra, Milan Kuchař, Gabriela Miková, Lenka Skří ovská, Tatiana Kubičárová, and Jiří Fajkus. 2004. 'Characterization of two Arabidopsis thaliana myb-like proteins showing affinity to telomeric DNA sequence', Genome, 47: 316-24.

Schrumpfová, Petra Procházková, Šárka Schořová, and Jiří Fajkus. 2016. 'Telomere-and Telomerase-Associated Proteins and Their Functions in the The Plant Cell', Frontiers in Plant Science, 7.

`

Sengupta, Sonali, and Arun Lahiri Majumder. 2009. 'Insight into the salt tolerance factors of a wild halophytic rice, Porteresia coarctata: a physiological and proteomic approach', Planta, 229: 911-29.

Seo, Pil Joon, Saet Buyl Lee, Mi Chung Suh, Mi-Jeong Park, Young Sam Go, and Chung-Mo Park. 2011. 'The MYB96 transcription factor regulates cuticular wax biosynthesis under drought conditions in Arabidopsis', The Plant Cell, 23: 1138-52.

Shabala, Sergey, and Tracey A Cuin. 2008. 'Potassium transport and plant salt tolerance', Physiologia Plantarum, 133: 651-69.

Sharp, Robert E, Mary E LeNoble, Mark A Else, Eleanor T Thorne, and Francesca Gherardi. 2000. 'Endogenous ABA maintains shoot growth in tomato independently of effects on plant water balance: evidence for an interaction with ethylene', Journal of Experimental Botany, 51: 1575-84.

Shi, Huazhong, Manabu Ishitani, Cheolsoo Kim, and Jian-Kang Zhu. 2000. 'The Arabidopsis thaliana salt tolerance gene SOS1 encodes a putative Na+/H+ antiporter', Proceedings of the National Academy of Sciences of USA, 97: 6896-901.

Shi, Huazhong, Byeong-ha Lee, Shaw-Jye Wu, and Jian-Kang Zhu. 2003. 'Overexpression of a plasma membrane Na+/H+ antiporter gene improves salt tolerance in Arabidopsis thaliana', Nature Biotechnology, 21: 81-85.

Shi, Huazhong, Francisco J Quintero, Jose M Pardo, and Jian-Kang Zhu. 2002. 'The putative plasma membrane Na+/H+ antiporter SOS1 controls long-distance Na+ transport in plants', The Plant Cell, 14: 465-77.

Sievers, Fabian, Andreas Wilm, David Dineen, Toby J Gibson, Kevin Karplus, Weizhong Li, Rodrigo Lopez, Hamish McWilliam, Michael Remmert, and Johannes Söding. 2011. 'Fast, scalable generation of high-quality protein multiple sequence alignments using Clustal Omega', Molecular Systems Biology, 7: 539.

Smogorzewska, Agata, Bas van Steensel, Alessandro Bianchi, Stefan Oelmann, Matthias R Schaefer, Gisela Schnapp, and Titia de Lange. 2000. 'Control of human telomere length by TRF1 and TRF2', Molecular and Cellular Biology, 20: 1659-68.

Smyth, David R, John L Bowman, and Elliot M Meyerowitz. 1990. 'Early flower development in Arabidopsis', The Plant Cell, 2: 755-67.

Sonoda, Yutaka, Kaori Sako, Yuko Maki, Naoko Yamazaki, Hiroko Yamamoto, Akira Ikeda, and Junji Yamaguchi. 2009. 'Regulation of leaf organ size by the Arabidopsis RPT2a 19S proteasome subunit', The Plant Journal, 60: 68-78.

Sugimoto-Shirasu, Keiko, Gethin R Roberts, Nicola J Stacey, Maureen C McCann, Anthony Maxwell, and Keith Roberts. 2005. 'RHL1 is an essential component of

the plant DNA topoisomerase VI complex and is required for ploidy-dependent cell growth', Proceedings of the National Academy of Sciences of USA, 102: 18736-41.

Sugimoto-Shirasu, Keiko, and Keith Roberts. 2003. '"Big it up": endoreduplication and cell-size control in plants', Current Opinion in Plant Biology, 6: 544-53.

Sugimoto-Shirasu, Keiko, Nicola J Stacey, Julia Corsar, Keith Roberts, and Maureen C McCann. 2002. 'DNA topoisomerase VI is essential for endoreduplication in Arabidopsis', Current Biology, 12: 1782-86.

Swarup, Ranjan, Paula Perry, Dik Hagenbeek, Dominique Van Der Straeten, Gerrit TS Beemster, Göran Sandberg, Rishikesh Bhalerao, Karin Ljung, and Malcolm J Bennett. 2007. 'Ethylene upregulates auxin biosynthesis in Arabidopsis seedlings to enhance inhibition of root cell elongation', The Plant Cell, 19: 2186-96.

Taji, Teruaki, Motoaki Seki, Masakazu Satou, Tetsuya Sakurai, Masatomo Kobayashi, Kanako Ishiyama, Yoshihiro Narusaka, Mari Narusaka, Jian-Kang Zhu, and Kazuo Shinozaki. 2004. 'Comparative genomics in salt tolerance between Arabidopsis and Arabidopsis-related halophyte salt cress using Arabidopsis microarray', Plant Physiology, 135: 1697-709.

Tamura, Koichiro, Glen Stecher, Daniel Peterson, Alan Filipski, and Sudhir Kumar. 2013. 'MEGA6: molecular evolutionary genetics analysis version 6.0', Molecular Biology and Evolution, 30: 2725-29.

Taylor, Neil G, Rhian M Howells, Alison K Huttly, Kate Vickers, and Simon R Turner. 2003. 'Interactions among three distinct CesA proteins essential for cellulose synthesis', Proceedings of the National Academy of Sciences of USA, 100: 1450-55.

Tester, Mark, and Romola Davenport. 2003. 'Na+ tolerance and Na+ transport in higher plants', Annals of Botany, 91: 503-27.

Tsabary, Galit, Ziv Shani, Levava Roiz, Ilan Levy, Joseph Riov, and Oded Shoseyov. 2003. 'Abnormalwrinkled'cell walls and retarded development of transgenic Arabidopsis thaliana plants expressing endo-1, 4-β-glucanase (cell) antisense', Plant Molecular Biology, 51: 213-24.

Tsuge, Tomohiko, Hirokazu Tsukaya, and Hirofumi Uchimiya. 1996. 'Two independent and polarized processes of cell elongation regulate leaf blade expansion in Arabidopsis thaliana (L.) Heynh', Development, 122: 1589-600.

Tsukagoshi, Hironaka, Takamasa Suzuki, Kouki Nishikawa, Sakae Agarie, Sumie Ishiguro, and Tetsuya Higashiyama. 2015. 'RNA-seq analysis of the response of the halophyte, Mesembryanthemum crystallinum (ice plant) to high salinity', PLoS One, 10: e0118339.

`

Tsukaya, Hirokazu. 2003. 'Organ shape and size: a lesson from studies of leaf morphogenesis', Current Opinion in Plant Biology, 6: 57-62.

———. 2008. 'Controlling size in multicellular organs: focus on the leaf', PLoS Biology, 6.

Tuteja, Narendra. 2007. 'Chapter twenty-four-mechanisms of high salinity tolerance in plants', Methods in Enzymology, 428: 419-38.

Umezawa, Taishi, Naoyuki Sugiyama, Masahide Mizoguchi, Shimpei Hayashi, Fumiyoshi Myouga, Kazuko Yamaguchi-Shinozaki, Yasushi Ishihama, Takashi Hirayama, and Kazuo Shinozaki. 2009. 'Type 2C protein phosphatases directly regulate abscisic acid-activated protein kinases in Arabidopsis', Proceedings of the National Academy of Sciences of USA, 106: 17588-93.

Usami, Takeshi, Gorou Horiguchi, Satoshi Yano, and Hirokazu Tsukaya. 2009. 'The more and smaller cells mutants of Arabidopsis thaliana identify novel roles for SQUAMOSA PROMOTER BINDING PROTEIN-LIKE genes in the control of heteroblasty', Development, 136: 955-64.

Van Sandt, Vicky ST, Dmitry Suslov, Jean-Pierre Verbelen, and Kris Vissenberg. 2007. 'Xyloglucan endotransglucosylase activity loosens a plant cell wall', Annals of Botany, 100: 1467-73.

Verkest, Aurine, Christina Weinl, Dirk Inzé, Lieven De Veylder, and Arp Schnittger. 2005. 'Switching the cell cycle. Kip-related proteins in plant cell cycle control', Plant Physiology, 139: 1099-106.

Vlad, Florina, Silvia Rubio, Americo Rodrigues, Caroline Sirichandra, Christophe Belin, Nadia Robert, Jeffrey Leung, Pedro L Rodriguez, Christiane Laurière, and Sylvain Merlot. 2009. 'Protein phosphatases 2C regulate the activation of the Snf1-related kinase OST1 by abscisic acid in Arabidopsis', The Plant Cell, 21: 3170-84.

Volkov, V, B Wang, PJ Dominy, W Fricke, and A Amtmann. 2004. 'Thellungiella halophila, a salt-tolerant relative of Arabidopsis thaliana, possesses effective mechanisms to discriminate between potassium and sodium', Plant, Cell & Environment, 27: 1-14.

Wada, Takuji, Tatsuhiko Tachibana, Yoshiro Shimura, and Kiyotaka Okada. 1997. 'Epidermal cell differentiation in Arabidopsis determined by a Myb homolog, CPC', Science, 277: 1113-16.

Wang, Hongyan, Honglei Wang, Hongbo Shao, and Xiaoli Tang. 2016. 'Recent advances in utilizing transcription factors to improve plant abiotic stress tolerance by transgenic technology', Frontiers in Plant Science, 7.

Wang, Yanping, Li Yang, Zhimin Zheng, Rebecca Grumet, Wayne Loescher, Jian-Kang Zhu, Pingfang Yang, Yuanlei Hu, and Zhulong Chan. 2013. 'Transcriptomic and

physiological variations of three Arabidopsis ecotypes in response to salt stress', PLoS One, 8: e69036.

Wang, Zhen-Yu, Liming Xiong, Wenbo Li, Jian-Kang Zhu, and Jianhua Zhu. 2011. 'The plant cuticle is required for osmotic stress regulation of abscisic acid biosynthesis and osmotic stress tolerance in Arabidopsis', The Plant Cell, 23: 1971-84.

Wang, Zhi-Yong, and Elaine M Tobin. 1998. 'Constitutive expression of the CIRCADIAN CLOCK ASSOCIATED 1 (CCA1) gene disrupts circadian rhythms and suppresses its own expression', Cell, 93: 1207-17.

Xiong, Y., and J. Sheen. 2012. 'Rapamycin and glucose-target of rapamycin (TOR) protein signaling in plants', Journal of Biological Chemistry, 287: 2836-42.

Xiong, Yan, Matthew McCormack, Lei Li, Qi Hall, Chengbin Xiang, and Jen Sheen. 2013. 'Glucose-TOR signalling reprograms the transcriptome and activates meristems', Nature, 496: 181-86.

Xu, Chongzhi, Xiaoli Tang, Hongbo Shao, and Hongyan Wang. 2016. 'Salinity Tolerance Mechanism of Economic Halophytes From Physiological to Molecular Hierarchy for Improving Food Quality', Current Genomics, 17: 207-14.

Yamaguchi, Toshio, Shin Hamamoto, and Nobuyuki Uozumi. 2013. 'Sodium transport system in plant cells', Frontiers in Plant Science, 4: 410.

Yang, Chunhua, Dayong Li, Xue Liu, Chengjun Ji, Lili Hao, Xianfeng Zhao, Xiaobing Li, Caiyan Chen, Zhukuan Cheng, and Lihuang Zhu. 2014. 'OsMYB103L, an R2R3-MYB transcription factor, influences leaf rolling and mechanical strength in rice (Oryza sativa L.)', BMC Plant Biology, 14: 158.

Yang, K., H. Wang, S. Xue, X. Qu, J. Zou, and J. Le. 2014. 'Requirement for A-type cyclin-dependent kinase and cyclins for the terminal division in the stomatal lineage of Arabidopsis', Journal of Experimental Botany, 65: 2449-61.

Yanhui, Chen, Yang Xiaoyuan, He Kun, Liu Meihua, Li Jigang, Gao Zhaofeng, Lin Zhiqiang, Zhang Yunfei, Wang Xiaoxiao, and Qiu Xiaoming. 2006. 'The MYB transcription factor superfamily of Arabidopsis: expression analysis and phylogenetic comparison with the rice MYB family', Plant Molecular Biology, 60: 107-24.

Yin, Yanhai, Hyeonsook Cheong, Danielle Friedrichsen, Yunde Zhao, Jianping Hu, Santiago Mora-Garcia, and Joanne Chory. 2002. 'A crucial role for the putative Arabidopsis topoisomerase VI in plant growth and development', Proceedings of the National Academy of Sciences of USA, 99: 10191-96.

Yoshida, Takuya, Junro Mogami, and Kazuko Yamaguchi-Shinozaki. 2014. 'ABA-dependent and ABA-independent signaling in response to osmotic stress in plants', Current Opinion in Plant Biology, 21: 133-39.

`

Zhang, J. L., and H. Shi. 2013. 'Physiological and molecular mechanisms of plant salt tolerance', Photosynthesis Research, 115: 1-22.

Zhang, Yi, Staffan Persson, and Patrick Giavalisco. 2013. 'Differential regulation of carbon partitioning by the central growth regulator target of rapamycin (TOR)', Molecular Plant Pathology, 6: 1731-33.

Zhao, Xin'Ai, Hirofumi Harashima, Nico Dissmeyer, Stefan Pusch, Annika K Weimer, Jonathan Bramsiepe, Daniel Bouyer, Svenja Rademacher, Moritz K Nowack, and Bela Novak. 2012. 'A general G1/S-phase cell-cycle control module in the flowering plant Arabidopsis thaliana', PLoS Genetics, 8: e1002847.

Zhu, Jian-Kang. 2001. 'Plant salt tolerance', Trends in Plant Science, 6: 66-71.

Zhu, M., G. Chen, T. Dong, L. Wang, J. Zhang, Z. Zhao, and Z. Hu. 2015. 'SlDEAD31, a Putative DEAD-Box RNA Helicase Gene, Regulates Salt and Drought Tolerance and Stress-Related Genes in Tomato', PLoS One, 10: e0133849.